Transition Matrix Monte Carlo Methods for Complex Systems

by

Yong Hwan Lee

A thesis
presented to the University of Waterloo
in fulfillment of the
thesis requirement for the degree of
Doctor of Philosophy
in
Physics

Waterloo, Ontario, Canada, 2019

Examining Committee Membership

The following served on the Examining Committee for this thesis. The decision of the Examining Committee is by majority vote.

External Examiner:	Erik Sorensen Professor, McMaster University
Supervisor:	David Yevick Professor
Internal Member:	Bae-Yeun Ha Professor
Internal Member:	Donna Strickland Professor
Internal-External Member:	George Freeman Associate Professor

Author's Declaration

This thesis consists of material all of which I authored or co-authored: see Statement of Contributions included in the thesis. This is a true copy of the thesis, including any required final revisions, as accepted by my examiners.

I understand that my thesis may be made electronically available to the public.

Statement of Contributions

I am the primary author of the material discussed in this thesis which was studied under the supervision of Prof. David Yevick. Most of the chapters of this thesis have been published or are submitted for publication. The list of the published or submitted articles are the following:

[1] Y. H. Lee and D. Yevick, *"Renormalized multicanonical sampling in multiple dimensions"*, Phys. Rev. E **94**, 043323 (2016).

[2] D. Yevick and Y. H Lee, *"Dynamic canonical and microcanonical transition matrix analyses of critical behavior"*, Eur. Phys. J. B **90**, 81 (2017).

[3] D. Yevick and Y. H Lee, *"Accelerated rare event sampling: Refinement and Ising model analysis"*, Int. J. Mod. Phys. C **28**, 1750012 (2017).

[4] Y. H. Lee and D. Yevick, *"Evidence for a nonzero temperature phase transition in the two-dimensional Ising spin glass by the transition matrix Monte Carlo analysis"*, submitted to Phys. Rev. E in March 2019.

Abstract

The aim of this thesis is to develop efficient transition matrix Monte Carlo simulation methods for complex systems(e.g., spin glasses) that enable one to construct the transition matrix from which the density of states is calculated with high accuracy. In this thesis, I explore a series of the transition matrix Monte Carlo techniques that are newly developed to generate the density of states with high accuracy for various systems that exhibit phase transitions. The Ising model and the Potts model are used to demonstrate the performance of each methods. Especially, the specific heat curve of the two-dimensional Ising model is evaluated and compared to the exact result as a stringent accuracy test in many cases. I extend the *monovariate* multicanonical transition matrix Monte Carlo method to a *bivariate* version for the calculation of the joint density of states which depends on the energy and a second variable associated with the order parameter. This bivariate version is applied to the Edward-Anderson spin glass model which is one of the most challenging model in the field of computer simulation.

After presenting the theoretical basis of the transition matrix Monte Carlo method, I explain the regulated temperature method which populates the transition matrix by the Metropolis algorithm with continuously varying temperature according to a certain schedule. I introduce new techniques that can produce the optimized temperature schedule in the context of the two-dimensional Ising model. Next I proceed to present the multicanonical transition matrix Monte Carlo method in which the transition matrix is constructed through the multicanonical iteration procedure. Although this method itself is faster than other existing techniques such as the broad histogram method and Wang-Landau algorithm, its simulation speed can be further increased by the renormalization idea which utilizes the simulation results for a small system to obtain an accurate initial estimate of the density of states for a large system through the convolution procedures. Especially a novel procedure about how to apply the renormalization idea in multiple dimensions is presented.

To study the critical behavior of the spin glasses, to my knowledge for the first time, I employ the *bivariate* multicanonical sampling to construct the transition tensor from which the joint density of states can be calculated with high accuracy. I introduce a calculation technique that transforms the massive transition tensor to a normal transition matrix to avoid the cumbersome manipulation of tensors. Using the joint density of states, Landau free energies, the probability distribution functions of spin overlap and Binder parameters are calculated. Contrary to the majority of the previous reports in the literature, the results of my method provide evidences that nonzero temperature phase transition occurs in the two-dimensional Ising spin glass. For the $\pm J$ Ising spin glass, the critical temperature

obtained by my method is $T_c/J \approx 0.45$ However, a definite conclusion can not be made due to small systems sizes and the limitted number of samples of random couplings.

Acknowledgements

First of all, I would like to thank my supervisor, professor David Yevick for giving me an opportunity to join his research projects, for tremendous and constant support and for his inspiring guidance.

I also would like to thank the members of my committee, professor Bae-Yeun Ha, professor Donna Strickland, professor George Freeman and professor Erik Sorensen (McMaster University) for taking their precious time to serve in my committee.

Lastly, I would like to express special thanks to my wife, Bo Mi for her continuous support, understanding and patience in a difficult situation where she had to work and study at the same time.

Dedication

This is dedicated to Bo Mi and Helen.

Table of Contents

List of Tables

List of Figures

List of Abbreviations

BMCTM Bivariate Multilcanonical Transition Matrix Monte Carlo

DOS Density of States

JDOS Joint Density of States

MC Monte Carlo

MCTM Multicanonical Transition Matrix Monte Carlo

RMCTM Renormalized Multicanonical Transition Matrix Monte Carlo

RTTM Regulated Temperature Transition Matrix Monte Carlo

RWLTM Renormalized Wang-Landau Transition Matrix Monte Carlo

TM Transition Matrix

TMMC transition matrix Monte Carlo

WLTM Wang-Landau Transition Matrix Monte Carlo

Chapter 1

Introduction

Since the monumental work was done by Metropolis *et al* [40], the Monte Carlo (MC) simulation has become a powerful tool in various fields of science, engineering and even in finance. The equilibrium thermodynamic properties of a variety of systems can be predicted from the canonical distribution generated by the Metropolis importance sampling. However, for systems that exhibit continuous phase transitons, the Metropolis algorithm becomes very inefficient due to the diverging autocorrelation time near a critical point(so called *critical slowing down* problem). For systems with first order phase transitions, exponential suppression of the tunneling between metastable states makes hard to use the Metropolis algorithm for simulations near the critical points. Furthermore, for systems with rough potential energy landscapes as in spin glasses, polymers and proteins, the traditional Metropolis type simulations suffer from the severe trapping in a potential energy minimum for large numbers of simulation steps resulting in an extreme inefficiency [43, 10].

For lattice spin systems with continuous phase transitions, the critical slowing down was overcome by the cluster algorithm in which a group of spins(called a *cluster*) is formed and flipped at once insted of a single spin flip[59, 69]. To resolve the severe trapping problems occuring in the simulations for systems with rugged energy landscapes, the replica exchange method(sometimes called parallel tempering) simulates multiple copies(or replicas) of the original system independently at different temperatures and allows the swapping of configurations between neighboring replicas with a specific probability[58, 36]. However, even with these breakthroughs, there is another problem when we need to evaluate a physical quantity as a function of temperature; to obtain the canonical average of an observable as a function of temperature varying over a significant range, due to the narrow width of the canonical distribution for a fixed temperature, multiple runs are required with the traditional methods such as Metropolis sampling and the cluster algorithm. As the system size

increases, the required number of different temperatures grows very fast and the selection of appropriate temperatures becomes extremely time consuming.

Instead of generating samples drawn from the canonical distribution, a number of MC methods taking different approaches were developed to directly attain the density of states (DOS) $g(E)$ which is the number of all microstates having energy E. The multiple histogram reweighting technique [19], multicanonical sampling [5, 6, 4], Wang-Landau algorithm[63, 64], broad histogram method[14, 13] and the transition matrix Monte Carlo method(TM)[68, 67](the detailed procedures of most of these methods are explained in the next chapter) are included in this category. Once the DOS $g(E)$ is given, the canonical average $\langle A \rangle$ of an observable $A(E)$ at any temperature T is calculated by

$$\langle A \rangle = \frac{1}{Z} \sum_{E} A(E) g(E) e^{-E/k_B T}, \tag{1.1}$$

where k_B is the Boltzmann constant and $Z = \sum_E g(E) e^{-E/k_B T}$ is the partition function. Especially the transition matrix Monte Carlo method yields a very accurate estimate of the DOS compared to other methods due to its unique features that will be explored in the next chapter.

Sometimes, it is required to express the DOS as a function of two variables. For instance, to obtain the Landau free energy F, which is useful to study phase transitions, it is necessary to acquire the joint DOS $g(E, q)$ which depends on both the energy E and a second variable q which is associated with the order parameter. The Landau free energy at a temperature T is then calculated by

$$F(q, T) = -k_B T \ln \left[\sum_{E} g(E, q) e^{-E/k_B T} \right]. \tag{1.2}$$

In the simulations for spin glasses (the details are presented in chapter 6), it is required to evaluate the probability distribution of the spin overlap q at temperature T, $P(q, T)$ which is given by

$$P(q, T) = \frac{1}{Z} \sum_{E} g(E, q) e^{-E/k_B T}, \tag{1.3}$$

where $Z = \sum_{E,q} g(E, q) \exp(-E/k_B T)$. In terms of the CPU time and the required memory, it is typically far more difficult to obtain an accurate estimate of $g(E, q)$ than

$g(E)$. Thus the development of an efficient algorithm is essential to obtain the joint DOS $g(E, q)$.

One of the recent trends in computer simulations is designing an optimal method for a specific problem of interest by modifying or combining numerous existing algorithms; Wnag-Landau TM method[50, 7], multicanonical TM method[35, 76, 77, 34], replica exchange multicanonical algorithm[17, 57] and replica exchange Wang-Landau[61, 62, 48] etc. Especially for complicated systems such as spin glasses, specially designed techniques for specific systems are used[38, 52, 31, 18, 60]. The detailed discussion about the development of various Monte Carlo algorithms may be found in [43, 10].

In this thesis, I employed the transition matrix Monte Carlo method to evaluate the densities of states for various systems with high accuracy. The evaluation of an accurate estimate of the DOS of a system of interest completely solves most of related physical problems once and for all. The accuracy of the DOS generated by the transition matrix Monte Carlo method depends on how the transition matrix is constructed; the entire region of the phase space of interest should be visited with appropriate frequencies and the information about all the allowed transitions must be collected to populate the transition matrix. To achieve this, the transition matrix Monte Carlo method can combine with various broad sampling techniques, *e.g.,* multicanonical sampling and Wang-Landau algorithm. The Metropolis algorithm with slowly varying temperature, which is called *regulated temperature method*, can also be adopted to construct the transition matrix [27, 73]. The aim of this thesis is to develop efficient transition matrix simulation methods for complex systems(*e.g.,* spin glasses) that enable one to construct the transition matrix from which the DOS is calculated with high accuracy.

The theoretical basis of the transition matrix Monte Carlo method together with the explanation of related algorithms is presented in chapter 2. The regulated temperature method is explained in the context of the two-dimensional(2D) Ising model in chapter 3. The optimization of the temperature schedule of the regulated temperature method is also discussed. In chapter 4, the construction of the transition matrix through the multicanonical iterations is introduced and its performance is demonstrated in the applications to the 2D Ising model and the 2D 10-state Potts model. In chapter 5, the renormalized sampling idea, which utilizes the result for a small system to produce an accurate initial estimate of the DOS for a large system, is introduced and the dramatic increase of the simulation speed is demonstrated in the context of the 2D Ising model. The comparison of the CPU times of different simulation methods is also presented. In chapter 6, as an efficient and accurate method to obtain the joint DOS, the bivariate multicanonical transition matrix Monte Carlo method is introduced; the transition tensor is constructed through the bivariate multicanonical iteration procedure in this method. The results in the applications of

this method to the Ising model, Potts model and Ising spin glass are presented. Especially the possibility of the existence of a nonzero temperature phase transition in the 2D Ising spin glass is discussed. Finally, the summary and conclusions including comments on the future work are presented in chapter 7.

Chapter 2

Transition Matrix Monte Carlo Methods

2.1 Markov Chain Monte Carlo Simulations

A stochastic process is a set of random variables $\{X_n : n = 1, 2, 3, \cdots\}$. The set of values-usually possible states of a system of interest-that X_n can take forms the state space Ω. If the states are denoted by by nonnegative integers, $\Omega = \{0, 1, 2, 3, \cdots\}$. Let's suppose

$$P(X_{n+1} = j | X_n = i, X_{n-1} = i_{n-1}, \cdots, X_o = i_o) = P(X_{n+1} = j | X_n = i) \equiv W_{ij}, \qquad (2.1)$$

where W_{ij} is dependent on i and j, but independent of n. Then this stochastic process is called *Markov chain*. W_{ij} is the probability that the process will make a transition to state j given it is in state i. The matrix $\mathbf{W}$ constructed by W_{ij}, which is called the *transition matrix* (TM), contains all the essential features of the Markov chain and governs the whole process. Since a transition to some state should be made in any case,

$$\sum_j W_{ij} = 1. \qquad (2.2)$$

Let $\mathbf{p}^{(0)}$ be the initial probability distribution of states, i.e., $p_i^{(0)} = P(X_0 = i)$, then

$$P(X_n = j) = \sum_i p_i^{(0)} (\mathbf{W}^n)_{ij} \equiv p_j^{(n)}. \qquad (2.3)$$

More compactly this can be written as

$$\mathbf{p}^{(n)} = \mathbf{p}^{(0)} \mathbf{W}^n, \qquad (2.4)$$

where $\mathbf{p}^{(n)} = (p_o^{(n)}, p_1^{(n)}, p_2^{(n)}, \cdots)$ is the probability distribution of states in n steps starting in a state drawn from $\mathbf{p}^{(0)}$. If for all i and j, $(\mathbf{W}^n)_{ij} > 0$ for some finite n, the Markov chain is called *irreducible*. This means the process can go from any state to any state in an irreducible Markov chain. For any state i, if $(\mathbf{W}^n)_{ii} > 0$ for some finite n, the Markov chain is called *positive recurrent*. If the recurrence is not periodic, the Markov chain is called *aperiodic*. For any Markov chain which is irreducible, positive recurrent and aperiodic,

$$\lim_{n\to\infty} (\mathbf{W}^n)_{ij} \equiv W_{ij}^{\infty} \tag{2.5}$$

exists and is independent of i [49]. This means the columns of $\mathbf{W}^\infty$ are constant vectors. Let's define $\mathbf{\Pi} = (\pi_0, \pi_1, \pi_2, \cdots)$ where $\pi_j = W_{ij}^{\infty}$. Note that $\sum_j \pi_j = 1$ is automatically satisfied. Then, $\mathbf{\Pi}$ is the unique normalized solution of the following equation:

$$\mathbf{\Pi} = \mathbf{\Pi}\mathbf{W} \quad \text{or} \quad \pi_j = \sum_i \pi_i W_{ij}. \tag{2.6}$$

In other words, $\mathbf{\Pi}$ is the normalized left eigenvector of $\mathbf{W}$ with unit eigenvalue. Once $\mathbf{\Pi}$ is established, from the Eq. (2.4), for any m, the probability distribution in m steps is $\mathbf{\Pi}\mathbf{W}^m = (\mathbf{\Pi}\mathbf{W})\mathbf{W}^{m-1} = \mathbf{\Pi}\mathbf{W}^{m-1} = \cdots = \mathbf{\Pi}$. Thus $\mathbf{\Pi}$ is called the *stationary or invariant distribution* of the Markov chain. The stationary distribution is independent of the initial distribution upto the normalization constant because $\mathbf{p}^{(\infty)} = \lim_{n\to\infty} \mathbf{p}^{(n)} = \lim_{n\to\infty} \mathbf{p}^{(0)}\mathbf{W}^n = \mathbf{p}^{(0)}\mathbf{W}^\infty = \left(\sum_i p_i^{(0)}\right)\mathbf{\Pi}$. The interpretation of π_j is the long run proportion of time that the Markov chain is in state j. From Eq. (2.2) and Eq. (2.6), the following relation is derived:

$$\sum_i \pi_j W_{ji} = \sum_i \pi_i W_{ij} \tag{2.7}$$

This is called the *global balance* of a stationary Markov chain. This can be automatically satisfied if we require

$$\pi_j W_{ji} = \pi_i W_{ij}, \tag{2.8}$$

which is called the *detailed balance* condition. Any stationary Markov chain that satisfies the detailed balance condition is called *reversible*.

In a Markov chain Monte Carlo simulation, by the Markov process, a sequence of states $X_0, X_1, X_2, \cdots$, whose stationary distribution is a desired $p_i = P(X = x_i)$, is generated. Then the expectation value of $f(X)$ is simply evaluated by

$$Exp(f(X)) = \sum_i f(x_i)p_i = \lim_{n\to\infty} \frac{\sum_{j=1}^n f(X_j)}{n} \approx \frac{\sum_{j=1}^N f(X_j)}{N} \quad \text{for large} N \tag{2.9}$$

To accomplish this, the transition probabilities W_{ij} should be properly designed. First we need to select the transition matrix Q of any irreducible, positive recurrent and aperiodic Markov chain. Next define the transition probabilities in the following way [49]:

$$\begin{aligned} W_{ij} &= Q_{ij}\alpha(i \to j) \quad for\ i \neq j \\ W_{ii} &= Q_{ii} + \sum_{k \neq i} Q_{ik}(1 - \alpha(i \to k)), \end{aligned} \tag{2.10}$$

where $\alpha(i, j)$ is determined by requiring the satisfaction of the detailed balance condition. If we set

$$\alpha(i \to j) = \min\left(\frac{p_j Q_{ji}}{p_i Q ij}, 1\right), \tag{2.11}$$

we obtain

$$p_j W_{ji} = p_i W_{ij}. \tag{2.12}$$

In the Markov chain Monte Carlo simulations, usually Q_{ij} is called the probability to propose a transition from state i to state j and $\alpha(i \to j)$ is called the *acceptance probability*. In many cases, $Q_{ij} = Q_{ji}$, then

$$\alpha(i \to j) = \min\left(\frac{p_j}{p_i}, 1\right). \tag{2.13}$$

Thus the acceptance probability can be constructed only by the target distribution p_i. If the Boltzmann distribution $p_i = \exp(-\beta E(i))/Z$ is desired, the acceptance probability becomes

$$\alpha(i \to j) = \min\left(\exp\left[-\beta(E(j) - E(i))\right], 1\right). \tag{2.14}$$

This is the well-known *Metropolis algorithm* [40]. If N_s samples are drawn from $p_i = \exp(-\beta E(i))/Z$, then $\sum_{k=1}^{N_s} O_{i_k} \approx \sum_j N_s p_j O_j \approx N_s \langle O \rangle$. Thus

$$\langle O \rangle \approx \frac{1}{N_s} \sum_{k=1}^{N_s} O_{i_k}, \tag{2.15}$$

where $\langle O \rangle$ is the canonical average of an observable O. Even with N_s samples drawn from a non-Boltzmann distribution p_i,

$$\langle O \rangle \approx \frac{\sum_{k=1}^{N_s} \frac{O_{i_k}}{p_{i_k}} \exp(-\beta E(i_k))}{\sum_{k=1}^{N_s} \frac{1}{p_{i_k}} \exp(-\beta E(i_k))}. \tag{2.16}$$

More rigorous and detailed explanation of the Markov chains and the Markov chain Monte Carlo simulations can be found in [49, 43].

2.2 Simulation Methods for Density of States

2.2.1 Density of States

In a Markov chain Monte Carlo simulation for a physical system, the state space Ω consists of all possible configurations or microstates of the system. For example, the state space of the Ising model of N spins consists of 2^N different configurations. Any macrostate (usually we are interested in macrostates) has degeneracy in general. In other words, many different microstates can have the same value of a macrostate variable. The degeneracy of energy E which is denoted by $g(E)$ is called the density of states (DOS). If a probability distribution of the configurations is written as $p_i = f(E(C_i))$, where C_i is the ith configuration and $E(C_i)$ is the energy of the configuration, the probability distribution of energy $p(E)$ is

$$p(E) = \sum_{i \in E} f(E(C_i)) = g(E) f(E). \tag{2.17}$$

From Eq. (2.13), if we set

$$\alpha(i \to j) = \min\left(\frac{f(E(C_j))}{f(E(C_i))}, 1\right), \tag{2.18}$$

the stationary energy distribution function becomes

$$p(E) \propto g(E) f(E). \tag{2.19}$$

In a Metropolis algorithm, $f(E(C_i)) = \exp(-\beta E(C_i))/Z$, $p(E) = g(E)\exp(-\beta E)/Z$ and the partition function Z is

$$Z = \sum_i \exp(-\beta E(C_i)) = \sum_E g(E)\exp(-\beta E). \tag{2.20}$$

The canonical average of an observable O is

$$\langle O \rangle = \frac{1}{Z} \sum_E O(E) g(E) \exp(-\beta E). \tag{2.21}$$

Once the DOS $g(E)$ is given, the partition function Z is readily calculated by the above equation and most essential physical quantities can be calculated as functions of temperature from the partition function. Thus if a simulation method which can produce the DOS with high accuracy is available, we can solve many problems once and for all.

The DOS can not be obtained directly from the Metropolis algorithm or any other canonical sampling methods. Even though it is possible to determine the DOS by the unweighting method (multiplying $\exp(\beta E)$ to $p(E)$), the simulation should be performed multiple times at different temperatures which must be judiciously selected to cover the whole energy region of interest since the Boltzmann distribution at a fixed temperature is narrow. This is no doubt a very tedious job especially for large systems. Furthermore, the Metropolis algorithm suffers from a so-called *critical slowing down* in the simulations for systems that exhibit phase transitions due to the divergence of the correlation time or the exponential suppression of the tunnelling between meta stable states at the critical point. During the last a few decades, various simulation methods have been developed to obtain the DOS from a single simulation. A few of them which are relevant to this thesis are presented in the following subsections.

2.2.2 Multicanonical Algorithm

In 1991, B. A. Berg and T. Neuhaus [5, 6, 4] proposed the multicanonical sampling method to resolve the problems of the canonical sampling mentioned briefly in the previous subsection. The entropic sampling which was introduced by J. Lee [33] is almost identical to the multicanonical sampling. In the multicanonical simulation, a random walk in the energy space is realized by the non-Boltzmann weight factor. By the random walk, any energy barrier can be overcome and the trapping in a local energy minimum can be avoided. The canonical average of any physical observable can be obtained at any desired temperature from the multicanonical ensemble formed by the single multicanonical simulation.

From Eq. (2.18) and (2.19), if we set

$$f(E) = \frac{1}{g(E)}, \tag{2.22}$$

the acceptance probability is

$$\alpha(i \to j) = \min\left(\frac{g(E(C_i))}{g(E(C_j))}, 1\right) \quad \text{or} \quad A_{acc} = \min\left(\frac{g(E_{old})}{g(E_{new})}, 1\right), \tag{2.23}$$

and the stationary energy distribution function becomes

$$p(E) \propto g(E)f(E) = constant. \tag{2.24}$$

Thus the energy histogram $H(E)$ of the visited states by the random walker is expected to be flat. Since $H(E) \propto p(E) = g(E)f(E)$, the DOS can be written as $g(E) \propto H(E)f^{-1}(E)$.

From Eq. (2.21), the calculation of the canonical average of an observable O from the multicanonical ensemble with the histogram $H(E)$ can be done by

$$\langle O \rangle \approx \frac{\sum_E O(E) H(E) f^{-1}(E) \exp(-\beta E)}{\sum_E H(E) f^{-1}(E) \exp(-\beta E)}. \tag{2.25}$$

In an actual multicanonical simulation, however, $g(E)$ whose reciprocal is the multicanonical weight factor is not known *a priori*. It is determined by an iterative way. The multicanonical iteration procedure to determine the DOS $g(E)$ can be summarized as the following table:

---

1. Choose energy range $E_{min} \leq E \leq E_{max}$ and the number of MCS per iteration N_{it}.

2. Set $g(E) = 1$ and $H(E) = 1$ for all energy bins.

3. Select the initial configuration C_1 and start the simulation.

4. From the current configuration with E_{old} make a small random change to generate a new configuration with E_{new}.

5. Accept the transition to the new configuration with the probability
   $A_{acc} = \min\left(\frac{g(E_{old})}{g(E_{new})}, 1\right)$

6. If the proposed transition is accepted, set $H(E_{new}) = H(E_{new}) + 1$, if rejected, set $H(E_{old}) = H(E_{old}) + 1$.

7. If N_{it} MCS is reached, update $g(E)$ by $g(E) = g(E)H(E)$, and set $H(E) = 1$.

8. Repeat from 3 to 7 until the configuration with E_{min} is visited.

Table 2.1: Multicanonical iteration procedure to determine $g(E)$

After the determination of the estimate of $g(E)$ from the above iteration procedure (sometimes this procedure is called *learning run*), the estimate of $g(E)$ is used in a long *production run* during which the histogram $H(E)$ of the multicanonical ensemble is record.

Using Eq. (2.25), the canonical average of an observable O is calculated at any desired temperature. In a typical multicanonical simulation, the DOS $g(E)$ is obtained as a byproduct in some sense. Usually the accuracy of $g(E)$ obtained in the multicanonical iteration procedure is not very high.

The procedure described in Table 2.1 is the simplest form of the multicanonical algorithm. This is simple and works well for small systems. However, this suffers from unacceptable slowing down in real situations where we need to deal with large systems [3]. The slowing down is caused by the following simple update scheme (this is called *histogram update* scheme in this thesis):

$$g^{(k+1)}(E) = g^{(k)}(E)H^{(k)}(E), \tag{2.26}$$

where $g^{(k)}(E)$ is the estimate of the DOS used in the kth iteration and $H^{(k)}(E)$ is the histogram of the visited states during the kth iteration. If we define $S^{(k)}(E) = \ln g^{(k)}(E)$, the histogram update scheme becomes

$$S^{(k+1)}(E) = S^{(k)}(E) + \ln H^{(k)}(E), \tag{2.27}$$

which is mostly used because $g(E)$ contains usually huge numbers having very large number of digits. Let's suppose the sampled region is down to $E^{(k)}_{min}$ in the kth iteration. Then for $E < E^{(k)}_{min}$, $g^{(k+1)}(E) = g^{(k)}(E)$ since still $H^{(k)}(E) = 1$. This means all transition proposals are accepted (recall the acceptance rule $A_{acc} = \min\left(\frac{g(E_{old})}{g(E_{new})}, 1\right)$). In a simulation for a spin lattice system with N spins with the single-spin-flip dynamics, in the low energy region, typically

$$\frac{g(E_{i-1})}{g(E_i)} \sim \frac{1}{N}, \tag{2.28}$$

which implies about N spin flip trials are required to realize the transition from E_i to E_{i-1}. This is the reason why $H^{(k)}(E)$ spreads at extremely slow pace in the low energy region for large systems.

To reduce the slowing down problem, B. A. Berg *et. al.* [5, 6, 3] introduced parameters $\beta(E)$ and $\alpha(E)$ such that

$$S^{(k)}(E) = \beta^{(k)}(E)E - \alpha^{(k)}(E). \tag{2.29}$$

If we set $k_B = 1$, $S(E) = \ln g(E)$ is the microcanonical entropy. From the Helmholtz free energy $F = E - TS$,

$$S = \frac{1}{T}E - \frac{F}{T}. \tag{2.30}$$

Thus the parametrization Eq. (2.29) has a physical basis. To set up the update scheme for $\beta^{(k)}$ and $\alpha^{(k)}$, we have to note

$$\beta = \frac{\partial S}{\partial E}, \qquad \frac{\partial \alpha}{\partial E} = \frac{\partial \beta}{\partial E}E, \tag{2.31}$$

where the second equation is derived by differentiating $S = \beta E - \alpha$ with respect to E. If the bin width is ε, from the above equations

$$\beta(E) = \frac{S(E+\varepsilon) - S(E)}{\varepsilon}, \qquad \alpha(E) - \alpha(E-\varepsilon) = \left[\beta(E) - \beta(E-\varepsilon)\right] E. \tag{2.32}$$

Use the above equations to derive

$$\begin{aligned} \beta^{(k+1)}(E) &= \frac{S^{(k+1)}(E+\varepsilon) - S^{(k+1)}(E)}{\varepsilon} \\ &= \frac{S^{(k)}(E+\varepsilon) + \ln H^{(k)}(E+\varepsilon) - S^{(k)}(E) - \ln H^{(k)}(E)}{\varepsilon} \\ &= \beta^{(k)}(E) + \frac{1}{\varepsilon}\ln\frac{H^{(k)}(E+\varepsilon)}{H^{(k)}(E)} \end{aligned} \tag{2.33}$$

and

$$\alpha^{(k)}(E-\varepsilon) = \alpha^{(k)}(E) - \left[\beta^{(k)}(E) - \beta^{(k)}(E-\varepsilon)\right]. \tag{2.34}$$

After setting $\alpha^{(k)}(E_{max}) = 0$, the above equation can be used recursively to obtain $\alpha^{(k)}(E)$ for $E < E_{max}$. It should be noted that Eq. (2.33) can be used only for the region where $H^{(k)}(E)$ is reliable. For the region where $H^{(k)}(E)$ is unreliable, B. A. Berg *et. al.* used the following rule:

$$\beta^{(k+1)}(E) = \begin{cases} \beta^{(k)}(E) & \text{for } E \geq E^{(k)}_{median} \\ \beta^{(k+1)}(E^{(k)}_{cutoff}) & \text{for } E < E^{(k)}_{cutoff} \end{cases} \tag{2.35}$$

where $E^{(k)}_{median}$ is the median of $H^{(k)}(E)$ and $E^{(k)}_{cutoff} < E^{(k)}_{median}$ is the energy cutoff that is selected such that $H^{(k)}(E)$ is unreliable for $E < E^{(k)}_{cutoff}$ and the temperature is kept constant for $E < E^{(k)}_{cutoff}$ in the $(k+1)$th iteration. This recursive update with parameters β and α, which is called *parametrization update* scheme in this thesis, enables the histogram to spread toward E_{min} way faster than the histogram update scheme.

The parametrization update scheme can be interpreted as a *linear extrapolation* of $S^{(k)}$ from the well sampled region to the poorly sampled region; $S = \beta E - \alpha$ is a straight line if β and α are constants. A linear extrapolations means the Metropolis sampling with the fixed inverse temperature $\beta^{(k)}(E^{(k)}_{cutoff})$ is performed in the region $E < E^{(k)}_{min}$. Since the with of the Boltzmann distribution is of order $\sqrt{N}$, this amount of expansion toward E_{min} is expected in each iteration. The linear extrapolation can be seen in Fig. 2.1 which displays a few estimates of the DOS used in the multicanonical simulation for a 16×16 Ising model with the parametrization update scheme. The first visit of the ground state was made in the 7th iteration with the parametrization update scheme whereas 13 iterations were required to make a first visit to the ground state with the histogram update scheme. For larger systems, the difference is expected to be huge. The gradual changes of the histograms in the multicanonical iteration with each update scheme are shown in Fig. 2.2 and Fig. 2.3.

The problem of the parametrization update scheme is its complexity compared to the attractive simplicity of the histogram update scheme. Especially, it is not easy to choose appropriate $E^{(k)}_{cutoff}$. In the low energy region, slight error in the parameters causes a severe trapping because the linear extrapolation can not fit well any more. As an example, see Fig. 2.4; the exact $S(E) = \ln g(E)$ becomes zigzag near the ground state. In 3D, the situation becomes worse as shown in Fig. 2.5. One remedy that I used in my simulations is to go back to the histogram update scheme right after the first visit of the ground state and perform a few more iterations. Usually this eliminates the subtle problems involved with the parametrization update scheme.

For the parametrization update scheme, there is another important issue when it combines with the TMMC. As discussed in chapter 4, the gradual broadening of the sampling region in the multicanonical iteration procedure is well suited for the construction of the transition matrix. When the parametrization update scheme is used, even though it can speed up the multicanonical iteration procedure, the accuracy of the transition matrix is

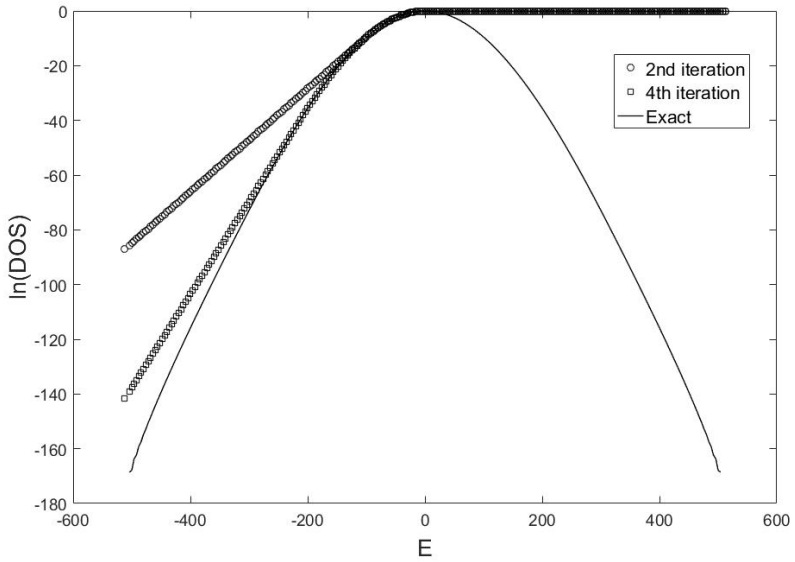

Figure 2.1: The evolution of the estimate of the DOS in the multicanonical iteration with the parametrization update scheme for 16×16 Ising model. The circle is $S^{(2)}(E)$, the square is $S^{(4)}(E)$ and the solid line is the exact curve.

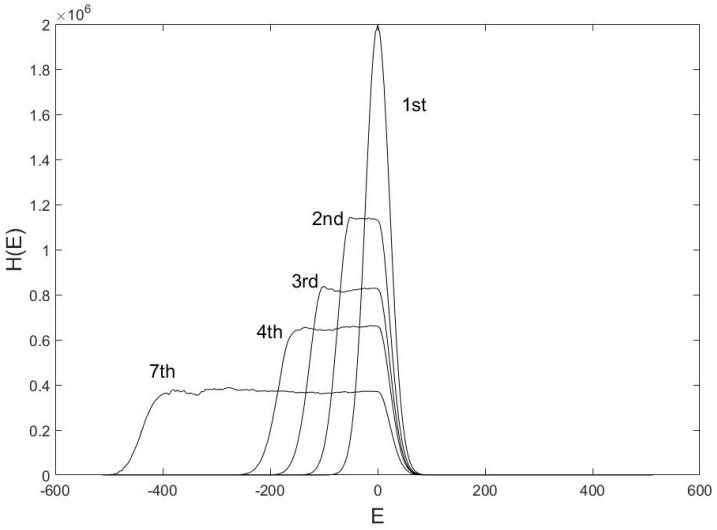

Figure 2.2: The histograms in several iteration stages during the multicanonical iteration for a 16×16 Ising model with the parametrization update scheme.

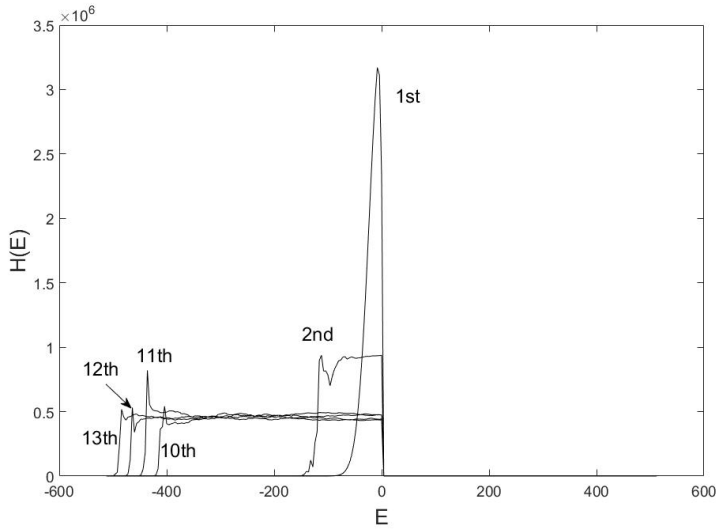

Figure 2.3: The histograms in several iteration stages during the multicanonical iteration for a 16×16 Ising model with the histogram update scheme.

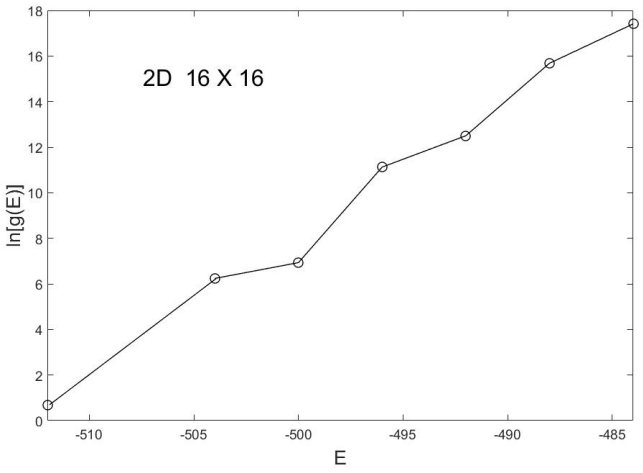

Figure 2.4: The exact DOS of a 2D 16×16 Ising model near the ground state.

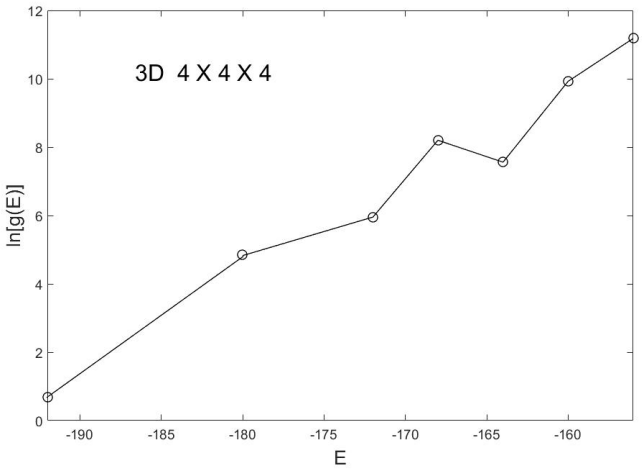

Figure 2.5: The exact DOS of a 3D $4 \times 4 \times 4$ Ising model near the ground state. The exact DOS is from Pearson's calculation [47].

lower than when the histogram update scheme is used probably because the fast broadening causes insufficient sampling for all possible transitions. For this reason, I adopted the histogram update scheme in the multicanonical transition matrix Monte Carlo method which is discussed in chapter 4.

2.2.3 Wang-Landau Algorithm

Wang and Landau[63, 64] introduced a new iteration method to determine the DOS of a system in 2001. Due to its simplicity, it has drawn wide attention of researchers and become very popular in various fields. The same acceptance rule (Eq. (2.23)) as the one used in the multicanonical sampling is adopted, but the convergence of the DOS $g(E)$ is determined by monitoring the flatness of the energy histogram $H(E)$ of the visited states. The outline of the iteration procedure is described in the following table:

In most simulations, $f_1 = e^1, f_{min} = \exp(10^{-8})$. If the minimum entry of $H(E)$ is not smaller than 80% of the mean of $H(E)$, it is considered reasonably flat. More specifically the flatness criterion is

$$\frac{\min\left[H(E)\right]}{\langle H(E)\rangle} > \gamma, \quad 0 < \gamma < 1.$$

1. Choose the desired energy range $E_{min} \leq E \leq E_{max}$.

2. Set $g(E) = 1$ and $H(E) = 0$ for all energy bins. Set the initial modification factor $f = f_1$.

3. Select the initial configuration C_1 and start the simulation.

4. From the current configuration with E_{old} make a small random change to generate a new configuration with E_{new}.

5. Accept the transition to the new configuration with the probability
$$A_{acc} = \min\left(\frac{g(E_{old})}{g(E_{new})}, 1\right)$$

6. If the proposed transition is accepted, set $g(E_{new}) = g(E_{new})f$, $H(E_{new}) = H(E_{new}) + 1$. If rejected, set $g(E_{old}) = g(E_{old})f$, $H(E_{old}) = H(E_{old}) + 1$.

7. If the flatness of $H(E)$ satisfies the predefined criterion, set $f = \sqrt{f}$, $H(E) = 0$.

8. Repeat from 3 to 7 while $f \leq f_{min}$.

Table 2.2: Wang-Landau iteration procedure to determine $g(E)$

If higher accuracy is required, γ can be increased, e.g., upto 0.9 (or 90%). The above flatness criterion has a subtle problem when there are empty bins. The above criterion can never be satisfied with empty bins since $\min[H(E)]$ is always zero. If the bin width is fixed, which is the most common case, empty bins can exist in the simulations for lattice spin systems. For example, in a simulation for the 2D Ising model, the bin right next to the ground state energy is empty. In a simulation for the spin glasses, the empty bins are not even known a priori. To deal with this problem, the following criterion can be used instead :

$$\frac{\max[H(E)]}{\langle H(E)\rangle} < \gamma, \quad \gamma > 1,$$

where γ is typically close to one, e.g., 1.2 in many cases. The DOS $g(E)$ obtained in the Wang-Landau method is usually accurate enough to be directly used to calculate the

partition function and the canonical averages of physical quantities by Eq. (2.20) and Eq. (2.21).

2.2.4 Broad Histogram Method

A New random walk dynamics based on the microcanonical averages of the numbers of possible moves was introduced by de Oliveira et al. [14, 13] in 1996. This method is called *broad histogram method* because the histogram of the samples taken by this method is broad. A minor systematic error in the original formulation was pointed out by Wang [66]. A microcanonical ensemble with energy E is formed by all microstates having the same energy E. Let's denote a microstate by σ. The microcanonical average of a quantity A is defined as

$$\langle A \rangle_E = \frac{1}{g(E)} \sum_{\sigma \in E} A(\sigma) \tag{2.36}$$

Let's suppose whenever a move from σ to σ' is possible, the reverse move is also possible (*microreversibility*). For lattice spin systems, single-spin-flip dynamics satisfies this. If the total number of possible moves from σ with E to σ' with $E' = E + \Delta E$ is $N(\sigma, \Delta E)$ and the total number of the reverse moves is $N(\sigma', -\Delta E)$, due to the microversibility,

$$\sum_{\sigma \in E} N(\sigma, \Delta E) = \sum_{\sigma' \in E'} N(\sigma', -\Delta E) \tag{2.37}$$

Using the microcanonical averages, this can be rewritten as

$$g(E) \langle N(\sigma, \Delta E) \rangle_E = g(E') \langle N(\sigma', -\Delta E) \rangle_{E'}. \tag{2.38}$$

This is called *broad histogram relation*. From this relation, the random walk acceptance rule (Eq. (2.23)) can be written as

$$A_{acc} = \min \left(\frac{g(E)}{g(E')}, 1 \right) = \min \left(\frac{\langle N(\sigma', -\Delta E) \rangle_{E'}}{\langle N(\sigma, \Delta E) \rangle_E}, 1 \right), \tag{2.39}$$

which makes it possible to realize a random walk in the energy space without any knowledge of $g(E)$ by keeping track of $\langle N(\sigma, \Delta E) \rangle_E$ and $\langle N(\sigma', -\Delta E) \rangle_{E'}$ and updating them in every move. In the early stage of the simulation $\langle N(\sigma, \Delta E) \rangle_E$ can be zero if σ' is never visited. In such a case, the move is unconditionally accepted. Keeping track of the microcononical averages in every move requires a significant computational cost and causes slowing down.

2.3 Transition Matrix Monte Carlo Methods

2.3.1 Formulation of the Method

Anderson et al. [16] used the transition probabilities first in the Monte Carlo simulations. Smith and Bruce [55] used the transition probabilities as an efficient way of obtaining a good approximation to the multicanonical weight factor. Fitzgerald et al. [21] took a slightly different approach to utilize the transition probabilities to reduce the variance compared to the method of Smith and Bruce. J. S. Wang and his colleagues [68, 67] generalized and refined the method that incorporate the transition matrices in the Monte Carlo simulations. Since then various transition matrix Monte Carlo (TMMC) methods have been developed by employing broad sampling techniques in widespread applications [50, 7, 23, 76, 77].

The transition matrix $\mathbf{W} = (W_{ij})$ introduced in section 2.1 is formed by the *microstate* transition probabilities. Since the macrostate observables such as energy and magnetization are of our interest, the macrostate transition matrix must be defined. In a Markov chain Monte Carlo simulation, the *macrostate* transition matrix $\mathcal{T}$ (from here on, transition matrix refers to macrostate transition matrix unless otherwise mentioned) is defined such that its element $\mathcal{T}_{IJ}$ coincides with the probability that a Markov chain evolves from a macrostate I with energy E_I to a macrostate J with energy E_J in a single Monte Carlo step. Then from the microstate transition probability W_{ij} and the DOS $g(E)$,

$$\mathcal{T}_{IJ} = \frac{1}{g(E_I)} \sum_{i \in I} \sum_{j \in J} W_{ij}. \tag{2.40}$$

From $\sum_{j \in \Omega} W_{ij} = 1$, where the summation runs over the entire configuration space Ω,

$$\begin{aligned} \sum_J \mathcal{T}_{IJ} &= \frac{1}{g(E_I)} \sum_J \left(\sum_{i \in I} \sum_{j \in J} W_{ij} \right) = \frac{1}{g(E_I)} \sum_{i \in I} \left(\sum_J \sum_{j \in J} W_{ij} \right) \\ &= \frac{1}{g(E_I)} \sum_{i \in I} \left(\sum_{j \in \Omega} W_{ij} \right) = \frac{1}{g(E_I)} \sum_{i \in I} 1 = \frac{1}{g(E_I)} g(E_I) = 1. \end{aligned}$$

Thus we derive,

$$\sum_J \mathcal{T}_{IJ} = 1. \tag{2.41}$$

The probability that the Markov chain occupies a state I at the $(k+1)$st step is related to the corresponding occupation probabilities at the kth step by

$$P^{(k+1)}(E_J) = \sum_I P^{(k)}(E_I)\mathcal{T}_{IJ}. \tag{2.42}$$

The macrostate transition matrix $\mathcal{T}$ retains all the properties of the microstate transition matrix $\mathbf{W}$. Thus if $\lim_{n\to\infty} W_{ij}^n$ exists, then $\lim_{n\to\infty} \mathcal{T}_{IJ}^n$ exists. In the same way as explained in section 2.1, the stationary macrostate distribution $\mathcal{P}$ can be constructed from $\mathcal{T}^\infty$ (any row vector of $\mathcal{T}^\infty$ can be picked up for $\mathcal{P}$) so that it satisfies

$$\mathcal{P} = \mathcal{P}\mathcal{T}. \tag{2.43}$$

From Eq. (2.10) and (2.40) the explicit form of $\mathcal{T}$ is,

$$\mathcal{T}_{IJ} = \frac{1}{g(E_I)} \sum_{i\in I} \sum_{j\in J} Q_{ij}\alpha(i\to j), \tag{2.44}$$

where Q_{ij} is the probability to propose the microscopic transition from i to j and $\alpha(i\to j)$ is the acceptance probability as explained in section 2.1. If $Q_{ij} = Q_{ji}$ is assumed (this is satisfied in most Markov chain Monte Carlo simulations),

$$\frac{\mathcal{T}_{IJ}}{\mathcal{T}_{JI}} = \frac{g(E_J)}{g(E_I)} \frac{\sum_{i\in I}\sum_{j\in J}\alpha(i\to j)}{\sum_{i\in I}\sum_{j\in J}\alpha(j\to i)}. \tag{2.45}$$

If we further assume the following condition (unconditional acceptance),

$$\alpha(i\to j) = 1 \quad for\ all\ i, j, \tag{2.46}$$

the following relation is obtained:

$$\frac{\mathcal{T}_{\infty IJ}}{\mathcal{T}_{\infty JI}} = \frac{g(E_J)}{g(E_I)}, \tag{2.47}$$

where $\mathcal{T}_{\infty IJ}$ is sometimes called *infinite temperature transition matrix* because the unconditional acceptance is realized in the Metropolis algorithm at infinite temperature, i.e., $\beta = 0$ (however, this does not imply $\mathcal{T}_{\infty IJ}$ can be obtained only by the Metropolis algorithm at infinite temperature). The above relation looks similar to the broad histogram relation Eq. (2.38). Note

$$\mathcal{T}_{\infty E,E'} = \langle N(\sigma, E'-E)\rangle_E. \tag{2.48}$$

Because of this close relation, many researchers believe the root of TMMC goes down to the broad histogram method introduced by Oliveira et al. [14, 13]. From Eq. (2.41) and (2.47), we can derive

$$g(E_I) = \sum_J g(E_J)\mathcal{T}_{\infty JI}, \tag{2.49}$$

which means the DOS $g(E)$ is the left eigenvector with unit eigenvalue of $\mathcal{T}_\infty$. A big question is how to design a simulation that satisfies the unrealistic condition of Eq. (2.46) to produce the infinite temperature TM from which the DOS can be calculated by Eq. (2.47) and (2.49). Before answering this question, let's first figure out how to calculate the DOS from the TM.

2.3.2 Calculation of DOS from Transition Matrix

Suppose all information about the transitions occurred during the course of a simulation is stored in C_{IJ}. Then the estimate of the infinite temperature TM is

$$\tilde{\mathcal{T}}_{\infty IJ} = \frac{C_{IJ}}{D_I}, \tag{2.50}$$

where $D_I = \sum_K C_{IK}$. The use of Eq. (2.47) with the above estimate enables us to calculate the DOS $g(E)$. The simplest way is to use only neighbouring entries of $\tilde{\mathcal{T}}_{\infty IJ}$. With $g(E_1)$ given or set to a constant,

$$g(E_2) = \frac{\tilde{\mathcal{T}}_{\infty 12}}{\tilde{\mathcal{T}}_{\infty 21}} g(E_1), \quad g(E_3) = \frac{\tilde{\mathcal{T}}_{\infty 23}}{\tilde{\mathcal{T}}_{\infty 32}} g(E_2), \quad \cdots$$

The second method is to evaluate the best estimate of $g(E)$ with a multi-variable optimization procedure as described in [14, 67, 50]. If there are N_b energy bins, there are $N_b - 1$ unknown values of $g(E)$ and $N_b(N_b - 1)/2$ equations from Eq. (2.47). Thus this is an over-specified problem. Furthermore, the entries of $\mathcal{T}_\infty$ are not independent; they satisfy the following relations:

$$0 \le \mathcal{T}_{\infty IJ} \le 1, \quad \sum_J \mathcal{T}_{\infty IJ} = 1. \tag{2.51}$$

From the detailed balance condition, for any distinct I, J and K,

$$\mathcal{T}_{\infty IJ}\mathcal{T}_{\infty JK}\mathcal{T}_{\infty KI} = \mathcal{T}_{\infty JI}\mathcal{T}_{\infty IK}\mathcal{T}_{\infty KJ}, \tag{2.52}$$

which is called TTT identity. There are two possible optimization models for this situation. In the first model, the total variance with respect to $S_I = \ln g(E_I)$ is minimized;

$$\sigma_{tot}^2 = \sum_{IJ} \frac{\left(S_I - S_J + \ln \tilde{\mathcal{T}}_{\infty IJ}/\tilde{\mathcal{T}}_{\infty JI}\right)^2}{\sigma_{IJ}^2}, \tag{2.53}$$

where σ_{IJ}^2 is the variance of $\ln \tilde{\mathcal{T}}_{\infty IJ}/\tilde{\mathcal{T}}_{\infty JI}$. Its explicit form is

$$\sigma_{IJ}^2 = \frac{1}{C_{IJ}} + \frac{1}{D_I} + \frac{1}{C_{JI}} + \frac{1}{D_J}. \tag{2.54}$$

In the second model, the following is minimized to obtain the best estimate of $\mathcal{T}_\infty$:

$$\sum_{IJ} \frac{1}{\sigma_{IJ}^2} \left(\mathcal{T}_{\infty IJ} - \tilde{\mathcal{T}}_{\infty IJ}\right)^2. \tag{2.55}$$

The minimization is subject to the conditions given in Eq. (2.51) and (2.52).

The most straightforward way to find the best estimate of $g(E)$ from $\tilde{\mathcal{T}}_\infty$ is the method based on the existence of the stationary distribution under certain conditions which are usually satisfied in most simulations as discussed in section 2.1 (see Eq. (2.5) and (2.6)). The procedure is summarized in the following table:

This third method is called *repeated multiplication method* in this thesis. Since the left eigenvector of $\tilde{\mathcal{T}}_\infty$ with unit eigenvalue (left unit eigenvector) can be directly obtained from $\lim_{n\to\infty} \tilde{\mathcal{T}}_\infty^n$, this method is extremely simple. However, this procedure works only when the statistical quality of $\tilde{\mathcal{T}}_\infty$ is above certain level. If the statistics is not good enough, $\tilde{\mathcal{T}}_\infty^n \to 0$ as $n \to \infty$. In such a case, previously explained two methods can be applied to obtain $g(E)$.

2.3.3 Construction of TM by Accepted Transitions

In a Markov chain Monte Carlo simulation, since the stationary distribution is the left eigenvector of the TM with unit eigenvalue (left unit eigenvector), if the TM is constructed by all the *accepted* transitions in the course of the simulation, the stationary distribution can be calculated from the TM without taking any samples during the simulation. For the TM $\mathcal{T}$ constructed by the accepted transitions in the Metropolis algorithm at a fixed temperature T, if we find $\mathcal{P}$ such that $\mathcal{P} = \mathcal{P}\mathcal{T}$,

$$\mathcal{P}(E) \propto g(E) \exp(-E/T). \tag{2.56}$$

1. Normalize the estimate of TM : $\tilde{\mathcal{T}}_{\infty IJ} = \frac{C_{IJ}}{\sum_K C_{IK}}$.

2. Set $p(E) = 1$ for all energy bins. Calculate $p^n = p^{n-1}\tilde{\mathcal{T}}_\infty$.

3. Calculate $x =$ the sum of elements of $p^n - p^{n-1}$.

4. If $|x| < \epsilon$, where ϵ is the predefined positive small number, stop multiplication.

5. Set $\mathcal{P} = p^n$. Then $\mathcal{P}$ satisfies $\mathcal{P} = \mathcal{P}\tilde{\mathcal{T}}_\infty$ and $\mathcal{P} \propto g(E)$.

6. Normalize $\mathcal{P}$: $g(E) = \frac{g(E_1)}{\mathcal{P}_1}\mathcal{P}$, provided $g(E_1)$ is known.

Table 2.3: Determination of $g(E)$ by the Repeated Multiplication Method

From this equation, we obtain

$$g(E) \propto \mathcal{P}(E) \exp(E/T). \tag{2.57}$$

This implies that the DOS $g(E)$ can be obtained from the TM that is constructed by the accepted transitions in the Metropolis algorithm. The algorithm is not restricted to Metropolis; any canonical sampling method such as heat bath algorithm or cluster algorithm can be adopted to populate the TM. Since the canonical sampling methods have good convergence to its stationary distributions, the TM constructed in any one of these algorithms also has a good convergence character; the existence of $\lim_{n\to\infty} \mathcal{T}$ is guaranteed if reasonably large number of steps are taken to populate TM. Thus $\mathcal{P}$ can be readily calculated by the repeated multiplication method.

The normalized left unit eigenvector $\mathcal{P}$ of the TM constructed in the Metropolis sampling for the 32×32 Ising model at temperature $T = 3.0$ and the normalized histogram of samples taken during the simulation are plotted in Fig. 2.6. 2×10^5 samples were taken in every 32^2 spin flip trials (which is called one MCS). As expected, they are almost identical. The DOS obtained by the Eq. (2.57) is shown in Fig. 2.7. Near the critical temperature $T_c = 2.269$, due to long correlation time, cluster algorithm is more efficient in general. The results from the Wolff cluster algorithm for 32×32 Ising model at $T = 2.3$ are shown in Fig. 2.8 and Fig. 2.9. Samples were taken during 7×10^5 cluster spin flips. As in the Metropolis sampling, the normalized left unit eigenvector $\mathcal{P}$ of the TM is in great agreement with the

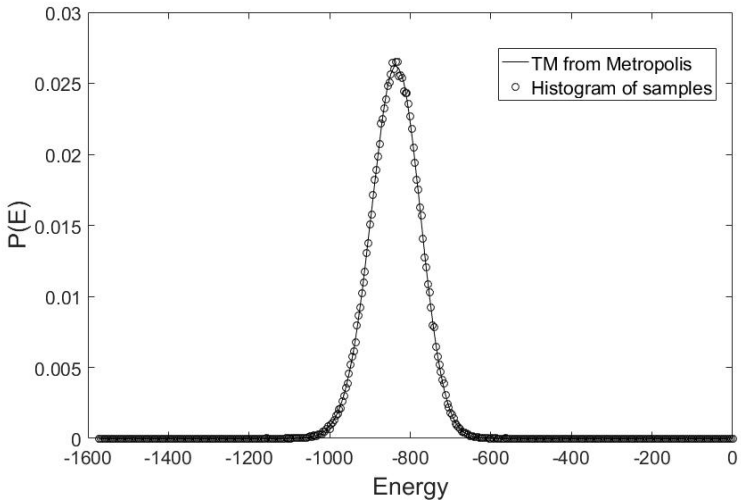

Figure 2.6: The solid line is the normalized left unit eigenvector $\mathcal{P}$ of the TM constructed in the Metropolis sampling for 32×32 Ising model at $T = 3.0$. The circle is the normalized histogram of the samples taken during the sampling.

histogram of samples in the Wolf cluster sampling. Note that the TM constructed in the single spin flip Metropolis algorithm at T and the TM constructed in the Wolff cluster spin flip algorithm at T have identical left unit eigenvector $\mathcal{P} \propto g(E) \exp(-E/T)$ even though they are totally different matrices. The exact DOS of the two dimensional (2D) Ising model was calculated by the Beale's method [2].

As shown in Fig. 2.7 and Fig. 2.9, the DOS's obtained from the canonical sampling methods are restricted in small region of the energy space due to the narrow Boltzmann distributions. To cover the entire energy region, the simulation should be performed multiple times at different temperatures. Temperatures must be chosen for the adjacent DOS's to have proper overlap. Fig. 2.10 shows the DOS covers the entire range of the energy of 32×32 Ising model obtained from the TM constructed in the Wolff cluster algorithm performed at 7 different temperatures. The DOS obtained in this method is so accurate that it is almost impossible to distinguish it from the the exact DOS. Since it is very difficult to obtain the correct location and height of the peak of the specific heat near the critical temperature T_c (the peak position is very sensitive to the estimate of the DOS), the calculation of the error in the specific heat is more stringent test of the accuracy of the DOS. The specific heat of the Ising model is evaluated by

$$C = k_B \beta^2 \left(\langle E^2 \rangle - \langle E \rangle^2 \right). \tag{2.58}$$

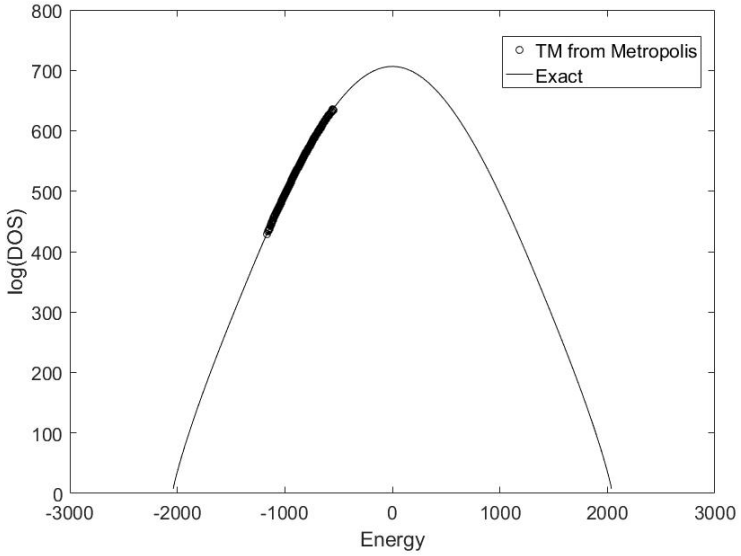

Figure 2.7: The circle is the DOS obtained from the TM constructed in the Metropolis sampling for 32×32 Ising model at $T = 3.0$. The solid line is the exact DOS.

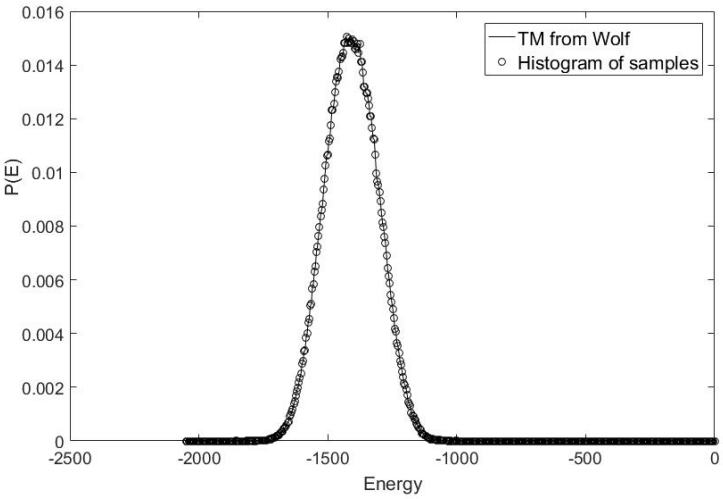

Figure 2.8: The solid line is the normalized left unit eigenvector $\mathcal{P}$ of the TM constructed in the Wolff cluster algorithm for 32×32 Ising model at $T = 2.3$. The circle is the normalized histogram of the samples taken during the sampling.

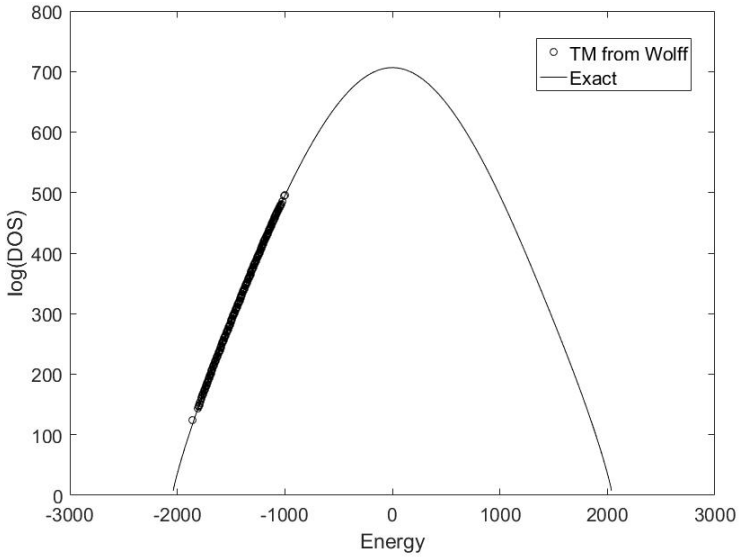

Figure 2.9: The circle is the DOS obtained from the TM constructed in the Wolff cluster algorithm for 32×32 Ising model at $T = 2.3$. The solid line is the exact DOS.

The relative error is defined as

$$\epsilon(C) = \frac{|C - C_{exact}|}{C_{exact}}. \tag{2.59}$$

The specific heat per spin is plotted in Fig. 2.11 with the inset of the relative error. Note the error is very low even near the peak. Furthermore this is the result of single simulation; the error can be lowered by taking average of multiple results. However, it costs a lot to attain this accuracy; long CPU time, additional efforts to select temperatures compared to other TMMC methods to be presented in what follows.

2.3.4 Construction of TM by Proposed Transitions

Now it is the time to answer the big question posed in the last part of subsection 2.3.1; how to design a simulation method to construct the TM with unconditional acceptance rule $\alpha(i \to j) = 1$. To find the answer, we need to note that a *proposed transition* in a simulation have valuable information about all possible transitions from the current state. As can be seen in Eq. (2.44), this information is essential to construct the TM. To obtain

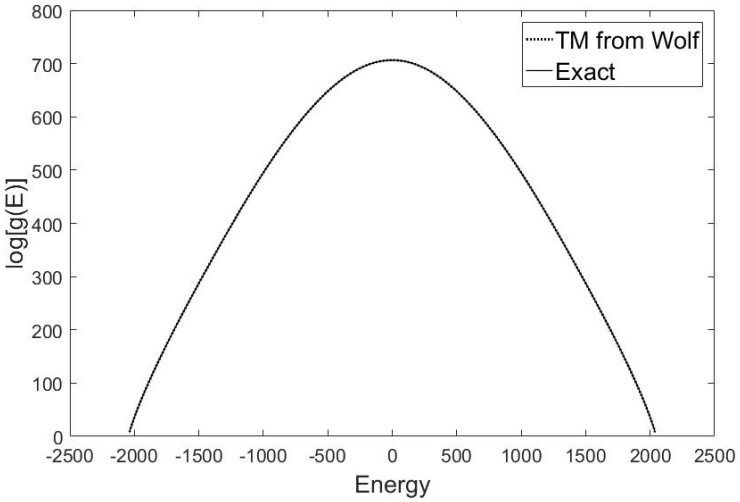

Figure 2.10: The dotted line is the logarithm of the DOS obtained from the TM constructed in the Wolff cluster algorithms for 32×32 Ising model at 7 different temperatures. The solid line is the logarithm of the exact DOS.

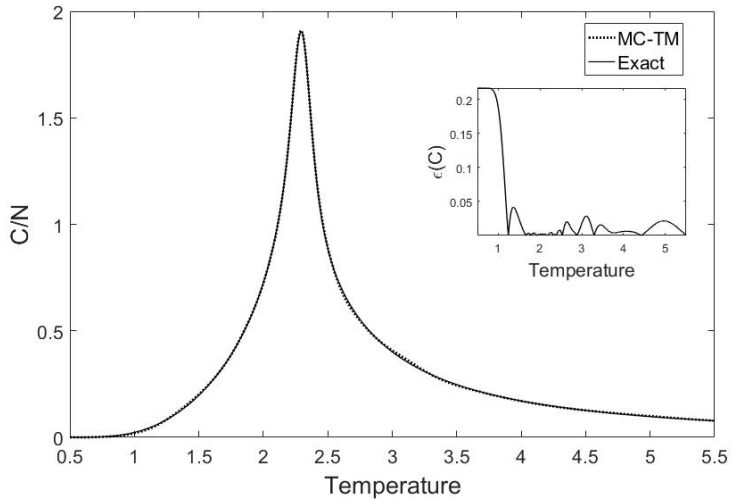

Figure 2.11: The dotted line is the specific heat per spin calculated by the the DOS obtained from the TM constructed in the Wolff cluster algorithms for 32×32 Ising model at 7 different temperatures. The solid line is the exact specific heat per spin. The inset shows the relative error at each each temperature.

a good estimate of $\mathcal{T}_{\infty IJ}$, it is required to visit all microstates $i \in I$ many times to record all possible transitions to $j \in J$. If we construct TM by the accepted transitions we lose some of (most of in some cases) the information about the allowed transitions because all proposed transitions are not accepted. Thus we have to populate the TM by the *proposed transitions* to make the most of the chosen simulation method. Moreover, if the TM (precisely C_{IJ} in an actual simulation) is updated by every proposed transition *regardless of the acceptance of it*, the TM is constructed as if $\alpha(i \to j) = 1$ even though the actual acceptance probability is not equal to one. Therefore, the estimate of $\mathcal{T}_\infty$ can be obtained in any simulation method by utilizing all the attempted transitions, i.e., *all the accepted and rejected transitions*, for the construction of the TM. The job of the algorithm with certain acceptance rule is steering the random walker and pushing it to the location in the configuration space where we want to collect the information on the possible transitions to construct the TM.

The DOS obtained from the TM constructed by the proposed transitions in the Metropolis algorithm for 16×16 Ising model at $T = 3.0$ is plotted in Fig. 2.12. Once the left unit eigenvector $\mathcal{P}$ of the TM is found, since $\mathcal{P} \propto g(E)$, multiplication of $\exp(E/T)$ is not required any more. Again note the range of $\mathcal{P}$ is restricted due to the narrow sampling region of the Metropolis algorithm. The Metropolis samplings were performed at 5 different temperatures to construct the TM that produces the DOS covering the entire energy bins as shown in Fig. 2.13. To check the accuracy of the DOS, I calculated the specific heat which is plotted in Fig. 2.14. Separate calculations of the DOS at each temperature and patching them up are not needed any more. Just adding up the TM's constructed from the simulations at different temperatures is enough to construct the final single TM from which the full range DOS is derived. This is a great advantage of the transition matrix Monte Carlo methods.

When the TM is constructed in the Metropolis algorithm, there is a close relation between the TM, $\mathcal{T}(\beta)$ constructed by the accepted transitions at $\beta = 1/T$ and the TM, $\mathcal{T}_\infty$ constructed by the proposed transitions. As discussed before, since

$$\mathcal{T}_{IJ} = \frac{1}{g(E_I)} \sum_{i \in I} \sum_{j \in J} Q_{ij} \alpha(i \to j),$$

and

$$\alpha(i \to j) = \min\left[\exp(-\beta(E_j - E_i), 1\right]$$

in the Metropolis algorithm,

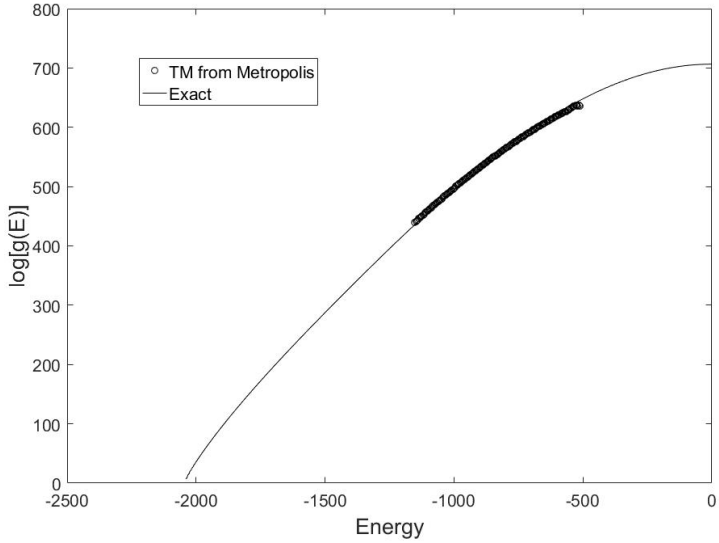

Figure 2.12: The dotted line is the logarithm of the DOS obtained from the TM constructed in the Metropolis algorithms for 16×16 Ising model at $T = 3.0$. The solid line is the logarithm of the exact DOS.

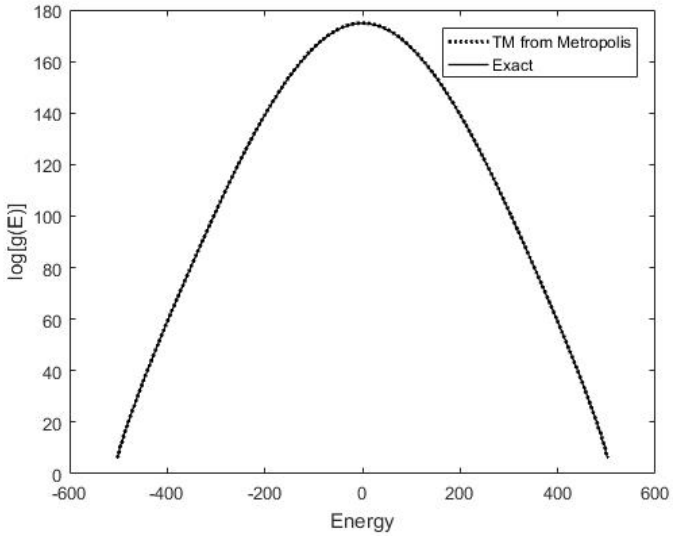

Figure 2.13: The dotted line is the logarithm of the DOS obtained from the TM constructed in the Metropolis algorithms for 16×16 Ising model at 5 different temperatures. The solid line is the logarithm of the exact DOS.

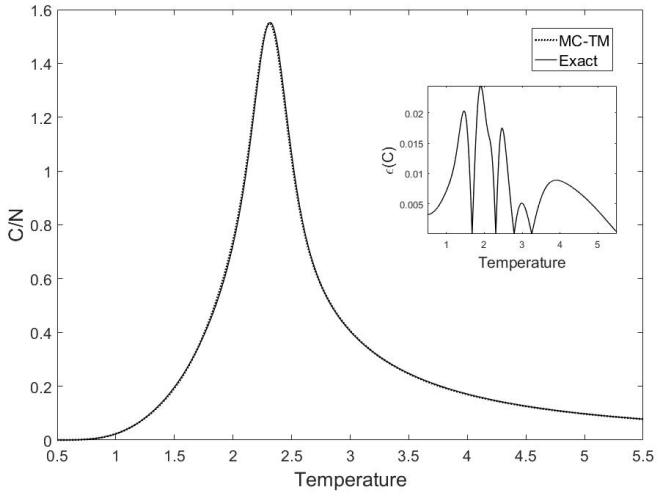

Figure 2.14: The dotted line is the specific heat per spin calculated by the the DOS obtained from the TM constructed in the Metropolis algorithms for 16×16 Ising model at 5 different temperatures. The solid line is the exact specific heat per spin. The inset shows the relative error at each each temperature.

$$
\begin{aligned}
&\mathcal{T}(\beta)_{IJ} = \mathcal{T}_{\infty IJ} \exp\left[-\beta(E_J - E_I)\right] \quad for\ E_I < E_J \\
&\mathcal{T}(\beta)_{IJ} = \mathcal{T}_{\infty IJ} \quad for\ E_I > E_J \\
&\mathcal{T}(\beta)_{II} = \mathcal{T}_{\infty II} + \sum_{J>I} \mathcal{T}_{\infty IJ} \left[1 - \exp(-\beta(E_J - E_I)\right],
\end{aligned}
\tag{2.60}
$$

where the third equation is derived from $\sum_J \mathcal{T}(\beta)_{IJ} = \sum_J \mathcal{T}_{\infty IJ} = 1$. In the same way, the following reversed relation can be derived:

$$
\begin{aligned}
&\mathcal{T}_{\infty IJ} = \mathcal{T}(\beta)_{IJ} \exp\left[\beta(E_J - E_I)\right] \quad for\ E_I < E_J \\
&\mathcal{T}_{\infty IJ} = \mathcal{T}(\beta)_{IJ} \quad for\ E_I > E_J \\
&\mathcal{T}_{\infty II} = \mathcal{T}(\beta)_{II} + \sum_{J>I} \mathcal{T}(\beta)_{IJ} \left[1 - \exp(\beta(E_J - E_I)\right].
\end{aligned}
\tag{2.61}
$$

2.3.5 Construction of TM by Broad Sampling Methods

It is not an efficient way, as discussed in the previous subsection, to construct the TM in the multiple Metropolis algorithms since a lot of time and effort are required to choose proper temperatures prior to the main simulation (significant improvement can be achieved though by employing continuously varying temperature as presented in the next chapter). We know the broad sampling methods, such as the multicanonical algorithm and Wang-Landau algorithm, are available. If the TM is constructed by the proposed transitions in any one of such methods, it is expected the DOS that covers any region of energy space can be obtained more efficiently since the simulation is performed just once. In this subsection, I present a method that can realize a random walk in the energy space without any knowledge of the DOS beforehand [67, 50, 7]. It is based on the following fundamental relation which was derived in subsection 2.3.1:

$$
\frac{\mathcal{T}_{\infty IJ}}{\mathcal{T}_{\infty JI}} = \frac{g(E_J)}{g(E_I)}
$$

From the above relation, the random walk acceptance rule $A_{acc} = \min\left(\frac{g(E_I)}{g(E_J)}, 1\right)$ can be replaced by

$$
A_{acc} = \min\left(\frac{\mathcal{T}_{\infty JI}}{\mathcal{T}_{\infty IJ}}, 1\right). \tag{2.62}
$$

The steps of the procedure is outlined in the following table:

1. Choose the desired energy range $E_{min} \leq E \leq E_{max}$.

2. Set the total number of steps N_s.

3. Set $C_{IJ} = 0 \; for \; all \; I, J$.

4. From the current configuration with E_I make a small random change to generate a new configuration with E_J.

5. Update $C_{IJ} = C_{IJ} + 1$. Calculate $\mathcal{T}_{\infty IJ} = \frac{C_{IJ}}{\sum_K C_{IK}}$ and $\mathcal{T}_{\infty JI} = \frac{C_{JI}}{\sum_K C_{JK}}$.

6. If $C_{JI} = 0$, accept the proposed transition. If $C_{JI} \neq 0$, accept with the probability $A_{acc} = \min\left(\frac{\mathcal{T}_{\infty JI}}{\mathcal{T}_{\infty IJ}}, 1\right)$.

7. Repeat from 4 to 6 for N_s steps.

8. Calculate the left unit eigenvector $\mathcal{P}$ of $\mathcal{T}_{\infty}$.

Table 2.4: The procedure of the Transition matrix Monte Carlo method

In this thesis, this method is called the *original* transition matrix Monte Carlo method. The total number of steps N_s should be large enough for the histogram $H(E)$ to be reasonably flat in the range of $E_{min} \leq E \leq E_{max}$. To increase the accuracy, from step 3 to step 7 in the above table can be repeated a few times. The great feature of this method is the random walk is realized from the beginning; the histogram $H(E)$ spreads very fast and $\mathcal{T}_{\infty IJ}$ is filled quickly compared to the multicanonical or Wang-Landau method. Apparently, in the early stage, $\mathcal{T}_{\infty IJ}$ is not accurate since all the possible transitions can not be thoroughly probed due to the fast moving random walker. The accuracy of $\mathcal{T}_{\infty IJ}$ improves slowly as the frequencies of the visits of the states increase. However, there are serious drawbacks of this method; this is *prohibitively slow* and the convergence is not guaranteed. The latter might not be a serious problem because it doesn't mean the TM doesn't converge; it can converge (actually it seems it converges in most simulations) even though the convergence is not guaranteed. The speed is a real issue; the additional time spent to normalize the TM in every move before being used in the acceptance rule is significant.

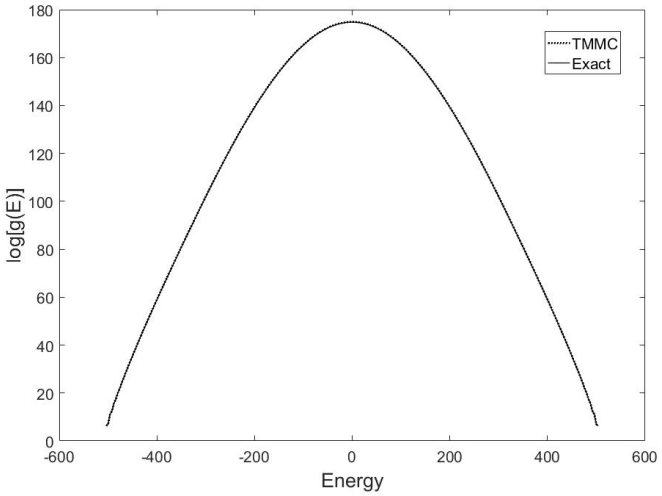

Figure 2.15: The dotted line is the logarithm of the DOS obtained from the original TMMC for 16×16 Ising model. The solid line is the logarithm of the exact DOS.

For the 16×16 Ising model, the original TMMC was performed with $N_s = 1.3 \times 10^8$ to obtain the results plotted in Fig. 2.15 and Fig. 2.16. N_s steps were taken 4 times repeatedly to construct the TM. In all 4 simulations, the histograms of the visited states are almost identical as shown in Fig. 2.17.

The construction of the TM from the single run of a broad sampling method is a great advantage. However, the original TMMC is too slow; to increase the simulation speed, it is required to employ other broad sampling methods such as the multicanonical algorithm or the Wang-Landau algorithm. It is also required to figure out how to control the random walker to make its movement in the phase space optimized for the construction of the TM.

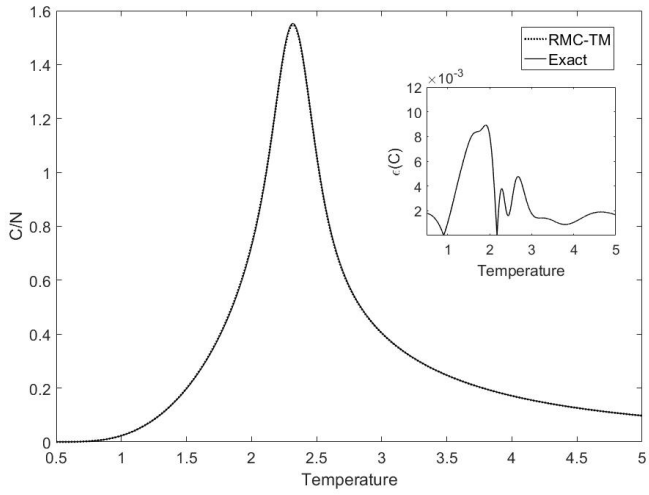

Figure 2.16: The dotted line is the specific heat per spin calculated by the the DOS obtained from the original TMMC for 16×16 Ising model. The solid line is the exact specific heat per spin. The inset shows the relative error at each each temperature.

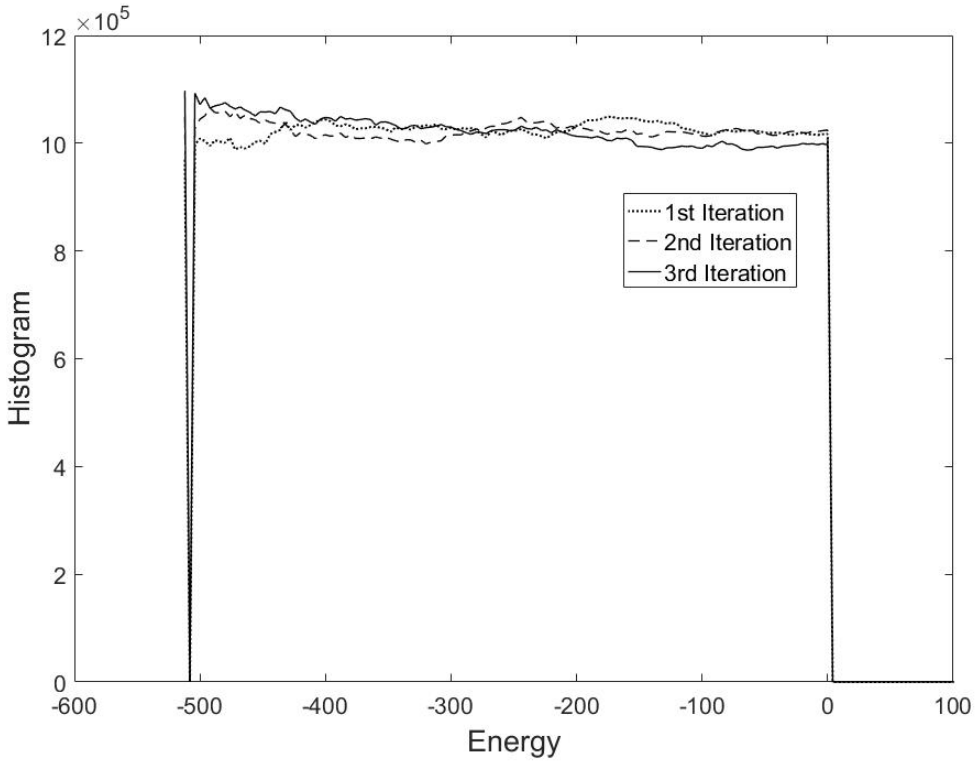

Figure 2.17: The histograms recorded in 4 repeated original TMMC simulations for the original TMMC for 16×16 Ising model. All of them are very flat and almost identical.

Chapter 3

Regulated Temperature Method

3.1 Introduction

It is required to perform the Metropolis algorithm multiple times at different temperatures to construct the TM that can generate the DOS valid for the entire energy range of interest. Even if this is a tedious job, the advantage of employing the TMMC is that the simple addition of the TM's obtained from each simulation is enough to construct the final TM. By introducing continuously changing temperature, we can construct the TM for the full range DOS from a single simulation [27, 73]. In this method, temperature T is expressed as a function of a parameter x which indicates the progress of the simulation. If the total number of steps (or the total number of spin flip trials in a simulation for a lattice spin system) is N_t and the index of the main loop of the Metropolis algorithm is i, the parameter x is defined as

$$x = \frac{i}{N_t}. \tag{3.1}$$

Then, this parameter x, which is called *progress parameter*, changes approximately from 0 to 1 as i increases from 1 to N_t. The acceptance probability becomes

$$P_{acc} = \min\{\exp\left[-(E_{new} - E_{old})/T(x)\right], 1\}. \tag{3.2}$$

By choosing an appropriate $T(x)$, the TM can be constructed over the entire energy range of interest. This method is called the *regulated temperature transition matrix Monte Carlo* (RTTM) method. This is closely related to the simulated annealing which was

proposed by Kirkpatrick et al. [32] as a simulation method to find the global minima of complex functions by gradually lowering temperature. However, in the RTTM, $T(x)$ is not necessarily a monotonically decreasing or increasing function since the purpose of the simulation is not the minimization but the construction of the TM. $T(x)$ is called *temperature schedule*. The numerical details of the RTTM and the optimization of the temperature schedule will be presented in the context of the 2D Ising model on a square lattice with the nearest neighbour interactions and the periodic boundary condition.

3.2 Various Temperature Schedules

3.2.1 Linear Temperature Schedule

The simplest form of the $T(x)$ would be a linear function. If a cooling down is chosen (a heating up works as well) the highest temperature T_{max} and the lowest temperature T_{min} must be selected. Then

$$T(x) = -(T_{max} - T_{min})x + T_{max}. \tag{3.3}$$

For the 2D Ising model with N spins, T_{max} and T_{min} must be selected so that the maximum energy 0 and the minimum energy $-2N$ can be visited in the Metropolis sampling. The DOS for the positive energy region can be obtained from $g(-E) = g(E)$.

For 32×32 Ising model, with $T_{max} = 50$ and $T_{min} = 1.4$, the TM was constructed by the RTTM with a linear temperature schedule. The total number of steps (N_t) was 1.0×10^9. The energy of the visited state as a function of time t measured in MCS as the simulation proceeds and the energy histogram of the all visited states are plotted in Fig. 3.1. It can be seen that samples are taken mostly in high temperature region. This implies the linear schedule is too crude for the 2D Ising model. The specific heat, which is shown in Fig. 3.2, was obtained by taking average over 10 independent results. The average relative error is 0.351 % which is very small in spite of the choice of the crude linear schedule.

3.2.2 Exponential Temperature Schedule

When there is no information about the better choice of the temperature schedule for the system of interest, the most common choice is the exponential cooling schedule. With T_{max} and T_{min} given,

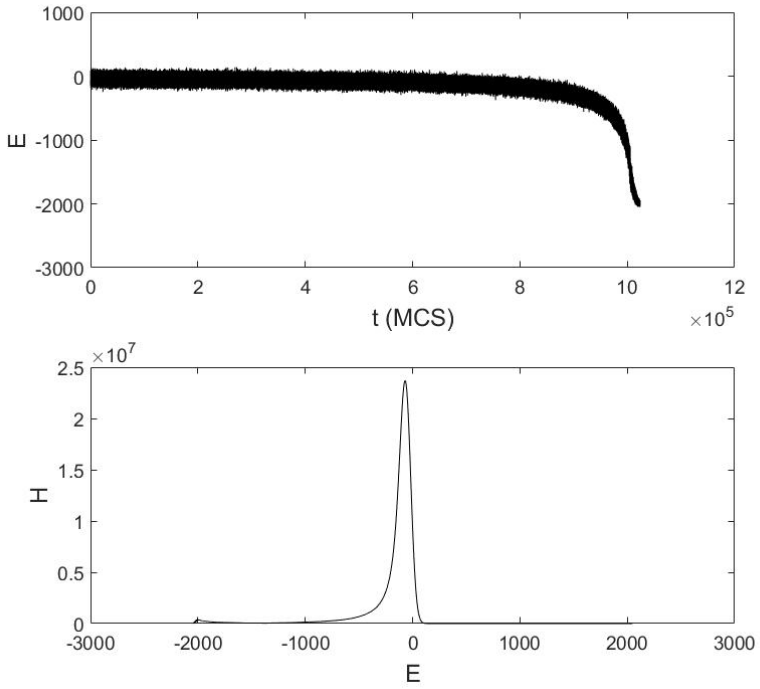

Figure 3.1: The upper graph is the energy of the visited states in RTTM with a linear schedule as a function of time t measured in MCS. The lower graph is the energy histogram of the total visited states.

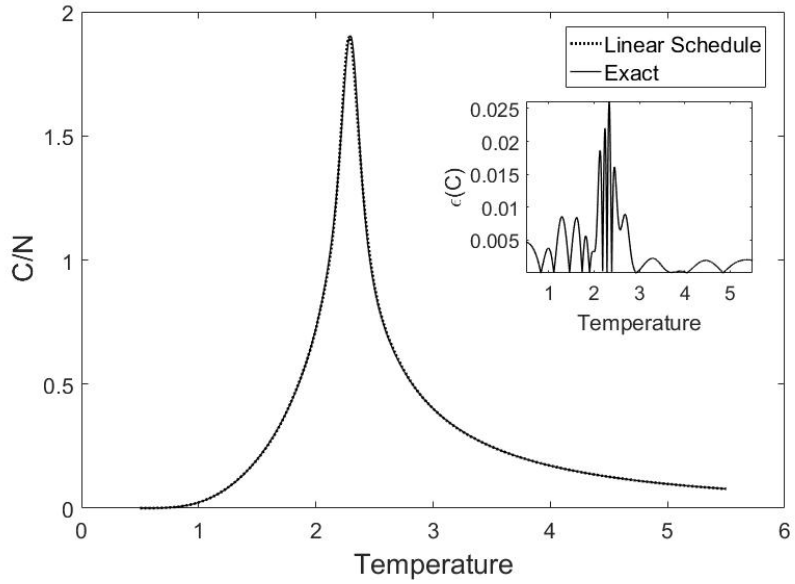

Figure 3.2: The specific heat of 32×32 Ising model obtained by taking average over the results of 10 independent RTTM simulations with a linear temperature schedule.

$$T(x) = T_{max} \exp\left[-\left(\ln \frac{T_{max}}{T_{min}}\right) x\right]. \tag{3.4}$$

For 32×32 Ising model, with $T_{max} = 50$ and $T_{min} = 1.4$, the results of the RTTM with an exponential temperature schedule are shown in Fig. 3.4. The total number of steps (N_t) was 1.0×10^8. Note that the samples in lower temperature region has increased. The specific heat was obtained by taking average over 10 independent results and plotted in Fig. 3.5. The average relative error is 0.256 % which is less than the one with a linear schedule.

3.2.3 Piecewise Linear Temperature Schedule

It is well known that the 2D Ising model exhibits a continuous phase transition at $T_c = 2.269$ in the thermodynamic limit. The fluctuation becomes larger as the temperature approaches T_c. This knowledge can be used to modify the simple linear schedule so that more samples are taken near T_c. There are many options; one example is the first graph

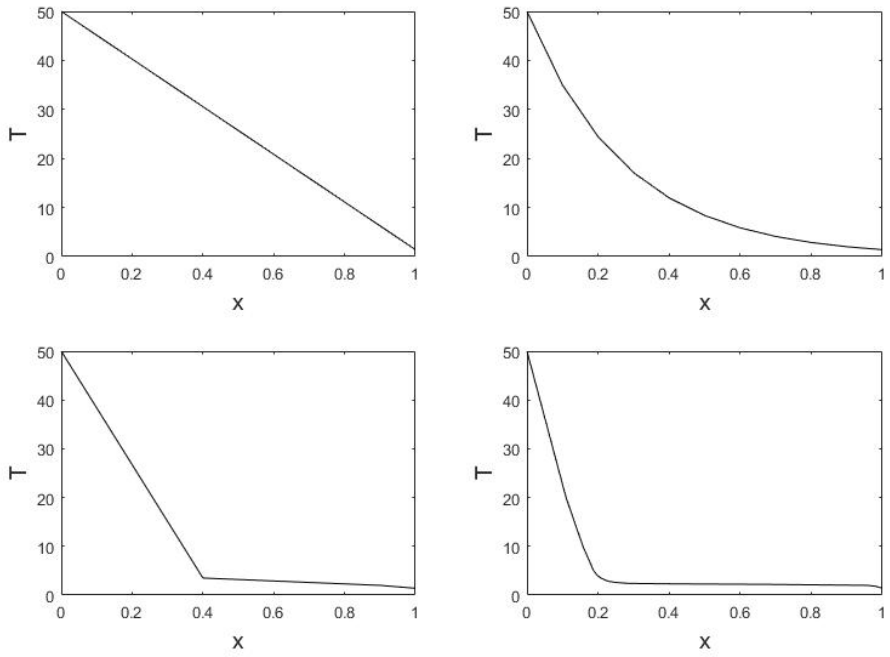

Figure 3.3: Various temperature schedules. The left and right graphs in the first row are the linear and the exponential schedule respectively. The left graph in the second row is the piecewise linear schedule. The right one in the second row is the schedule obtained by the use of the autocorrelation times.

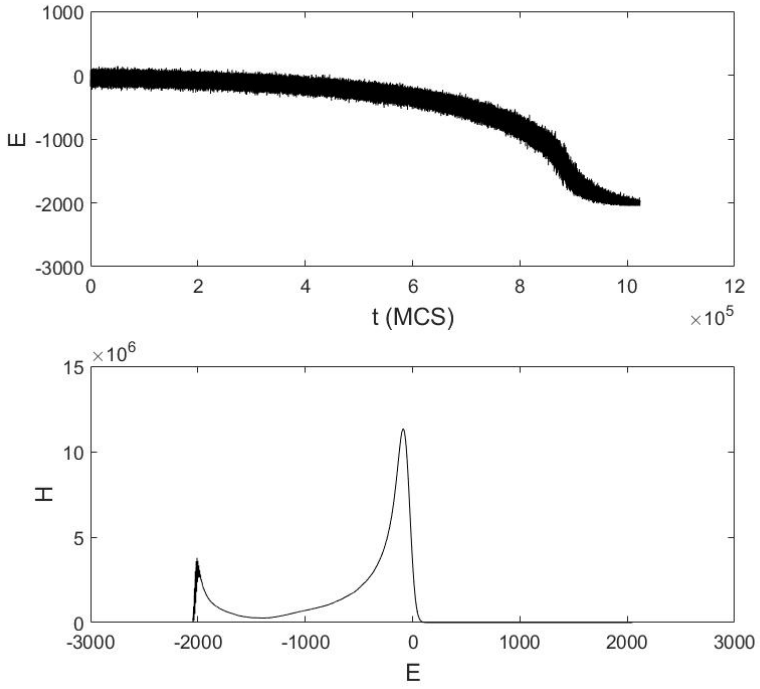

Figure 3.4: The upper graph is the energy of the visited states in RTTM with an exponential schedule as a function of time t measured in MCS. The lower graph is the energy histogram of the total visited states.

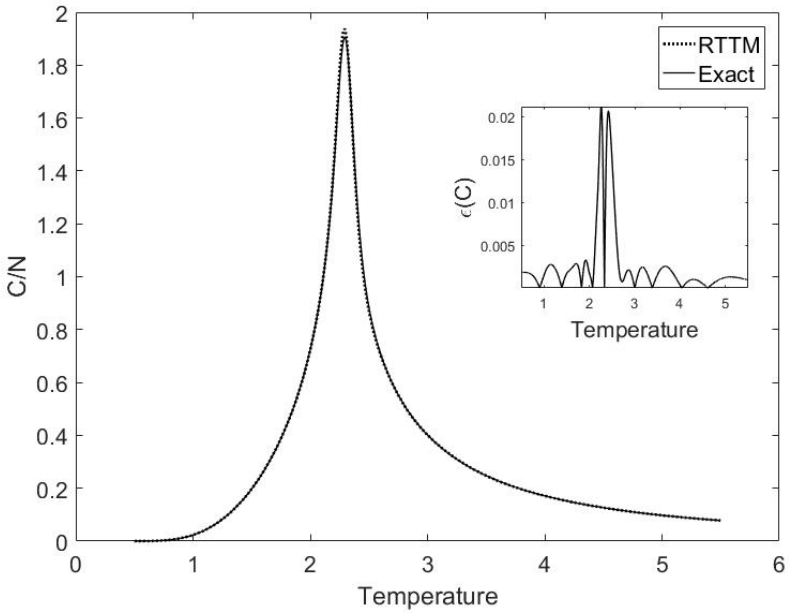

Figure 3.5: The specific heat of 32×32 Ising model obtained by taking average over the results of 10 independent RTTM simulations with an exponential temperature schedule.

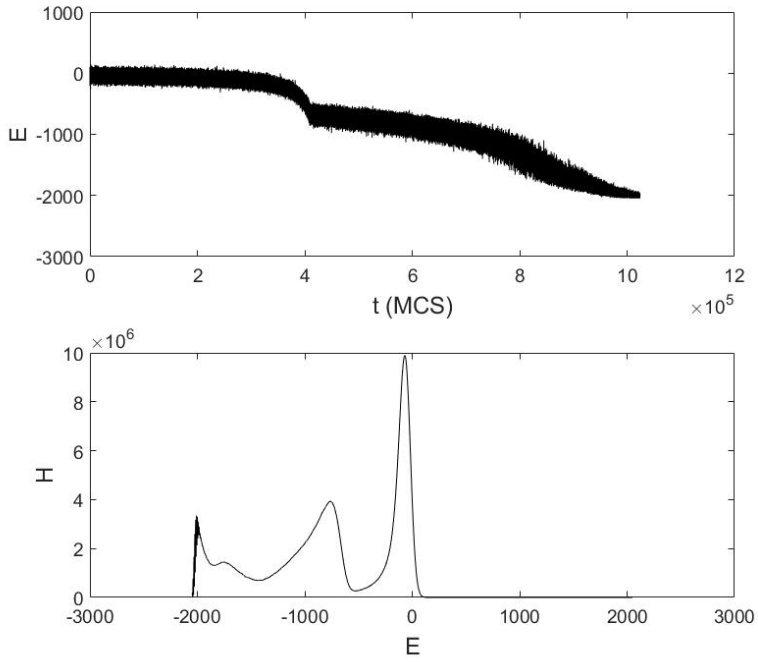

Figure 3.6: The upper graph is the energy of the visited states in RTTM with a piecewise linear schedule as a function of time t measured in MCS. The lower graph is the energy histogram of the total visited states.

in the second row in the Fig. 3.3. This schedule is applied to 32×32 Ising model without changing other conditions to obtain the results shown in Fig. 3.6 and Fig. 3.7. Note the samples in the low energy bins which corresponds to temperatures close to Tc are significantly increased. This modification of the temperature schedule based on the naive guess lowered the average relative error down to 0.174 % which means the DOS obtained in the TM constructed in the RTTM with the piecewise linear schedule is highly accurate.

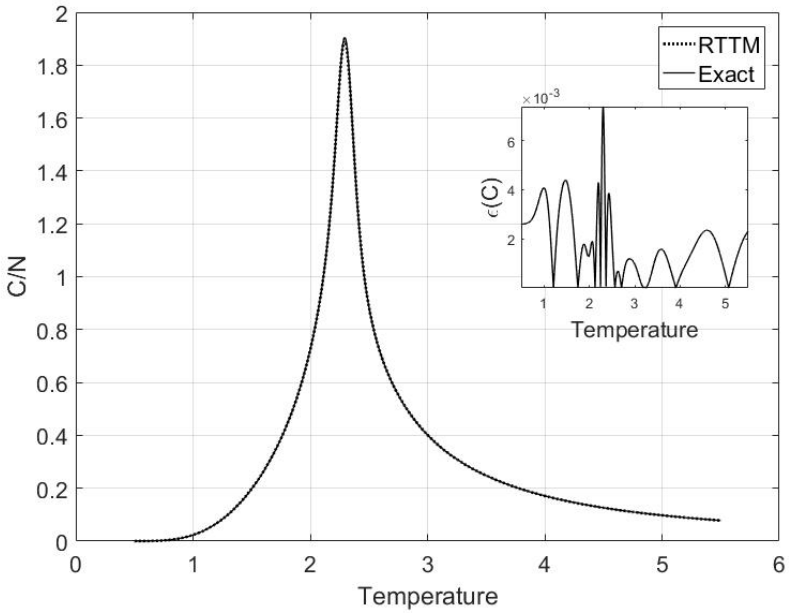

Figure 3.7: The specific heat of 32×32 Ising model obtained by taking average over the results of 10 independent RTTM simulations with a piecewise linear temperature schedule.

3.3 Optimized Temperature Schedule

3.3.1 Optimization by Autocorrelation Time

To improve the temperature schedule further, we need to know the regions in the energy space where we need to spend more time taking samples. In the Metropolis sampling for the Ising model, more samples are required as the temperature approaches the critical temperature since the autocorrelation time, which causes an error, increases dramatically near the critical point. The normalized autocorrelation function of an observable Q is defined as

$$A(t) = \frac{\langle Q_k Q_{k+t} \rangle - \langle Q_k \rangle^2}{\langle Q_k^2 \rangle - \langle Q_k \rangle^2}, \tag{3.5}$$

where t is measured in MCS. $A(t)$ can be approximated by the following exponential function :

$$A(t) \sim \exp(-t/\tau), \tag{3.6}$$

where τ is called the *autocorrelation time*. The autocorrelation functions of the 32×32 Ising model are plotted in Fig. 3.8 and Fig. 3.9. It can be seen that τ increases fast as T becomes near $T_c = 2.269$ (Of course there is no precise T_c for a finite system though). Fig. 3.10 shows the autocorrelation times measured at different temperatures for 32×32 Ising model.

To derive a temperature schedule from Fig. 3.10, I assumed the following relation :

$$\frac{dT}{dx} \propto -\frac{1}{\tau}, \tag{3.7}$$

which implies the slope of $T(x)$ becomes smaller, which means taking more samples, as τ becomes larger. This is a *bold* assumption. However, the derivation of the temperature schedule now at least has a reasonable and quantified basis instead of crude ad hoc assumptions presented in the previous section. To explain the detailed procedure of the derivation of $T(x)$ from Eq. (3.7), let's assume $\{T_1, T_2, \cdots, T_n\}$ and $\{\tau_1, \tau_2, \cdots, \tau_n\}$ are given. τ_i is the autocorrelation time at temperature T_i. We have to determine the corresponding $\{x_1, x_2, \cdots, x_n\}$ where $x_1 = 0, x_n = 1$. Set $dx/dT = -k\tau$ and determine the constant k in the following way :

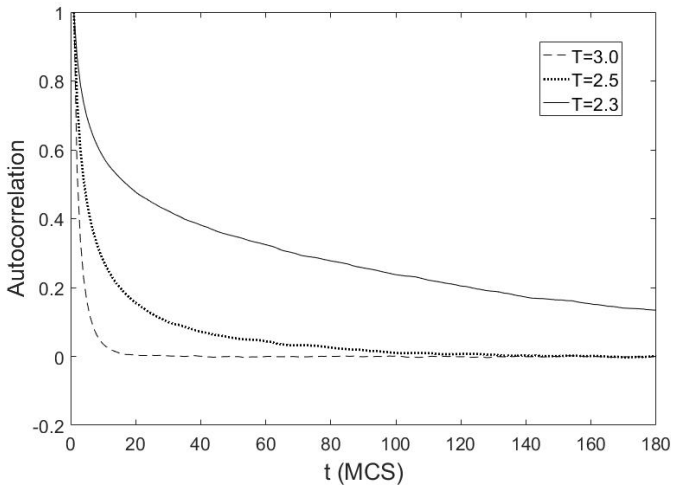

Figure 3.8: The autocorrelation function of 32×32 Ising model at three different temperatures in the Metropolis algorithm.

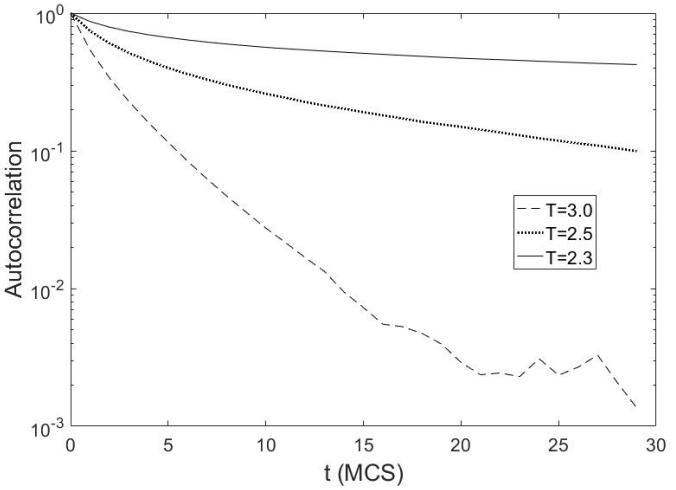

Figure 3.9: The semilog plot of the autocorrelation function of 32×32 Ising model at three different temperatures in the Metropolis algorithm.

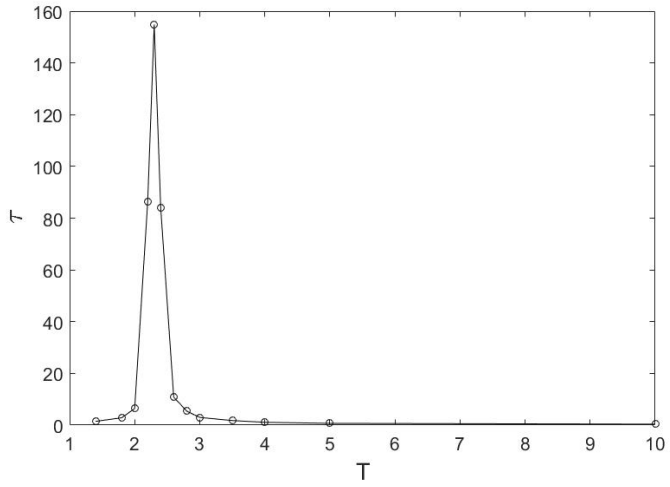

Figure 3.10: The autocorrelation times of 32×32 Ising model measured at different temperatures in the Metropolis algorithm.

$$x_2 - x_1 = -k\tau_1(T_2 - T_1), x_3 - x_2 = -k\tau_2(T_3 - T_2), \cdots, x_n - x_{n-1} = -k\tau_{n-1}(T_n - T_{n-1}). \quad (3.8)$$

Add up all the above equations to obtain

$$k = \frac{1}{\sum_{i=1}^{n-1} \tau_i(T_i - T_{i+1})}. \quad (3.9)$$

Then,

$$x_j = x_{j-1} + k\tau_{j-1}(T_{j-1} - T_j) = x_{j-1} + \frac{\tau_{j-1}(T_{j-1} - T_j)}{\sum_{i=1}^{n-1} \tau_i(T_i - T_{i+1})}. \quad (3.10)$$

The right graph in the second row of Fig. 3.3 is the schedule obtained by the use of the autocorrelation times plotted in Fig. 3.10. The results of the RTTM with this temperature schedule are shown in Fig. 3.11 and Fig. 3.12. Note the number of samples in the low temperature region has significantly increased. The average relative error of the specific heat is 0.21% in this case.

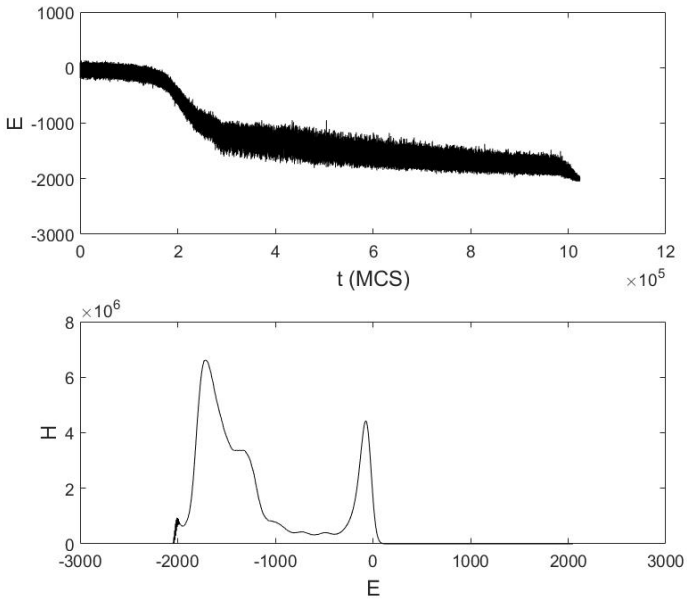

Figure 3.11: The upper graph is the energy of the visited states in RTTM with the schedule derived from the autocorrelation time as a function of time t measured in MCS. The lower graph is the energy histogram of the total visited states.

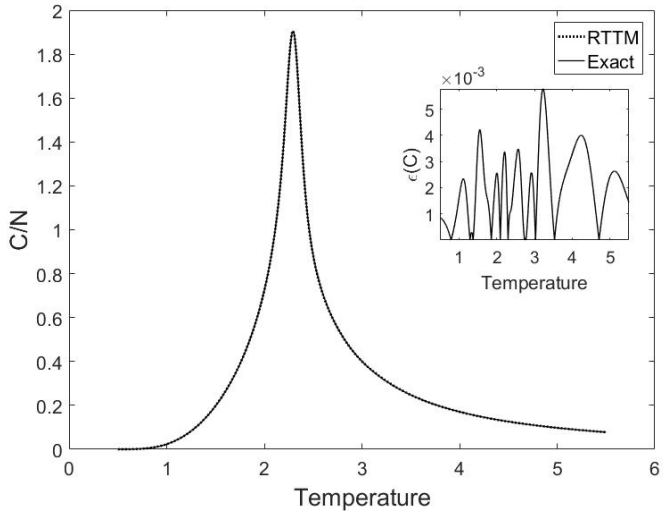

Figure 3.12: The specific heat of 32×32 Ising model obtained by taking average over the results of 10 independent RTTM simulations with the temperature schedule derived from the autocorrelation time.

3.3.2 Optimization by Magnetization Distribution

The ideal optimized temperature schedule should be *self-adapting*; instead of changing according to the predetermined schedule, the temperature should be adjusted adaptively to guide the random walker to the insufficiently sampled regions. For the 2D Ising model, if the the trace of the Markov chain is monitored in the energy and magnetization ($M = \sum \sigma_i$) space, it is found that the covered area in equilibrium is restricted and increases as temperature approaches the critical point as shown in Fig. 3.13. If the temperatures changes too quickly, the required area at each temperature can not be fully covered, which leads to an error in the TM. Whether the area in the E-M space is fully covered or not at each temperature can be determined by monitoring the histogram of magnetization since *the distribution of the magnetization won't change once the area is fully covered.*

The adaptive optimization of the temperature schedule based on the saturation of the magnetization histogram was proposed, to my knowledge for the first time, by D. Yevick and the author [74]. Let's suppose the RTTM starts at the maximum temperature T_{min}. Choose the maximum number of steps N_s and $N_m (< N_s)$ which is the period of the convergence check of the magnetization histogram. The following is the temperature update procedure by the convergence check of the magnetization histogram :

1. Set $H_{new}(M) = 0$ and $H_{old}(M) = 1$ for all M bins.

2. Update H_{new} for N_m steps in the RTTM at temperature T.

3. Normalize H_{old} and H_{new}. Calculate x = mean of $|H_{new} - H_{old}|$.

4. If $x \geq \epsilon$, where ϵ is the predetermined small number,
   set $H_{old} = H_{new}$ and $H_{new} = 0$. Repeat from 2 to 3.
   If $x < \epsilon$, Set $T = T - \Delta T$ and repeat from 1 to 3.

5. If the total steps reaches N_s, irrespective of x, set $T = T - \Delta T$
   and repeat from 1 to 3. This is to avoid infinite loop.

6. If $T = T_{min}$, terminate the procedure.

Table 3.1: Temperature Update Procedure

In this procedure, how long to stay at each temperature is determined automatically. The accuracy can be easily adjusted by ϵ. The temperature interval ΔT can also be adjusted for further acceleration of the simulation. I chose a cooling down procedure (decreasing temperature) as in the previous section. However, sometimes a heating up procedure is more convenient if the ground state is known. In a cooling down procedure for 32×32 Ising model, with $T_{max} = 20, T_{min} = 1.2$, I decreased ΔT gradually from 5.0 to 0.2 as T decreases. With this variable ΔT, the simulation time can be reduced without affecting the accuracy. The energy histogram of the visited states in the RTTM with this adaptive optimized temperature schedule is plotted in Fig. 3.14. The temperature schedule produced in the simulation is shown in Fig. 3.15. Interestingly this is very similar to the one derived from the autocorrelation time. If $\epsilon = 5 \times 10^{-6}$, $N_s = 3 \times 10^8$ and $N_m = 1 \times 10^7$, the CPU time is almost same as the one of other temperature schedules (linear, exponential or piecewise linear). The specific heat is plotted in Fig. 3.16. The average relative error is 0.113% which is the lowest error so far. Even though this optimization method seems valid only for the Ising model, the generalization to other systems which have the second order phase transitions is straightforward by replacing M with the corresponding order parameter.

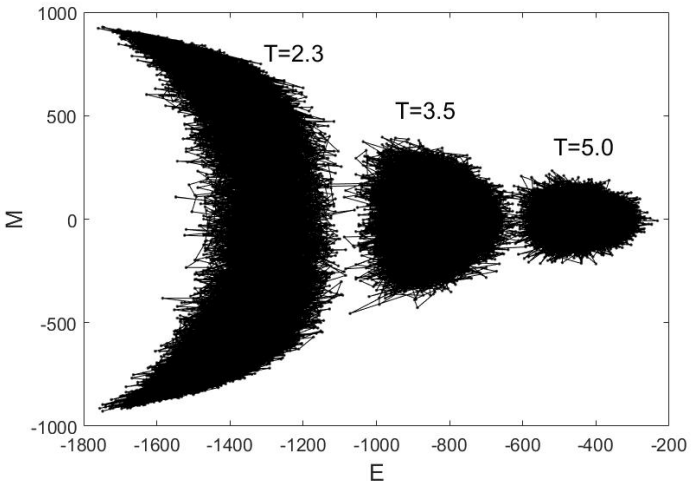

Figure 3.13: The trace of the sequence of the visited states in the Metropolis algorithm at a fixed temperature. The results at three different temperatures are plotted.

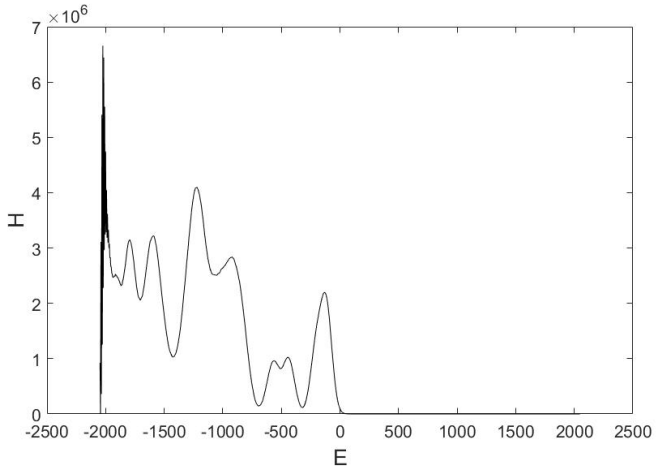

Figure 3.14: The energy histogram of the visited states in the RTTM for 32×32 Ising model with the optimized temperature schedule produced by the convergence check of magnetization histogram.

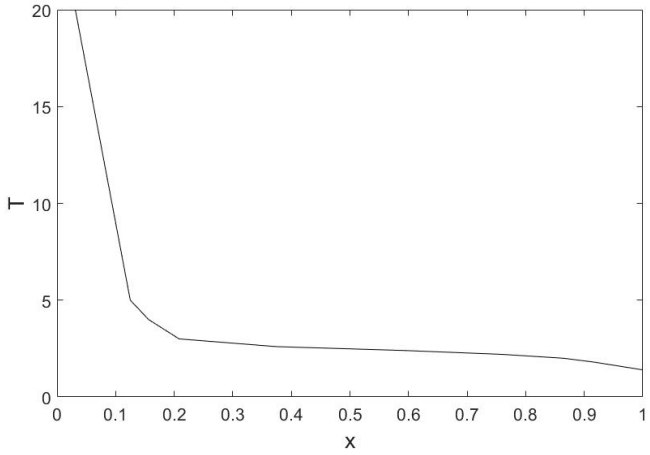

Figure 3.15: The temperature schedule derived by the adaptive optimization based on the convergence of the magnetization histogram.

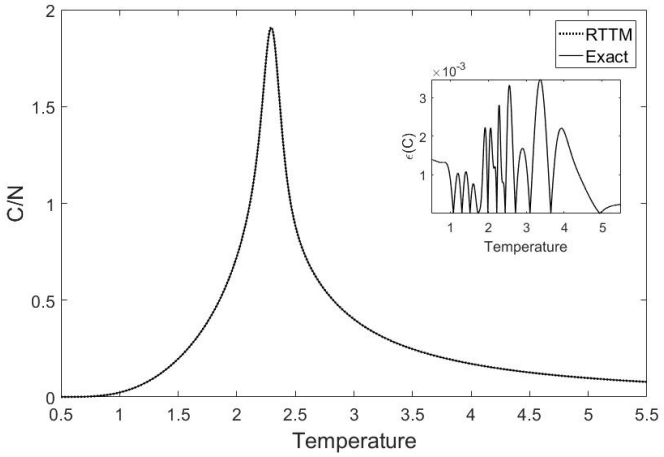

Figure 3.16: The specific heat of 32×32 Ising model obtained by taking average over the results of 10 independent RTTM simulations with the temperature schedule derived from the adaptive optimization method.

Chapter 4

Multicanonical Transition Matrix Methods

4.1 Introduction

From the discussion presented in the subsection 2.3.4, it is found that the infinite temperature TM elements can be populated by all accepted and rejected transitions during the simulation with any acceptance rule. In the subsection 2.3.4, it is presented that the infinite temperature TM for the full energy range of interest can be constructed in a single simulation by employing broad sampling methods such as multicanonical sampling, Wang-Landau algorithm and original TMMC method. The important feature of this method is that temperature is not involved in the construction of the TM. In the RTTM, which can be called a *temperature-driven* construction of the TM, a lot of work should be done for the selection of temperature range and the choice of the temperature schedule since those factors greatly affect the accuracy as well as the efficiency. Thus, by employing a broad sampling method, the TM construction procedure can be considerably simplified. In the original TMMC, with the following acceptance rule,

$$A_{acc} = \min\left(\frac{\mathcal{T}_{\infty JI}}{\mathcal{T}_{\infty IJ}}, 1\right),$$

all energy bins can be visited with approximately equal frequency. This eliminates all involving jobs required in the RTTM at the cost of the simulation speed; the original TMMC is very slow. Instead of the above acceptance rule, the multicanonical iteration

procedure can be employed to populate the transition matrix elements in a more efficient way [76, 77, 34]. This method is called the *multicanonical transition matrix Monte Carlo* method (MCTM).

4.2 Simulation Method

In the multicanonical iteration procedure (learning run), to find the estimate of the DOS $g(E)$, the following acceptance rule is used

$$A_{acc} = \min\left(\frac{g(E_I)}{g(E_J)}, 1\right)$$

as $g(E)$ is periodically updated in the following way :

$$g^{(k+1)}(E) = g(E)^{(k)} H^{k)}(E), \tag{4.1}$$

where $g^{(k)}$ and $H^{(k)}$ are the estimate of the DOS and the histogram in the kth iteration respectively. In contrast to the original TMMC, the histograms are not flat in the early stage of the iteration. As shown in Fig. 4.1, the histogram becomes wider and flatter as the iteration proceeds. Usually the total number of steps per iteration is gradually increased to deal with widening energy region. During the iteration, all proposed transitions are recorded in the C-matrix; for instance, $C_{IJ} = C_{IJ} + 1$ when the transition from I to J is proposed. C is never zeroed during the entire iteration procedure. After the first visit of the state with E_{min}, 2 or 3 more iterations are performed before the iteration procedure is terminated. Using the C-matrix populated during the iteration procedure, the infinite temperature TM is obtained by

$$\mathcal{T}_{\infty IJ} = \frac{C_{IJ}}{\sum_K C_{IK}}. \tag{4.2}$$

The DOS $g(E)$ is subsequently calculated from the TM by the repeated multiplication method for instance.

The MCTM is generally faster than the original TMMC; the reason, I guess, is the gradual broadening of the histogram. Note that there is no iteration procedure in the original TMMC and the simulation is performed until the the boundary states are visited to realize a flat histogram. The original TMMC spends long time to produce a single flat histogram as depicted in Fig. 2.17. The clear difference can be seen in the plot of the

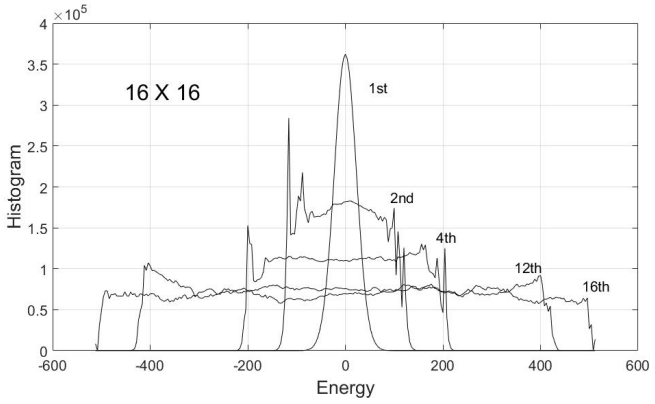

Figure 4.1: The histograms of the visited states recorded during several different iteration stages in the multicanonical simulation for the 2D 16×16 Ising model.

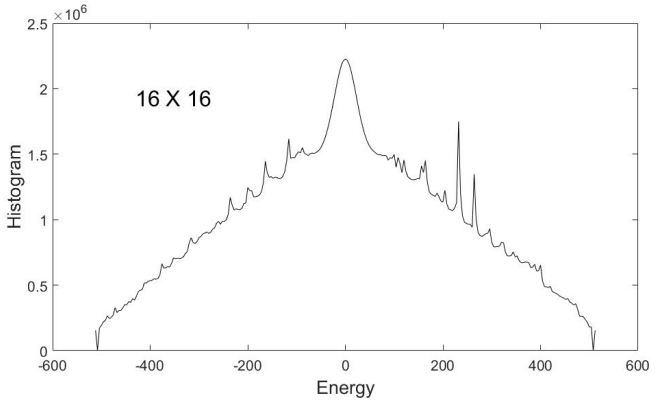

Figure 4.2: The histogram of the total visited states during the entire iteration procedure in the multicanonical simulation for the 2D 16×16 Ising model.

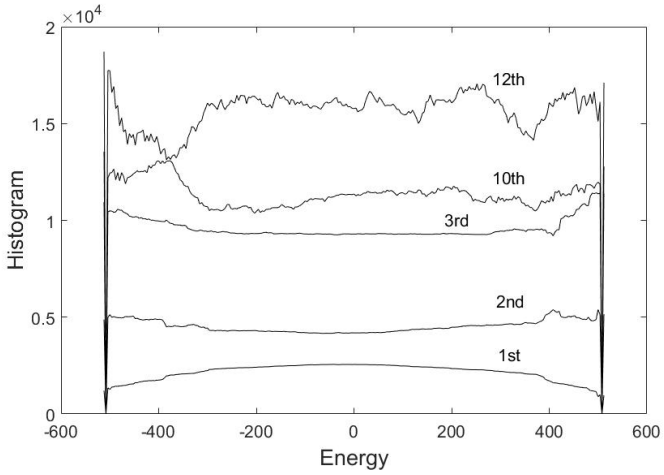

Figure 4.3: The histograms of the visited states recorded during several early iteration stages of the Wang-Landau simulation for the 2D 16×16 Ising model.

accumulated energy histogram of the visited states during the MCTM iteration as shown in Fig. 4.2. This is not flat in contrast to Fig. 2.17. The frequency of the visit is almost proportional to the energy E. I think this is reasonable because more time should be spent in the region where more states exist. The uniform sampling is simple, but it might be excessive and wasteful. It is interesting to see the histograms recorded during the Wang-Landau sampling. Obviously every histogram in each iteration is reasonably flat because the flatness criterion had to be satisfied as shown in Fig. 4.5. This is similar to the original TMMC. The unique feature is the total number of steps increases dramatically as the modification factor f approaches f_{min}. This can be seen in Fig. 4.6. I think this explains why the TMMC combined with the Wang-Landau algorithm (WLTM) is very slow [7, 34].

4.3 Simulation Results

4.3.1 2D Ising Model

In the RTTM simulations, lots of time and efforts are required to do the tedious preparation such as numerous try and error to select appropriate temperatures the number of which increases very fast as the system size increases. Since the MCTM is free from the concept of temperature, it is simple and straightforward even for large systems. Thus it can be said the MCTM has better scalability compared to the RTTM.

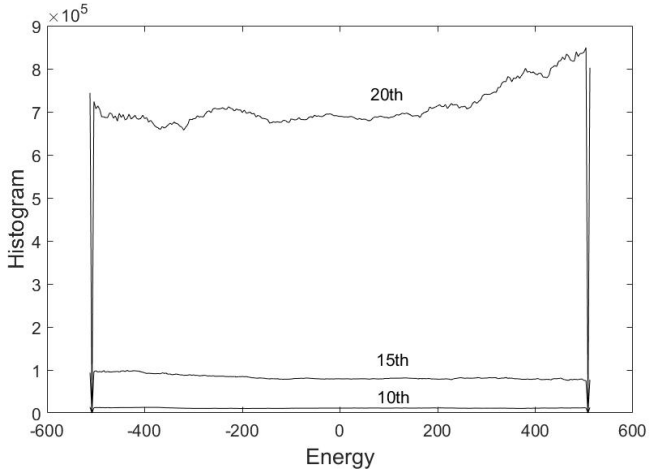

Figure 4.4: The histograms of the visited states recorded during a few latter iteration stages of the Wang-Landau simulation for the 2D 16×16 Ising model.

In a MCTM simulation of a 2D Ising model with N spins, $10N \sim 100N$ MCS are employed in each iteration. After the multicanonical iteration that first reaches the ground state, $2 \sim 5$ additional iterations are performed to make sure all possible transitions are recorded. This normally results in the average relative error for the specific heat, $\epsilon(C) = |C - C_{\text{exact}}|/C_{\text{exact}}$, below 1%. In the transition matrix calculations, the DOS is first obtained from $\mathcal{T}$, after which the specific heat is evaluated from the standard formula $C = k_B\beta^2(\langle E^2\rangle - \langle E\rangle^2)$. To attain the average relative error of C not exceeding 1% , the average relative error of $\log[g(E)]$ must be lower than roughly 0.1%. The MCTM was applied to a 64×64 Ising system, $\mathcal{T}$ was constructed as indicated in the preceding section from the accepted and rejected transitions occurring during 240 multicanonical iterations with 17×64^2 MCS per iteration. The average was taken over 5 independent simulations to obtain the specific heat which is plotted in Fig. 4.5. The inset displays the relative error over the temperature interval between 0.5 and 5.5. The average relative error over this interval is 0.14%. The average CPU time was 469 minutes when a MATLAB interpreter together with a 2.3GHz Intel Core i7 processor was employed.

4.3.2 2D 10-state Potts Model

To demonstrate the performance of the MCTM for a system that exhibits the first order phase transition, the MCTM was applied to the 2D 10-state Potts model. The Hamiltonian

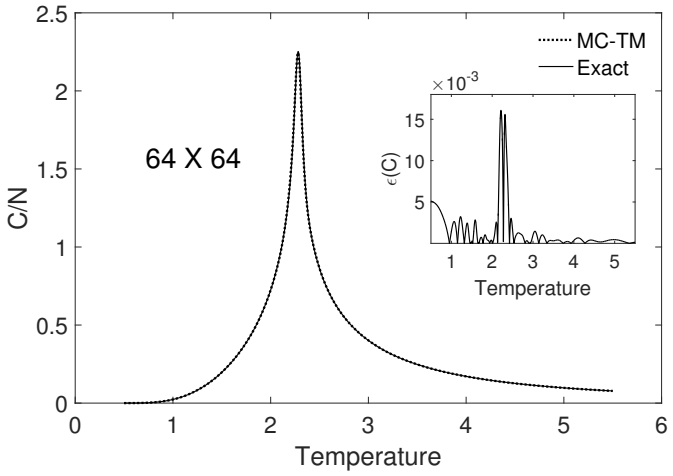

Figure 4.5: The MCTM result for the specific heat per spin of the 64×64 Ising model averaged over 5 independent simulations (dotted line) compared to the corresponding exact result. The inset displays the relative error with respect to the exact values. The average relative error equals 0.14%.

of r-state 2D Potts model of N spins is given by

$$H = -J \sum_{\langle i,j \rangle} \delta_{s_i,s_j}, \quad \text{where } s_i = 1, 2, \cdots, r. \tag{4.3}$$

If $r = 2$, this model becomes identical to the 2D Ising model. The magnetization M is defined as

$$M = (rN_m/N - 1)/(r - 1), \tag{4.4}$$

where N_m is the number of the majority spins in a spin configuration. It is known that a continuous phase transition occurs for $r \leq 4$ and a first order phase transition for $r > 4$. The critical temperature in the thermodynamic limit is

$$T_c = \frac{1}{\log(1 + \sqrt{r})}. \tag{4.5}$$

For the 10-state Potts model, $T_c = 0.7012$. At the critical point, the energy probability distribution function $P(E)$ has double peaks since the coexistence of the disordered states

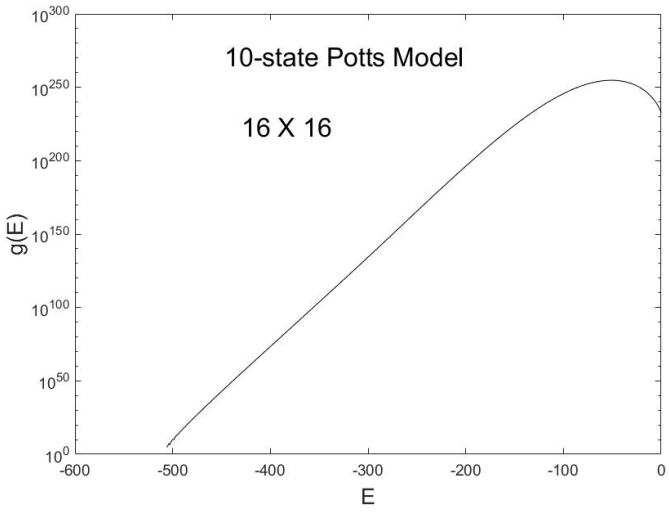

Figure 4.6: The semilog plot of the DOS obtained by the MCTM for a 16×16 10-state Potts model.

and the ordered states. For the states between the two metastable states, $P(E)$ is extremely small. Thus, as the system size increases, tunnelling between the two metastable states are exponentially suppressed, which in turn causes extreme slowing down.

The MCTM easily overcomes this problem and generates a highly accurate DOS. The TMMC was applied to a 16×16 10-state Potts model to obtain accurate double peaked distribution at the critical point and the specific heat. The number steps per iteration was gradually increased from 6.4×10^5 MCS to 25.6×10^5 MCS. To reach the ground state, 44 iterations were required and 2 more iterations were performed. The semilog plot of the DOS is shown in Fig. 4.6 and the energy probability distribution function $P(E)$ at the critical point is plotted in Fig. 4.7 which clearly shows double peaks. $P(E)$ is given by

$$P(E) \propto g(E) \exp(-E/T_c). \tag{4.6}$$

Because the size is small, the temperature at which the heights of two peaks become equal is slightly higher the $T_c = 0.7012$ in the thermodynamic limit. The specific heat per spin, which is displayed in Fig. 4.8, shows the typical spike due to the latent heat involved in the first order phase transition.

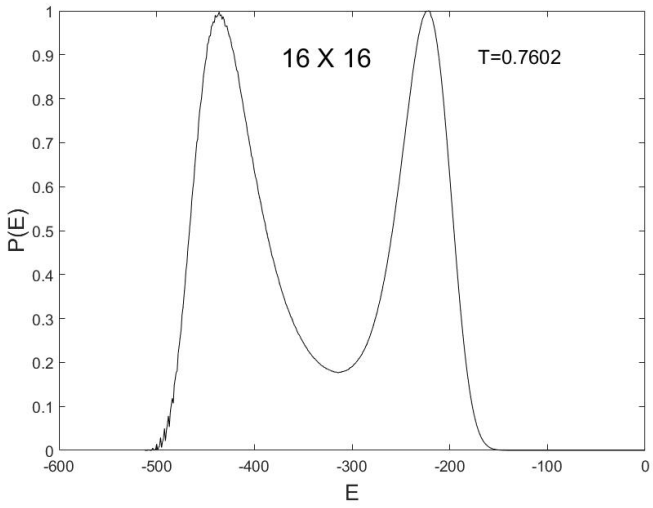

Figure 4.7: The canonical distribution of a 16×16 10-state Potts model at the critical point.

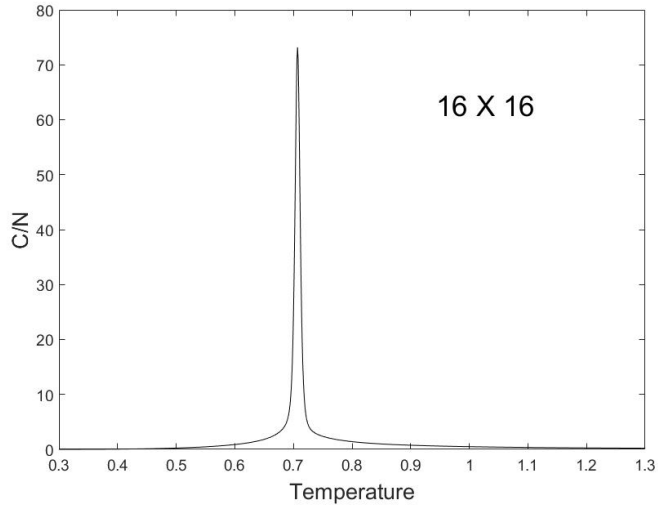

Figure 4.8: The MCTM result for the specific heat per spin of a 16×16 10-state Potts model.

Chapter 5

Renormalized Multicanonical Transition Matrix Methods

5.1 Introduction

The CPU time grows according to a power law as the system size increases. For a d dimensional lattice spin system with linear size L, it volume or number of spins is $V = L^d$. It holds typically that $E_{max} - E_{min} \sim V$. In the optimum random walk to obtain a flat histogram over the entire energy range, the CPU time $\sim V^2$ [5]. This implies, for 2D ($d = 2$) and 3D ($d = 3$), the CPU time increases by a factor of 16 and 64 respectively when the system size is doubled. To deal with the dramatic increase of the CPU time in a simulation for a larger system, the TM $\mathcal{T}$ or the DOS $g(E)$ of a smaller system can be utilized to produce better initial estimate of $\mathcal{T}$ or $g(E)$ of a larger system [35, 6, 4].

In 2016, for 1D systems, D. Yevick proposed a new method to utilize the DOS of a smaller system to model the DOS of a larger system by employing the convolution technique [70]. This method, which is called *renormalized multicanonical sampling*, was extended to higher dimensions resulting in a significant acceleration by the author [34]. The MCTM that employs the renormalized multicanonical sampling to increase the simulation speed is called the *renormalized multicanonical transition matrix Monte Carlo* method (RMCTM).

5.2 Simulation Method

In one dimension, the renormalized multicanonical procedure is based on approximating the density of states of a spin lattice system with short range interactions by the convolution of the density of states of two identical subsystems S_1 and S_2, each corresponding to one half of the original system [70]. That is, since in general the interaction between S_1 and S_2 is far weaker than the individual spin-spin coupling, to a first approximation the two systems can be considered isolated. If the probabilities that S_1 and S_2 possess energies E_1 and E_2 are given by $P_1(E_1)$ and $P_2(E_2)$, an initial estimate of the probability that the combined system has energy E is given by

$$P(E) = \sum_{E_1} P_1(E_1) P_2(E - E_1). \tag{5.1}$$

Employing an accurate initial estimate of $g(E)$, which corresponds to the infinite temperature probability distribution, in a multicanonical iteration significantly increases its rate of convergence. Especially for large systems, the efficiency can therefore be greatly enhanced by generating $g(E)$ for a small system and then applying the above procedure to obtain an approximation for $g(E)$ for a system with twice the linear size. This estimate can be further refined through multicanonical iterations. Repeated application of these latter two steps in principle enables the rapid simulation of systems with arbitrarily large sizes.

Previously, a similar methodology was advanced by B. A. Berg *et al.* [6, 4] to improve the efficiency of multicanonical algorithms by employing $g(E)$ for a smaller system to model the DOS of larger systems. While this method has proven highly effective in many contexts, renormalized multicanonical sampling is in certain respects both more straightforward as it directly manipulates the DOS and more general since it can be employed in conjunction with numerous other methods besides the multicanonical algorithm. For example, a renormalized WLTM (RWLTM) can be formulated that combines the convolution procedure with the WLTM.

When Eq. (5.1) is applied, the resulting number of bins must coincide with that of the enlarged system. For example, assuming a constant bin width and M initial energy bins, $2M - 1$ equal width bins are obtained after the convolution. Thus for a 1D system of N spins and $M = aN + 1$ bins where a represents an arbitrary positive integer, Eq. (5.1) yields the density of states over $2M-1 = 2(aN+1)-1 = a\cdot 2N+1$ bins, which corresponds to the appropriate number of discrete bins for a system of $2N$ spins. In contrast, for a two-dimensional $L \times L$ spin lattice system the spin numbers are quadrupled when the linear size L is doubled, while the number of bins resulting from the convolution of Eq. (5.1)

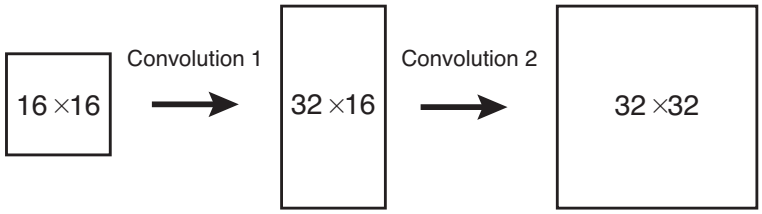

Figure 5.1: An illustration of the procedure employed for doubling the linear size of a two dimensional system for the RMCTM.

coincides with the number of bins of a spin system (subject to boundary conditions) with a linear size that is doubled in a single direction as indicated in Fig. 5.1. However, as apparent from the figure, a second convolution then yields the correct number of bins for a system with twice the linear size. Fig. 5.2 illustrates the excellent agreement between the exact normalized DOS of a 32×32 Ising system and the DOS resulting from two successive convolutions of the exact normalized DOS of a 16×16 Ising system.

In three dimensions, RMCTM procedure requires a series of three convolutions to double the linear system size. Similarly, if the DOS of a n dimensional system of N spins is expressed as a histogram over $M = aN + 1$ equal size bins, the DOS of a $2^n N$ spin system with twice the linear size can be approximated by performing n convolutions.

5.3 Numerical Results

When the RMCTM is applied to 2D Ising systems, the ground state is often already visited in the first iteration as a result of the accurate initial estimates of the DOS generated by the convolution procedure. Accordingly, an alternative convergence criterion is required to terminate a RMCTM simulation. For a system with N spins, $8 \sim 12$ iterations with $15N \sim 100N$ MCS per iteration is found to typically be sufficient to generate C with a relative error below 1%.

To apply RMCTM to a 64×64 system, the simulation was initialized with the MCTM result for a 8×8 system after which the system size was repeatedly doubled according to the procedure illustrated in Fig. 5.1. At the final system size of 64×64, 10 iterations with 30×64^2 MCS per iteration proved sufficient to generate the DOS to within the same level of accuracy as the MCTM. The specific heat per spin of the system calculated from the DOS obtained by RMCTM and averaged over 10 independent simulations is given by the dotted line in Fig. 5.3. The average relative error equals 0.17%. The CPU time was

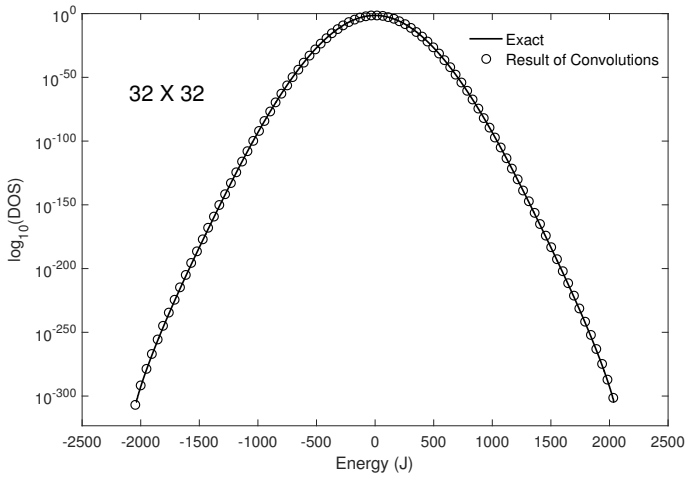

Figure 5.2: The result of convolving the exact normalized DOS of 16×16 Ising system twice (circle) compared to the exact normalized DOS of a 32×32 Ising system (solid line). Energy is in units of J which is the exchange energy between the nearest neighbour spins.

48 minutes on average. Hence the computation time was reduced almost by a factor of 10 from that of the MCTM calculation without a significant decrease in accuracy. This considerable reduction in CPU time enabled RMCTM simulations up to sizes of 128×128 on a normal Pentium laptop, for which the specific heat could be generated with a mean relative error of 0.27% in about 460 minutes as shown in Fig. 5.4.

As the density of states and specific heat of 3D Ising spin systems have not been analytically evaluated, the guidelines employed above for selecting the computational parameters in the 2D simulations are here assumed to ensure a similar degree of accuracy in 3D. Thus the MCTM results of a $16 \times 16 \times 16$ system were obtained by averaging over 5 independent simulations, each of which employed 236 iterations with 20×16^3 MCS per iteration to construct the transition matrix from which the DOS and specific heat were subsequently evaluated. The average CPU time per simulation was 787 minutes. The corresponding RMCTM calculation was initialized with the MCTM result for a $4 \times 4 \times 4$ system after which three convolutions were applied each time the linear system size was doubled. The final simulation stage for $16 \times 16 \times 16$ system then required 9 iterations with 25×16^3 MCS per iteration. The final result was then averaged over 10 independent simulations, each of which required on average 43 minutes. Despite the reduction by a factor of 19 in the required CPU time, the RMCTM result for the specific heat, shown as the dotted line in Fig. 5.5 is nearly identical to that of the MCTM (solid line). When the system size was

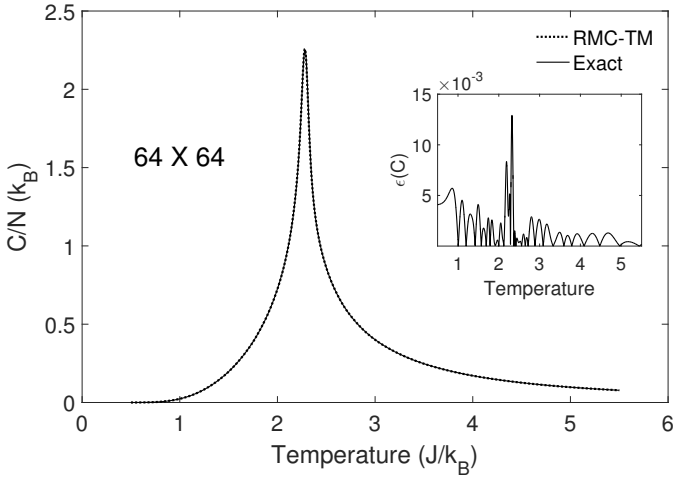

Figure 5.3: The RMCTM result for the specific heat per spin of the 64×64 Ising model averaged over 10 independent simulations (dotted line). The average relative error here equals 0.17%.

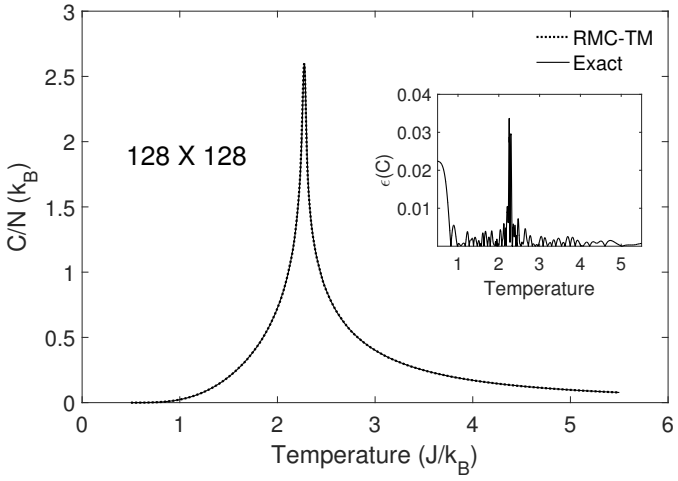

Figure 5.4: As in the previous figure but for the RMCTM applied to the 128×128 Ising model. The average relative error equals 0.27%.

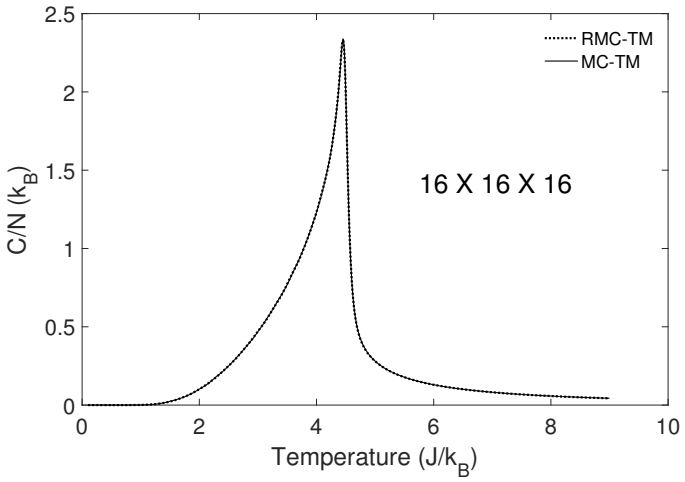

Figure 5.5: The specific heat per spin for the $16 \times 16 \times 16$ three-dimensional Ising model as calculated with RMCTM (dotted line) and MCTM (solid line).

further increased to $24 \times 24 \times 24$, the DOS and the specific heat of Fig. 5.6 were obtained in ≈ 490 minutes with the RMCTM. In the latter simulation, 8 iterations with 16×24^3 MCS/iteration were performed in the final step.

5.4 Scaling Behavior

In this section I investigate the dependence of the CPU time on system size at a prescribed level of computational accuracy for several algorithms that employ the TMMC. In particular, Fig. 5.7 displays the variation of the logarithm of the CPU time in minutes required to reach an average relative error $\epsilon(C)$ of between $0.1\% \sim 0.5\%$ as a function of the logarithm of the area $V = L^2$ of 2D Ising systems with linear size L for each of the hybrid TMMC algorithms discussed in the previous sections. The CPU times of all the methods obey power laws; however, the RMCTM possesses the smallest exponent. While the CPU times of both the WLTM and MCTM vary approximately as $V^{2.2}$ where the proportionality constant of the WLTM exceeds that of the MC-TM, those of the RTTM and RMCTM instead increase as $\sim V^{2.0}$ and $\sim V^{1.75}$ receptively. Precise linear fits to the MCTM and RMCTM curves yield the following scaling relations:

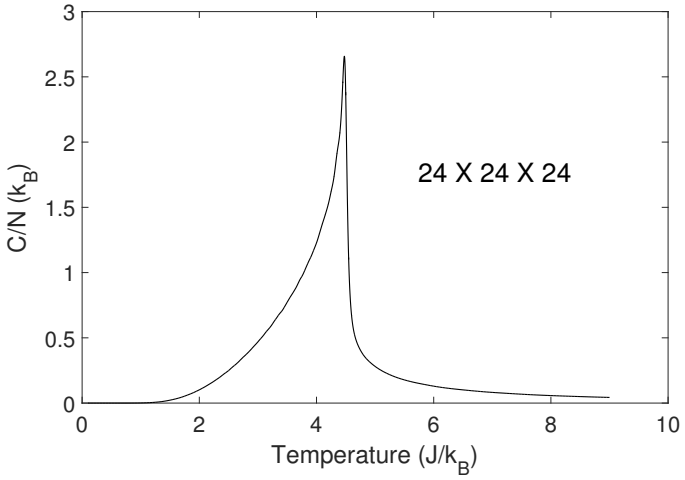

Figure 5.6: The specific heat per spin for the $24 \times 24 \times 24$ three-dimensional Ising model calculated with the RMCTM.

$$\tau_{CPU}^{MCTM} = e^{-12.1} V^{2.19}, \tag{5.2}$$
$$\tau_{CPU}^{RMCTM} = e^{-10.7} V^{1.75}, \tag{5.3}$$

The relative efficiency of MCTM and RMCTM can be expressed as a ratio of CPU times

$$r = \tau_{CPU}^{MCTM} / \tau_{CPU}^{RMCTM} = 0.247 V^{0.44}. \tag{5.4}$$

For $V = 128^2$, $r = 17.7$, indicating that for the 128×128 spin system, the RMCTM requires about 18 times less CPU time than the MCTM.

Turning to 3D Ising systems, the CPU times for MCTM and RMCTM calculations were obtained for several system sizes subject to the convergence criterion presented in the previous section. Fig. 5.8 displays the resulting log-log plots of the CPU times in minutes for the MCTM (squares), RMCTM (triangles) and the corresponding linear fits as a function of the system volume $V = L^3$. Linear fits yield the following relations:

$$\tau_{CPU}^{MCTM} = e^{-12.96} V^{2.36}, \tag{5.5}$$
$$\tau_{CPU}^{RMCTM} = e^{-9.94} V^{1.64}, \tag{5.6}$$
$$r = \tau_{CPU}^{MCTM} / \tau_{CPU}^{RMCTM} = 0.0488 V^{0.72}. \tag{5.7}$$

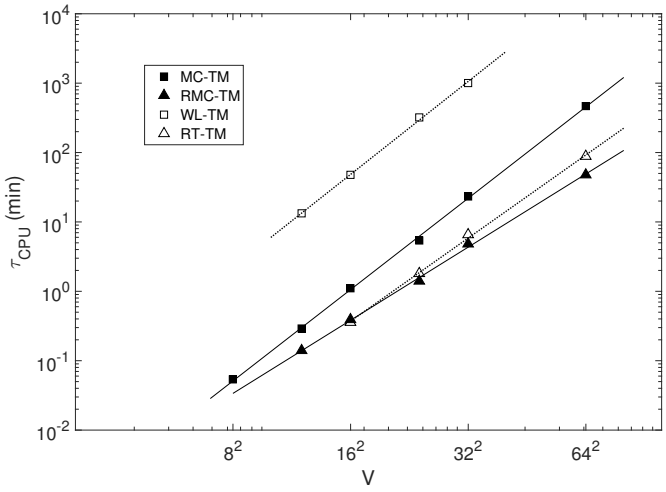

Figure 5.7: The scaling properties of the four methods employing the TMMC discussed in the text for the 2D Ising model together with the corresponding linear fits displayed as log-log plots of CPU time vs system area.

The significantly smaller slope of the RMCTM curve in Fig.5.8 shows that the relative efficiency of the renormalized procedure increases rapidly with system size. For instance, $r = 87$ for $V = 32^3$, which implies that the RMCTM will perform a 32^3 Ising model calculation 87 times faster than the MCTM.

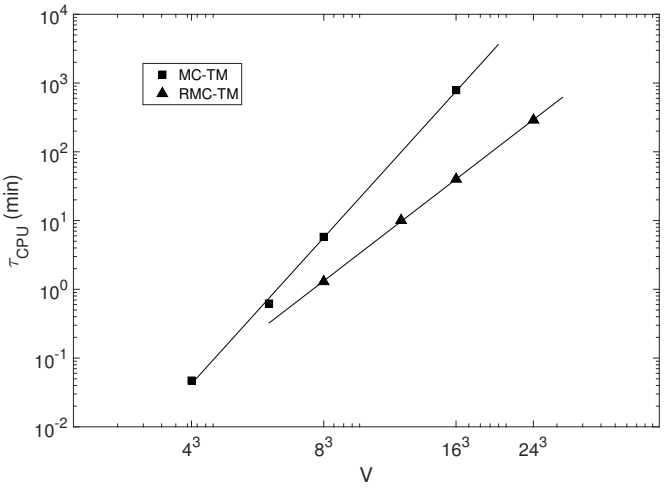

Figure 5.8: Log-log plots of the CPU time vs volume for the MCTM and RMCTM for 3D Ising systems.

Chapter 6

Bivariate Multicanonical Transition Matrix Methods

6.1 Introduction

As the thermodynamic variables of a system at any temperature can be obtained from the density of states (DOS) $g(E)$ by evaluating the partition function $Z = \sum_E g(E)e^{-\beta E}$, numerous methods, such as parallel tempering [22, 28], the broad histogram method [14], the multicanonical method [5, 6, 4, 24], the Wang-Landau algorithm [63, 64] and numerous variants of these [17, 61, 57] have been developed to estimate the DOS. The transition matrix Monte Carlo method (TMMC) [55, 66, 21] can further be combined with the above broad sampling procedures to generate the DOS with particularly high accuracy.

Quantities such as Landau free energy and the probability distribution of order parameter related variables, however, require the evaluation of the joint density of states (JDOS) $g(E, q)$ which depends on both the energy E and a second variable q which is associated with the order parameter. For lattice spin systems, q can represent either the magnetization or the spin overlap. The Landau free energy at a temperature T is given in terms of $g(E, q)$ by

$$F(q, T) = -k_B T \ln \left[\sum_E g(E, q) e^{-E/k_B T} \right], \tag{6.1}$$

where k_B is the Boltzmann constant. The order parameter corresponds to the value of q

that minimizes $F(q,T)$. The thermal average of any physical quantity $A(E,q)$ at temperature T is

$$\langle A(E,q)\rangle = \frac{1}{Z}\sum_{E,q} A(E,q)g(E,q)e^{-E/k_BT}, \tag{6.2}$$

where $Z = \sum_{E,q} g(E,q)\exp\left(-E/k_BT\right)$. The probability distribution of q at temperature T is

$$P(q,T) = \frac{1}{Z}\sum_{E} g(E,q)e^{-E/k_BT}. \tag{6.3}$$

F. Wang and D. P. Landau applied the bivariate version of Wang-Landau algorithm to the three-dimensional (3D) Ising spin glass [65]. The bivariate version of multicanonical sampling was applied to the 3D Ising spin glass by N. Hanato and J. E. Gubernatis [26]. M. S. Kalyan *et al* calculated the Landau free energies of various models using a modified Wang-Landau algorithm which is called two level method [29] . However, the computational effort required to obtain a reasonable level of accuracy with the bivariate version of Wang-Landau is excessive while despite relatively shorter computation times the JDOS obtained with the bivariate version of multicanonical method is not sufficiently accurate to provide a reliable result for Eq. (6.2) [34].

The TMMC has been successfully applied to various systems for accurate DOS calculations in many different hybrid forms in which it is combined with various methods such as Wang-Landau algorithm, multicanonical sampling and simulated annealing [50, 7, 23, 27, 71, 73, 34]. In this thesis, I demonstrate that the TMMC can be combined with the bivariate version of multicanonical sampling as well to generate an accurate JDOS with a high degree of computational efficiency. This method is called *bivariate multicanonical transition matrix Monte Carlo* method (BMCTM) in this thesis. In the next section, the simulation method is explained in detail. Subsequently, as an initial test, I apply the method to Ising models and Potts models to calculate the Landau free energies of systems some of which exhibit second order phase transitions, others of which do not. To demonstrate the applicability of the BMCTM to complex systems, the Landau free energies, the distributions of spin overlaps and the Binder parameters of the 2D and 3D Ising spin glasses are evaluated. The evidences that may imply the nonzero temperature phase transition of the 2D spin glass are presented.

6.2 Bivariate Multicanonical Transition Matrix Monte Carlo Method

6.2.1 Bivariate Multicanonical Sampling

The bivariate multicanonical method straightforwardly extends the monovariate procedure to realize a random walk in a two-dimensional space. To generate the two dimensional random walk, the multicanonical weight $w_{mu} = 1/g(E, q)$ is first determined. The iterative procedure is initialized by setting $g^{(1)}(E, q) = 1$. In the kth iteration, the transition from a state with E and q to a state with E' and q' is accepted with probability

$$P_{acc} = \min\left[\frac{g^{(k)}(E, q)}{g^{(k)}(E', q')}, 1\right]. \tag{6.4}$$

The number of samples $N_s^{(k)}$ in the kth iteration is preset to insure that the histogram $h^{(k)}(E, q)$ attains a certain degree of flatness. Usually $N_s^{(k)}$ is increased as the iteration proceeds since the size of the sampling region expands with k. Once kth iteration terminates after taking $N_s^{(k)}$ samples, $(k + 1)$th iteration begins with

$$g^{(k+1)}(E, q) = g^{(k)}(E, q)h^{(k)}(E, q). \tag{6.5}$$

If the ground state or the most rare state is visited, normally in the next iteration the histogram becomes flat in the entire region of interest and the iteration procedure ends. In a typical bivariate multicanonical simulation, an estimate of $g(E, q)$ can be used to construct a multicanonical ensemble of samples with high statistics. The thermal averages of the physical quantities of interest can be determined by the unweighting and reweighting techniques. However, in a bivariate TMMC method, the transition tensor is constructed during the iteration procedure as explained below.

6.2.2 Bivariate TMMC

Let us denote the transition probability from a state with E_I and q_J to a state with E_K and q_L by W_{IJKL}. Then,

$$\sum_{K,L} W_{IJKL} = 1. \tag{6.6}$$

Using the exactly same reasoning as explained in Sec. 3.2, the following can be derived:

$$g(E_I, q_J) = \sum_{K,L} g(E_K, q_L) W_{KLIJ}, \tag{6.7}$$

which implies that the JDOS $g(E, q)$ is the unit left eigenmatrix of the four-dimensional transition tensor W. Eq. (6.7) can be transformed to a matrix form corresponding to Eq. (2.49) by reducing the number of indices. For instance, if $g(E_I, q_J)$ is a $(m \times n)$ matrix, define $\tilde{g}$ and $\tilde{W}$ as

$$\tilde{g}_{\tilde{I}} = g(E_I, q_J), \ \tilde{I} = n(I-1) + J, \tag{6.8}$$

$$\tilde{W}_{\tilde{I},\tilde{J}} = W_{IJKL}, \ \tilde{I} = n(I-1) + J, \ \tilde{J} = n(K-1) + L. \tag{6.9}$$

Then the following relation is obtained:

$$\tilde{g}_{\tilde{I}} = \sum_{\tilde{J}} \tilde{g}_{\tilde{J}} \tilde{W}_{\tilde{J}\tilde{I}}. \tag{6.10}$$

Accordingly, the standard TMMC can be applied to the simulations for JDOS provided that W is populated efficiently. In this thesis, we employ the iteration procedure of the bivariate multicanonical sampling to populate W. In the iteration procedure, if there is a proposal of the transition from a state with E and q to a state with E' and q', *irrespective of acceptance*, W is updated according to

$$W(E, q, E', q') = W(E, q, E'q') + 1. \tag{6.11}$$

When the iteration procedure terminates, the calculation of the unit left eigenvector of $\tilde{W}$ is performed to obtain an estimate of the JDOS which is generally more accurate than the multicanonical estimate.

The downside of the BMCTM is that it requires large memory to store the transition tensor W and the histogram $h(E, q)$. The additional CPU time to calculate the eigenmatrix of W also grows fast as the system size increases. Thus for the case where the JDOS with a moderate accuracy is enough, the estimate of the JDOS obtained in the Muca iteration procedure can be used without the additional effort to handle W. The high computational cost of the BMCTM for the evaluation of the more accurate JDOS can be reduced by parallelizing the procedure or adopting the renormalized version which is explained in the next subsection.

6.2.3 Renormalized Version

Renormalized multicanonical sampling, as presented in chapter 5 in the context of the Ising model, considerably reduces the computation time of the multicanonical iteration procedure by providing an accurate initial estimate of the DOS. This estimate is obtained by convolving the simulation results of smaller systems according to the prescription of Ref. [70, 34]. Renormalized sampling can be adapted to the bivariate version of the multicanonical sampling by instead convolving the normalized bivariate probability densities:

$$P_L(E,q) = \sum_{E_i,q_i} P_S(E_i,q_i) P_S(E-E_i, q-q_i), \tag{6.12}$$

where $P_L(E,q)$ and $P_S(E_i,q_i)$ are the normalized JDOS's for a large and a small systems respectively.

However, to apply this methods, the coupling constant between neighbour spins should be uniform throughout the entire system. For systems with nonuniform coupling constants such as spin glasses in which the coupling constant is a random variable, this method can not be used.

6.3 Numerical Results

6.3.1 Ising Model

The Hamiltonian of an Ising spin system consisting of N spins with nearest neighbour interactions is given by $H = -J\sum_{\langle i,j\rangle} s_i s_j$. The second variable of JDOS is the magnetization $M = \sum_{i=1}^{N} s_i/N$ whose thermal average is the order parameter. The JDOS $g(E,M)$ of an 1D Ising spin system of 200 spins was obtained by the BMCTM. The Landau free energy $F(M,T)$, which is calculated by Eq. (6.1), is plotted in FIG. 6.1 at four different temperatures. The lack of a minimum of F except at $M = 0$ demonstrates that a finite temperature second order phase transition is absent in the 1D Ising spin systems.

It is well known that the 2D Ising model exhibits a finite temperature($T_c = 2.269J$) second order phase transition in the thermodynamic limit. BMCTM was next applied to a 16×16 square lattice Ising spin system to calculate the JDOS $g(E,M)$ and the Landau free energy $F(M,T)$ which is plotted in FIG. 6.2. For comparison, the rescaled Landau free energies at three different temperatures near T_c are plotted in FIG. 6.3. The

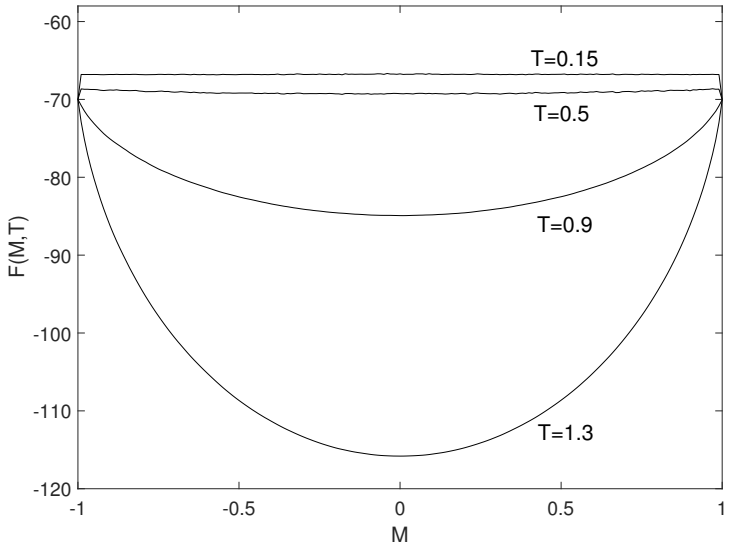

Figure 6.1: The Landau free energy $F(M,T)$ of an 1D Ising spin system of 200 spins at several different temperatures in units of J.

emergence of global minima of F at nonzero M establishes the presence of a second order phase transition. As a result of the small system size, the curve for F already starts to form minima at nonzero magnetizations for $T \approx 2.5J$. The precise value of T_c can be determined by calculating the Binder parameters which are calculated for Ising spin glasses in Sec. 6.4.3.

6.3.2 Two-dimensional Potts Model

The Hamiltonian of a r-state 2D Potts model with N spins is given by $H = -J\sum_{\langle i,j\rangle}\delta_{s_i,s_j}$ where $s_i = 1, 2, \cdots, r$. The second variable of the JDOS is the magnetization $M = (rN_m/N - 1)/(r-1)$ where N_m is the number of the majority spins in a spin configuration. A continuous phase transition occurs for $r \leq 4$ and a first order phase transition for $r > 4$.

The BMCTM was applied to 3-state and 10-state 8×8 Potts models. The Landau free energy of a 3-state Potts model is plotted in FIG. 6.4 and FIG. 6.5. The value of M that minimizes $F(M,T)$, which corresponds to $\langle M\rangle$, varies continuously from a near zero value towards unity as the temperature decreases. The abrupt change in $\langle M\rangle$ occurs at $T \approx 1.1J$, which approximates the exact value of $T_c = 0.995J$.

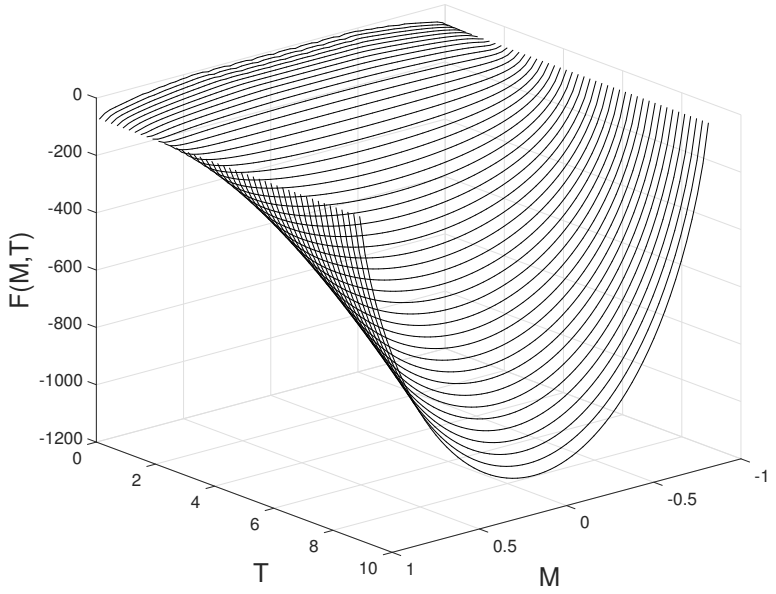

Figure 6.2: The Landau free energy $F(M,T)$ of a 16×16 square lattice Ising spin system.

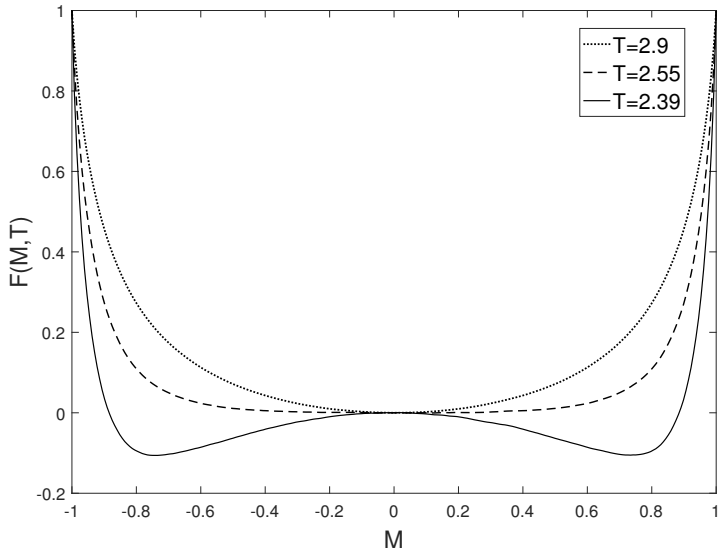

Figure 6.3: The rescaled Landau free energies of a 16×16 square lattice Ising spin system at three different temperatures(in units of J) near T_c.

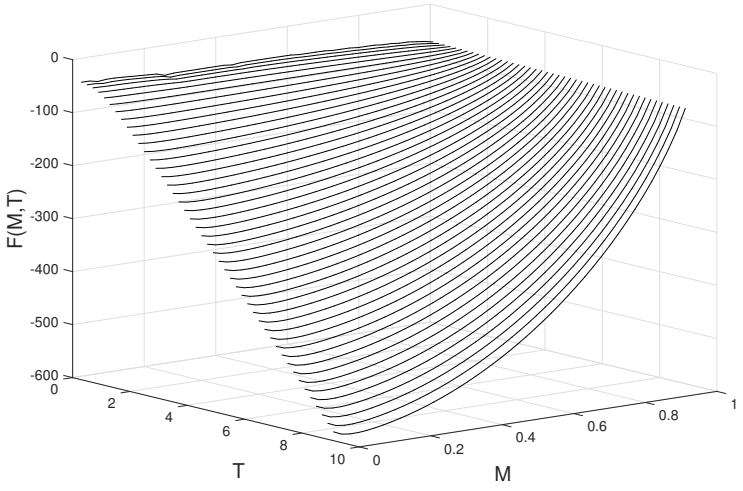

Figure 6.4: The Landau free energy $F(M, T)$ of a 8×8 3-state Potts model.

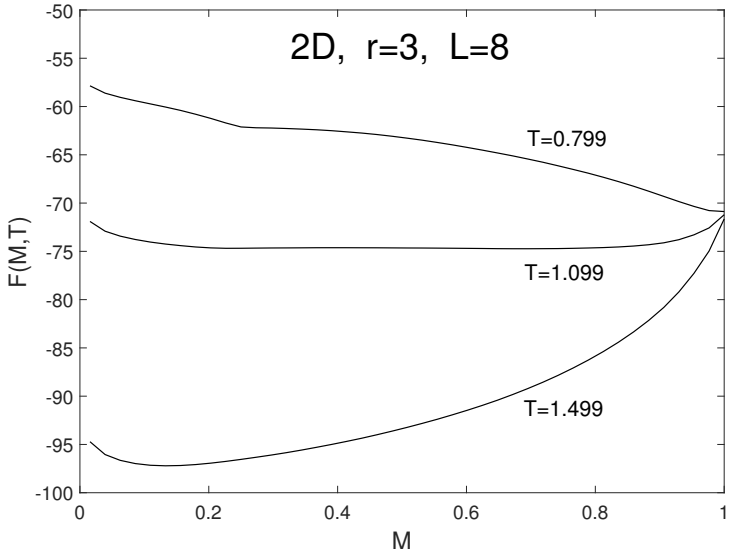

Figure 6.5: The Landau free energies of a 8×8 3-state Potts model at three different temperatures(in units of J) near T_c.

FIG. 6.6 displays the Landau free energies of a 8×8 10-state Potts model at three different temperatures near $T_c = 0.7012J$. From the curve of $F(M,T)$ at $T = 0.72J$, two coexisting phases with small and large M are apparent. The transitions of the shape of $F(M,T)$ near T_c shows that $\langle M \rangle$ jumps from near zero to near unity almost discontinuously indicating a first order phase transition.

6.3.3 Ising Spin Glasses

Spin glasses are randomly diluted magnetic alloys such as AuFe or CuMn in which a tiny percentage of magnetic ions are randomly scattered in a non-magnetic host metal. The interaction between the magnetic atoms in a spin glass is described by the RKKY interaction which is

$$J_{ij} = J_0 \frac{\cos(2k_F r_{ij}) - (2k_F r_{ij})^{-1} \sin(2k_F r_{ij})}{(k_F r_{ij})^3} \sim J_0 \frac{\cos(2k_F r_{ij})}{(k_F r_{ij})^3}, \tag{6.13}$$

where k_F is the Fermi wave number of the host conduction electrons and r_{ij} is the distance between two interacting magnetic atoms. Note the sign of the exchange interaction

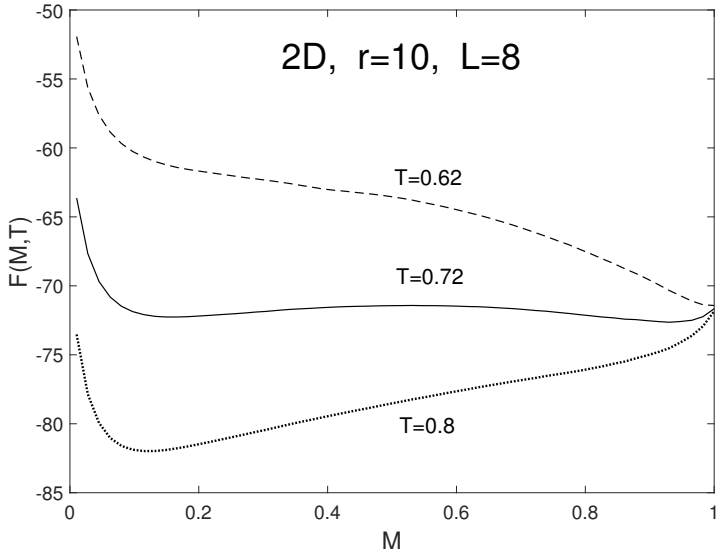

Figure 6.6: The Landau free energies of a 8×8 10-state Potts model at three different temperatures(in units of J) near T_c.

depends on the distance between the two magnetic atoms. Since magnetic atoms are randomly dispersed, there are roughly equal number of ferromagnetic and antiferromagnetic interactions in a spin glass. In 1972, V. Cannella and J. A. Mydosh [12] found a sharp cusp in the frequency dependent magnetic susceptibility which is reminiscent of the critical behavior associated with a typical second order phase transition. A few years later, Edwards and Anderson [15] introduced a theoretical model (EA model) of spin glasses that exhibits the essential properties of real spin glasses. The Hamiltonian of the EA model is

$$H = -\sum_{\langle i,j \rangle} J_{ij} \vec{s}_i \cdot \vec{s}_j, \tag{6.14}$$

where J_{ij} is a random variable with zero mean. If $\vec{s}_i$ takes only up or down orientation along a fixed direction ($s_i = \pm 1$), it is called Ising spin glass.

Ever since the work of Edwards and Anderson, intensive theoretical and experimental efforts have been made to understand the nature of spin glass ordering for decades. Immediately after the introduction of the EA model, Sherrington and Kirkpatrick [51] introduced a mean-field model (SK model) which replaces the short range interaction in the EA model with an unphysical infinite range interaction between all the spins. Soon

after, the Sherrington and Kirkpatrick's solution of the SK model, which was obtained by the use of replica trick, was found to be unstable with negative entropy. In 1979, G. Parisi presented a stable solution of SK model and introduced a novel concept of *replica symmetry breaking* [46]. Parisi's theory brought up an unprecedented level of complexity in the theoretical research of spin glasses. A new theory based on a scaling hypothesis on local excitations, which is called *droplet picture*, emerged [39, 20] and predicted conclusions strikingly different from the ones derived by the *replica symmetry breaking picture*. The different conclusions from the two different pictures regarding spin glasses with a short range interaction are still controversial. The problem of spin glasses, which has a long history, is rich and profound. Even mentioning the major experimental, theoretical and simulational issues in this problem is beyond the scope of this thesis because the focus of this thesis is developing efficient and accurate MC algorithms. The detailed information about spin glasses can be found, e.g., in [11, 41, 44, 56].

Two essential ingredients of a spin glass are *randomness* and *frustration*. Randomness means the locations of magnetic atoms and the directions of its spins are random. This is reflected in the random variable J_{ij} of the EA model. The randomness or the disorder encapsulated in J_{ij} is called *quenched* since it remains fixed during the evaluation of a thermal average. Frustration refers to the situation where no configuration of the system can simultaneously minimize each term of the Hamiltonian. A simple example illustrating frustration is shown in Fig. 6.7. A "+" indicates ferromagnetic interaction with which spins prefer parallel alignment and a "-" indicates antiferromagnetic interaction with which spins have to be antiparallel to lower the interaction energy. Note, regardless of the direction of spin 4, the interaction energy of spin 1 and spin 4 and the interaction energy of spin 3 and spin 4 can not be simultaneously minimized. This competition between ferromagnetic and antiferromagnetic interactions results in multiple local minima in the free energy (called *rugged energy landscape*) which makes it extremely non-trivial to determine the ground state as well as to reach a thermal equilibrium at low temperature. Due to the extremely slow relaxation process, despite the numerous Monte Carlo simulations performed for decades, many questions regarding the low temperature nature of spin glasses are still unanswered.

A d-dimensional Ising spin glass of $N = L^d$ spins on a hypercubic lattice with nearest neighbour interactions is described by the Hamiltonian

$$H = -\sum_{\langle i,j \rangle} J_{ij} s_i s_j, \tag{6.15}$$

where $s_i = \pm 1$ and J_{ij} is a random variable. The distribution of the random bonds $\{J_{ij}\}$

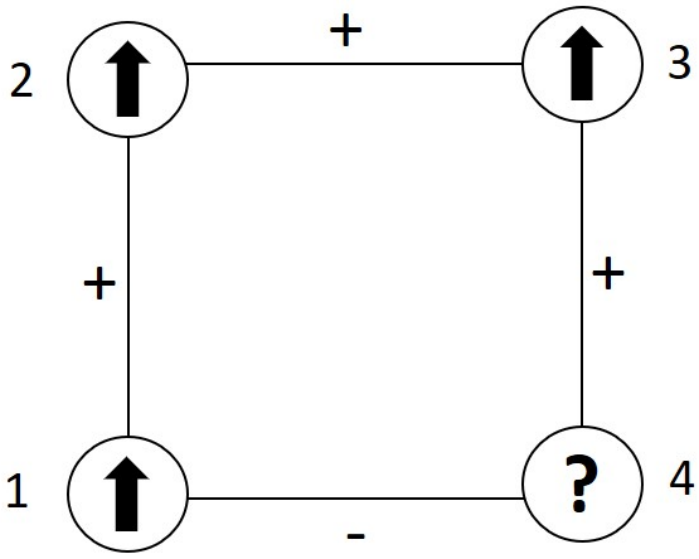

Figure 6.7: A simple example illustrating frustration. A "+" indicates ferromagnetic interaction with which spins prefer parallel alignment and a "-" indicates antiferromagnetic interaction with which spins have to be antiparallel to lower the interaction energy. No matter what direction spin 4 takes, the interaction energy of spin 1 and spin 4 and the interaction energy of spin 3 and spin 4 can not be simultaneously minimized.

in the $\pm J$ model (or bimodal model) is defined as

$$P(J_{ij}) = \frac{1}{2}\delta(J_{ij} + J) + \frac{1}{2}\delta(J_{ij} - J). \tag{6.16}$$

and in the Gaussian model

$$P(J_{ij}) = \frac{1}{\sqrt{2\pi}\Delta J} \exp\left(-J_{ij}^2/\Delta J^2\right), \tag{6.17}$$

where the variance ΔJ is typically set to unity. The order parameter of a spin glass system is defined as

$$q_{EA} = \left[\lim_{t\to\infty} \frac{1}{N}\sum_{i=1}^{N} \langle s_i(0)s_i(t)\rangle\right]_{av} = \left[\frac{1}{N}\sum_{i=1}^{N}\langle s_i\rangle^2\right]_{av}, \tag{6.18}$$

where $[\cdots]_{av}$ indicates an average over the quenched random couplings $\{J_{ij}\}$, i.e.,

$$\left[A_{\{J_{ij}\}}\right]_{av} = \prod_{\langle i,j\rangle} \int dJ_{ij} A_{\{J_{ij}\}} P(J_{ij}). \tag{6.19}$$

If N_s samples(N_s different realizations of $\{J_{ij}\}$) are taken,

$$\left[A_{\{J_{ij}\}}\right]_{av} \approx \frac{1}{N_s}\sum_{m=1}^{N_s} A_{\{J_{ij}\}_m}. \tag{6.20}$$

For the JDOS $g(E,q)$ of a spin glass system, the second variable q can be defined as

$$q = \frac{1}{N}\sum_{i=1}^{N} s_i s_i^g, \tag{6.21}$$

where $\{s_i^g\}$ is a ground state spin configuration. $[\langle q\rangle]_{av}$ is not exactly identical to q_{EA}, but its behavior is quite similar to q_{EA} [42, 65]. Once the JDOS $g_J(E,q)$ of a spin glass system with one realization of the random couplings $\{J_{ij}\}$ is given, the Landau free energy $F_J(q,T)$ can be calculated by Eq. (6.1) and the random average $F(q,T) = [F_J(q,T)]_{av}$ can be obtained from Eq. (6.20). The probability distribution of q which is denoted by

$P_J(q,T)$ and its random average $P(q,T) = [P_J(q,T)]_{av}$ are calculated by Eq. (6.3) and Eq. (6.20) respectively. With $P(q,T)$, the average of any q dependent quantity $f(q)$ can be calculated by

$$[\langle f(q)\rangle]_{av} = \sum_q f(q)P(q,T). \tag{6.22}$$

The Binder parameter, which is defined as

$$g_L(T) = \frac{1}{2}\left[3 - \frac{[\langle q^4\rangle]_{av}}{[\langle q^2\rangle]^2_{av}}\right], \tag{6.23}$$

is particularly important because the curves of $g_L(T)$ for different values of L intersect at T_c. More common method for the evaluation of $g_L(T)$ is to use a two-replica system consisting of two identical systems with the same couplings $\{J_{ij}\}$. As the two replicas are thermodynamically independent, the Hamiltonian is

$$\mathcal{H} = -\sum_{\langle i,j\rangle} J_{ij} s_i^{(1)} s_j^{(1)} - \sum_{\langle i,j\rangle} J_{ij} s_i^{(2)} s_j^{(2)}, \tag{6.24}$$

where the superscript indicates each replica in the system. For the two-replica system, the spin overlap is defined as

$$q = \frac{1}{N}\sum_{i=1}^{N} s_i^{(1)} s_i^{(2)}. \tag{6.25}$$

This can be regarded as the average of the multiplication of spins of two configurations at infinitely remote moments. Thus $[\langle q\rangle]_{av}$ is identical to q_{EA} defined in Eq. (6.18). The probability distribution function of the spin overlap can be calculated from the JDOS of the two-replica system using Eq. (6.3).

After the extensive theoretical, numerical and experimental studies on spin glasses that have been done for decades, now it is widely believed that a spin glass phase transition occurs at a finite, nonzero temperature ($T_c \approx 1.1J$) in 3D [37, 30, 45, 1] and at zero temperature ($T_c = 0$) in 2D [54, 25, 9]. However there are still other works that claim a nonzero phase transition temperature in 2D [53, 52].

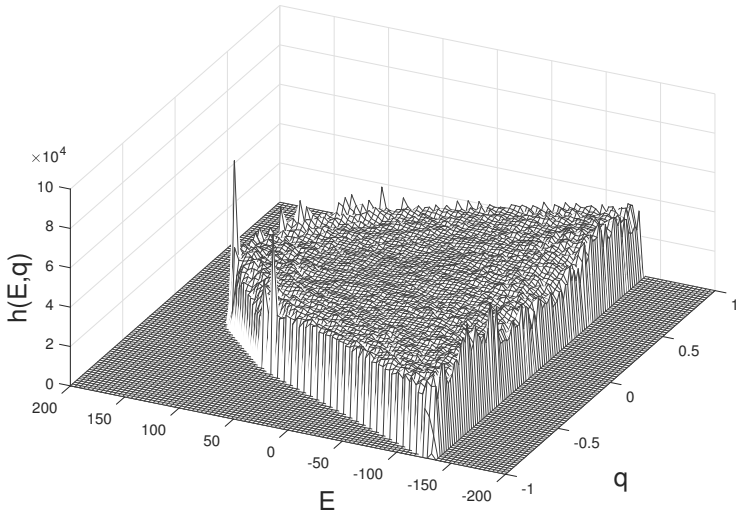

Figure 6.8: The joint histogram of the visited states in the last stage of the iteration procedure of the BMCTM for a 10×10 $\pm J$ Ising spin glass. It is almost flat in the 2D E-q space.

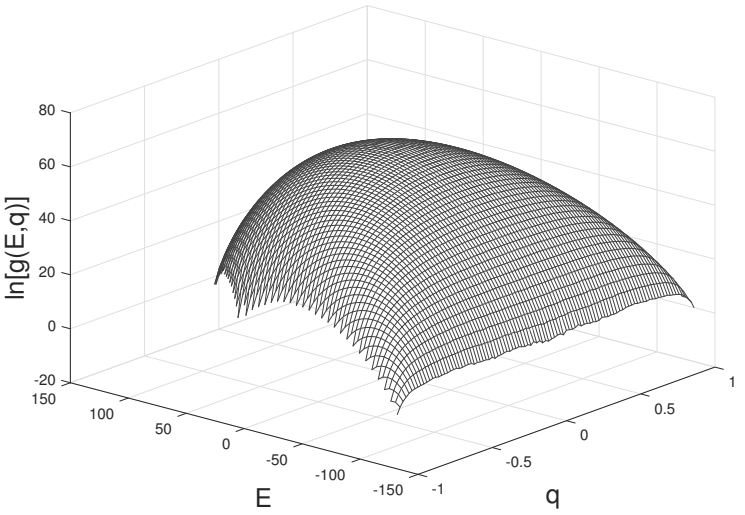

Figure 6.9: The logarithm of the JDOS $g(E, q)$ of a 10×10 $\pm J$ Ising spin glass obtained by the BMCTM.

I carried out BMCTM simulations for 2D spin glasses with bimodal and Gaussian bonds up to $L = 14$ and 3D spin glasses with bimodal bonds up to $L = 8$. To obtain the Landau free energy $F(q, T)$, the BMCTM simulation with the Hamiltonian given in Eq. (6.15) and the second variable q given in Eq. (6.21) was performed repeatedly for many different realizations of $\{J_{ij}\}$ and the average was computed according to Eq. (6.20). The joint histogram of the visited states and the JDOS acquired from the BMCTM simulation for a 10×10 system are shown in FIG. 6.8 and FIG. 6.9 respectively. The nearly flat histogram implies that a random walk in E-q space was realized and a good statistics was obtained even for the least probable states. The symmetry $g(E, -q) = g(E, q)$, which is due to the global spin reversal symmetry of the Hamiltonian, can be used to reduce the simulation time by limiting the sampling region. For the evaluation of the Binder parameter, the Hamiltonian of the two-replica system given in Eq. (6.24) and the spin overlap q given in Eq. (6.25) should be employed in the BMCTM simulation since the second variable q given in Eq. (6.21) can not represent all possible spin overlaps especially when the degeneracy is high. From the symmetry of the Hamiltonian of the two-replica system, $g(E, -q) = g(E, q)$ and $g(-E, q) = g(E, q)$ can be derived, which can be utilized to reduce the simulation time significantly. The probability distribution of the spin overlap $P(q, T)$ obtained from the BMCTM simulations with the two-replica Hamiltonian for a 12×12 system is plotted in FIG. 6.10.

For a $6 \times 6 \times 6$ 3D $\pm J$ Ising spin glass, the typical rugged shape of the Landau free energy at low temperature obtained by the BMCTM simulation is shown in FIG. 6.11. The average Landau free energy of 100 samples (i.e., 100 randomly chosen realizations of the bimodal bonds) is shown in FIG. 6.12. To increase visibility, the rescaled Landau free energies at four different temperatures are plotted in FIG. 6.13. The behavior of the Landau free energy apparent in FIG. 6.12 and FIG. 6.13 implies a continuous phase transition at a nonzero temperature. To evaluate the Binder parameters, 310, 54 and 21 samples were taken for $L = 4$, 6 and 8 respectively. As shown in FIG. 6.14, even with these limitted number of samples, the curves of g_L intersect at $T \sim 1.15J$ which is nearly equal to the result of previous studies $T_c \approx 1.1J$.

The average Landau free energy of 100 samples for a 10×10 system with $\pm J$ bonds were obtained by the BMCTM. Contrary to my expectation, as shown in FIG. 6.15, the rescaled Landau free energies at four different temperatures exhibit a feature of a continuous phase transition at a nonzero temperature. To find a more reliable evidence, the Binder parameters shown in FIG. 6.16 were obtained from 1100, 800, 616, 284 and 173 independent BMCTM simulations for $L = 6$, 8, 10, 12 and 14 respectively. The curves of g_L for various L cross at almost the same temperature of $T \sim 0.45J$ which is surprisingly high. This appears to imply a nonzero temperature phase transition in the 2D spin glass with $\pm J$

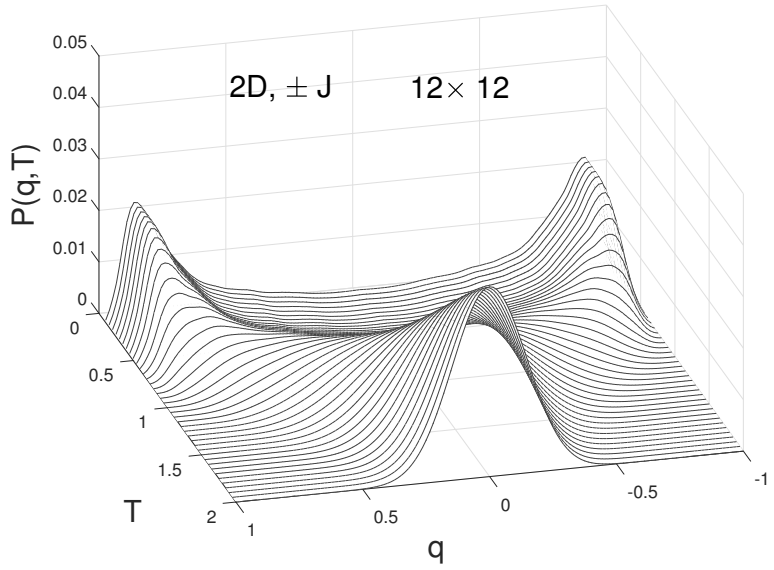

Figure 6.10: The probability distribution of the spin overlap q as a function of temperature T for a 12×12 $\pm J$ Ising spin glass. The simulation results of 140 samples were averaged to yield this.

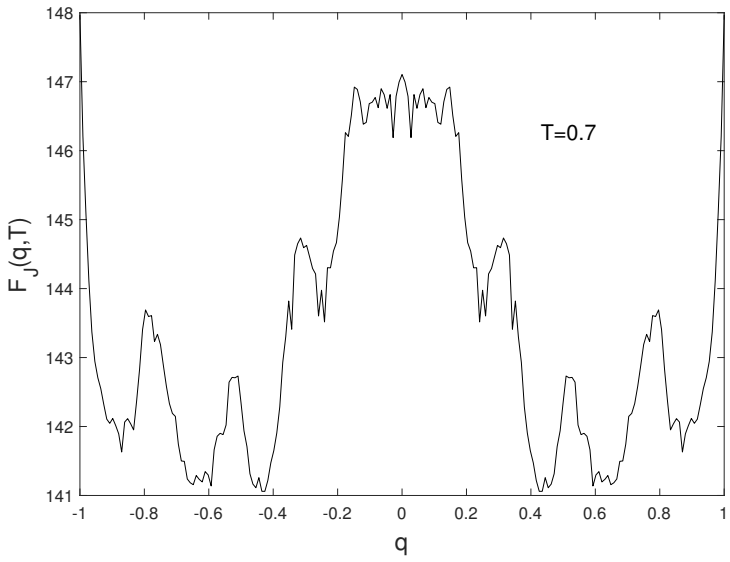

Figure 6.11: The Landau free energy of a $6 \times 6 \times 6$ $\pm J$ Ising spin glass with one realization of $\{J_{ij}\}$ at $T = 0.7J$.

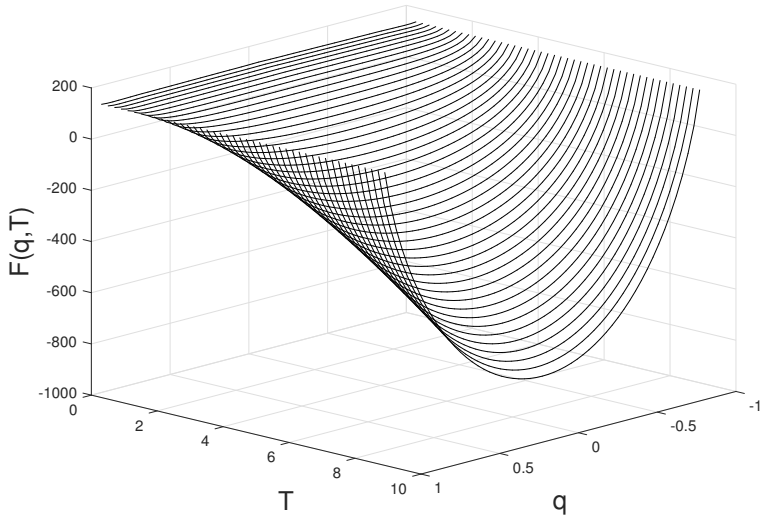

Figure 6.12: The Landau free energy of a $6 \times 6 \times 6$ $\pm J$ Ising spin glass.

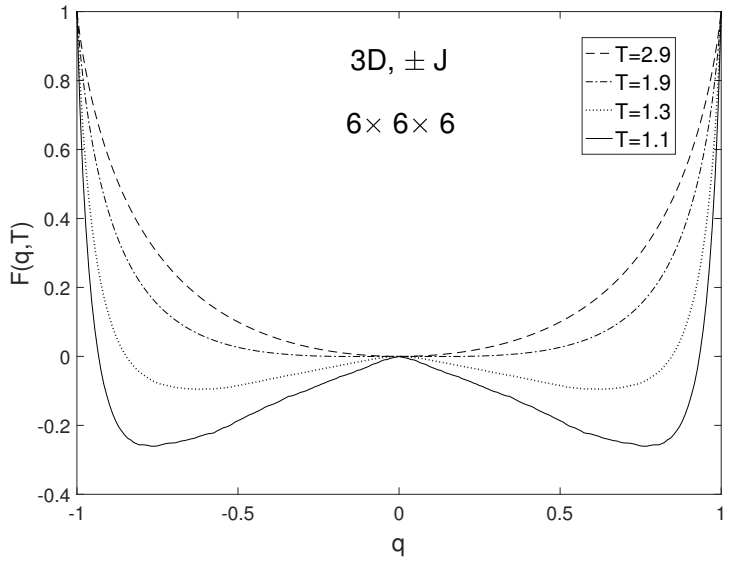

Figure 6.13: The plots of the rescaled Landau free energy at four different temperatures(in units of J) for a $6 \times 6 \times 6$ $\pm J$ Ising spin glass.

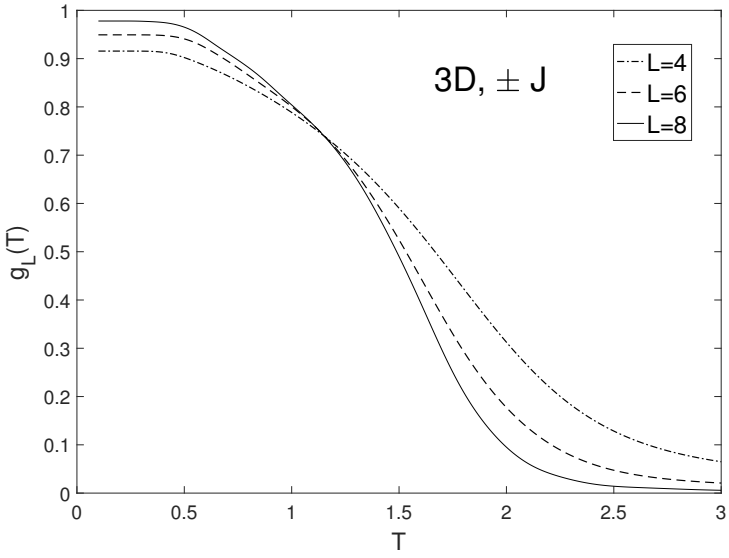

Figure 6.14: The temperature dependence of the Binder parameters for 3D $\pm J$ Ising spin glass with $L = 4$, 6 and 8.

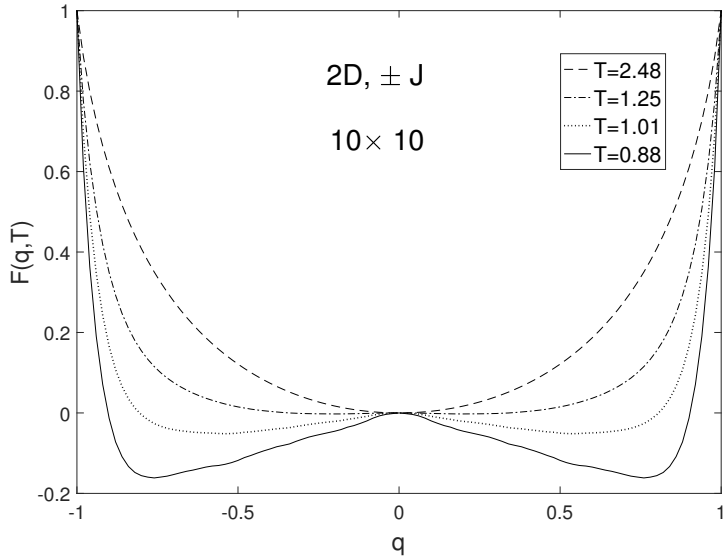

Figure 6.15: The plots of the rescaled Landau free energy at four different temperatures(in units of J) for a 10×10 $\pm J$ Ising spin glass.

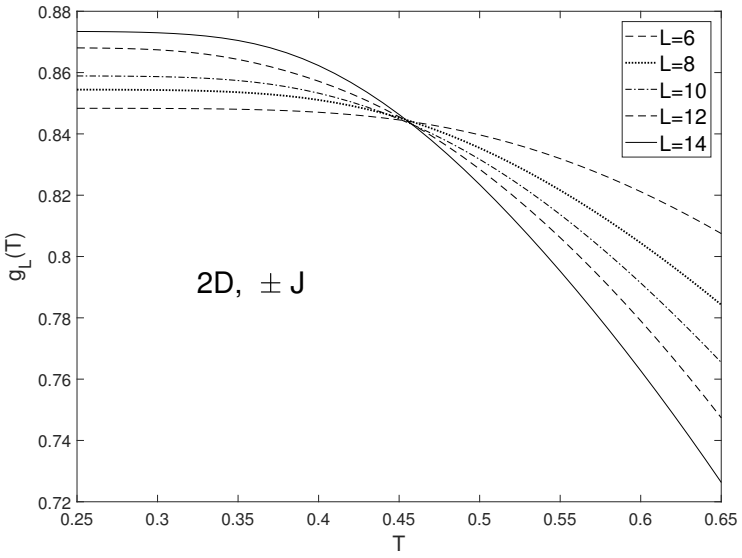

Figure 6.16: The temperature dependence of the Binder parameters for 2D $\pm J$ Ising spin glass with $L = 6$, 8, 10, 12 and 14.

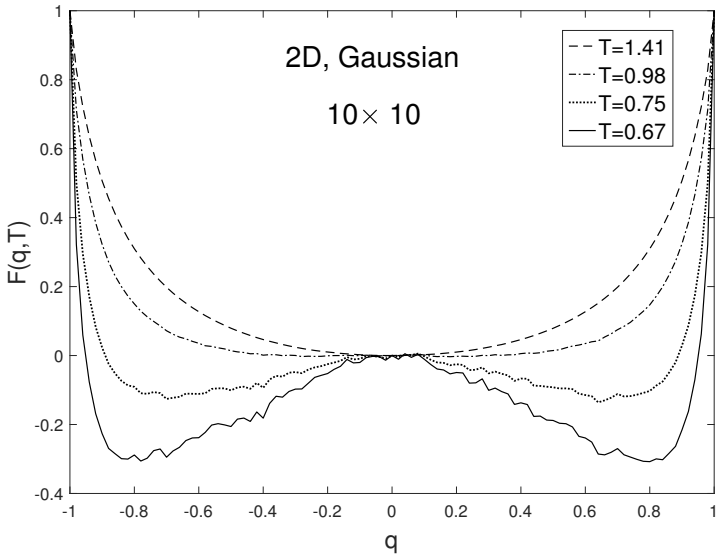

Figure 6.17: The plots of the rescaled Landau free energy at four different temperatures for a 10×10 Gaussian Ising spin glass.

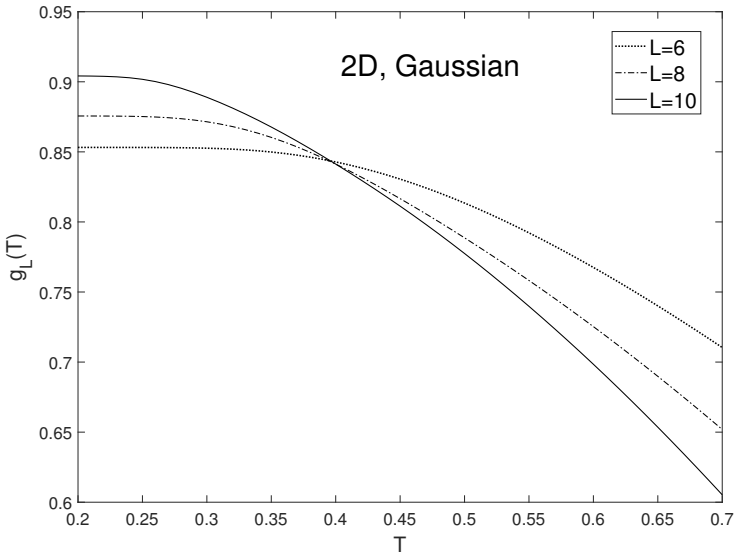

Figure 6.18: The temperature dependence of the Binder parameters for $L = 6$, 8 and 10.

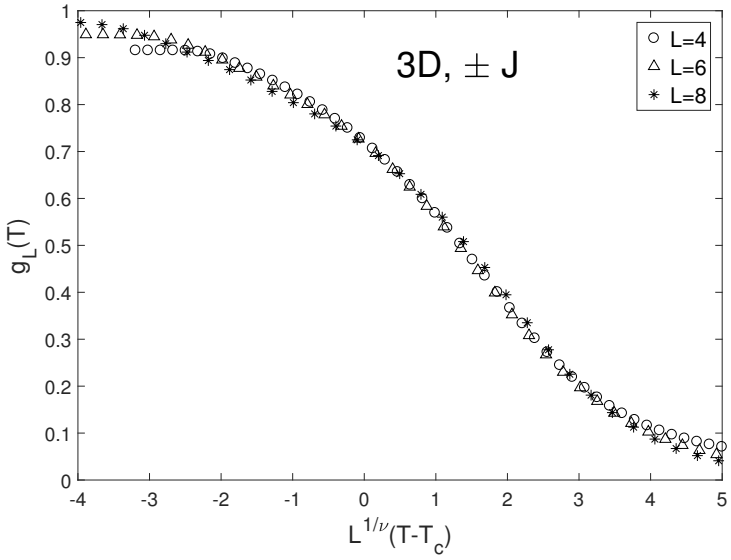

Figure 6.19: Scaling plot of g_L of the 3D $\pm J$ Ising spin glass according to Eq. (6.26) with $\nu = 1.3$ and $T_c = 1.2J$.

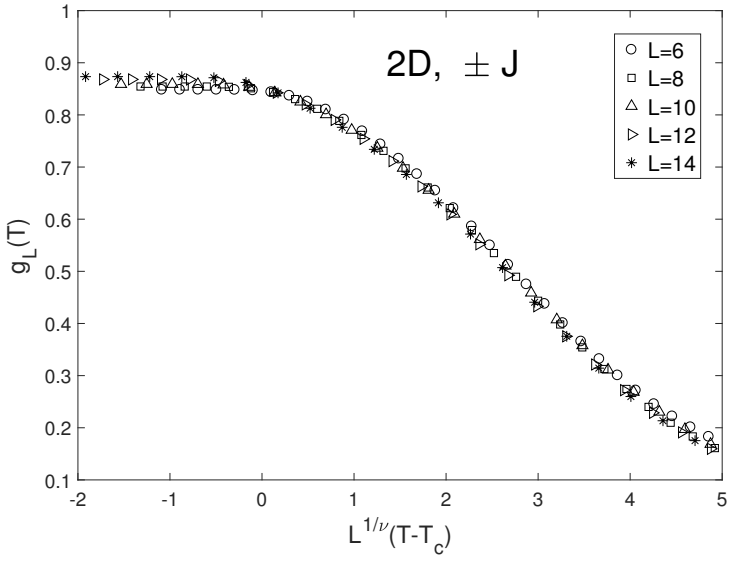

Figure 6.20: Scaling plot of g_L of the 2D $\pm J$ Ising spin glass according to Eq. (6.26) with $\nu = 1.5$ and $T_c = 0.43J$.

interactions. As shown in FIG. 6.17 and FIG. 6.18, I obtained the same results for the 2D spin glass with Gaussian interactions as well. The scaling behavior of g_L is expected to follow

$$g_L(T) = \bar{g}(L^{1/\nu}(T - T_c)), \tag{6.26}$$

where $\bar{g}$ is a scaling function and ν is the exponent of the correlation length [8]. For the 3D $\pm J$ spin glass, with $\nu = 1.3$ and $T_c = 1.2J$, a scaling plot of the data in FIG. 6.14 was obtained according to Eq. (6.26) as shown in FIG. 6.19. For the 2D $\pm J$ spin glass, with $\nu = 1.5$ and $T_c = 0.43J$, a scaling plot of the data in FIG. 6.16 is displayed in FIG. 6.20. It seems that the data collapses of g_L are acceptable in the scaling plots for both 2D and 3D.

The spin glass susceptibility when approached from high temperature is given by

$$\chi_{SG}(T) = N\left[\langle q^2\rangle\right]_{av} = N\sum_q q^2 P(q,T). \tag{6.27}$$

The spin glass susceptibility χ_{SG} diverges as T approaches T_c from above. χ_{SG} also has the following scaling form:

$$\chi_{SG} = L^{2-\eta}\bar{\chi}(L^{1/\nu}(T - T_c)), \tag{6.28}$$

where η describes the power law decay the spin correlation at T_c and $\bar{\chi}$ is a scaling function. For the 3D $\pm J$ spin glass, with $\nu = 1.3$, $\eta = -0.27$ and $T_c = 1.2J$, a scaling plot of χ_{SG} is displayed in FIG. 6.21. With $\nu = 1.5$, $\eta = 0.20$ and $T_c = 0.43J$, a scaling plot of χ_{SG} for the 2D $\pm J$ spin glass is shown in FIG. 6.22. Compared to the χ_{SG} for 2D, the quality of the data collapse of the χ_{SG} for 3D does not look good. This is possibly due to insufficient number of samples in the simulations for 3D systems.

All the results of the Landau free energy, the Binder parameters and the scaling analysis seem to support a nonzero temperature phase transition in the 2D Ising spin glass, which is an interesting result because this is contrary to the current consensus. I believe the JDOSs of spin glasses obtained by the BMCTM are very accurate since the accuracy of the method was proven in the applications to the Ising and Potts models. However, I can not definitely conclude that $T_c \neq 0$ for the 2D Ising spin glass because of the limitted number of samples. The number of different sets of random couplings $\{J_{ij}\}$ is huge; it is the order of 10^{20} (however, many of them would be identical due to the periodic boundary condition) even for a 6×6 Ising spin glass with the bimodal interactions. FIG. 6.23 shows

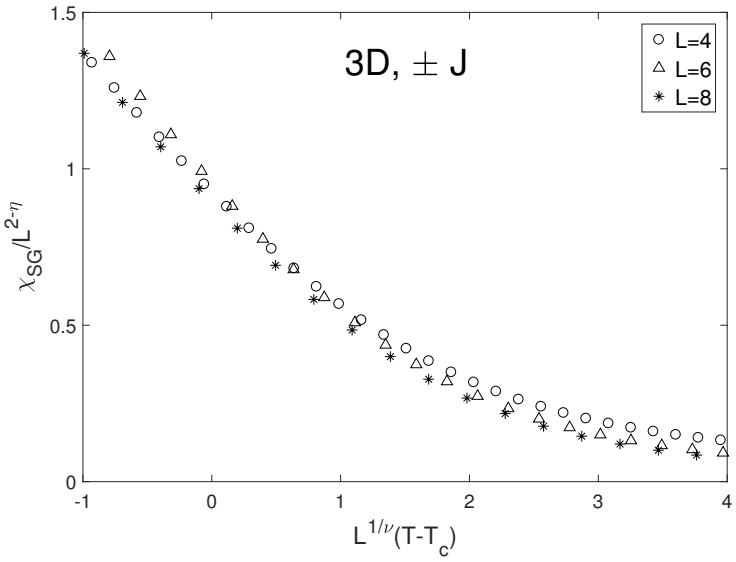

Figure 6.21: Scaling plot of χ_{SG} of the 3D $\pm J$ Ising spin glass according to Eq. (6.28) with $\nu = 1.3$ and $T_c = 1.2J$.

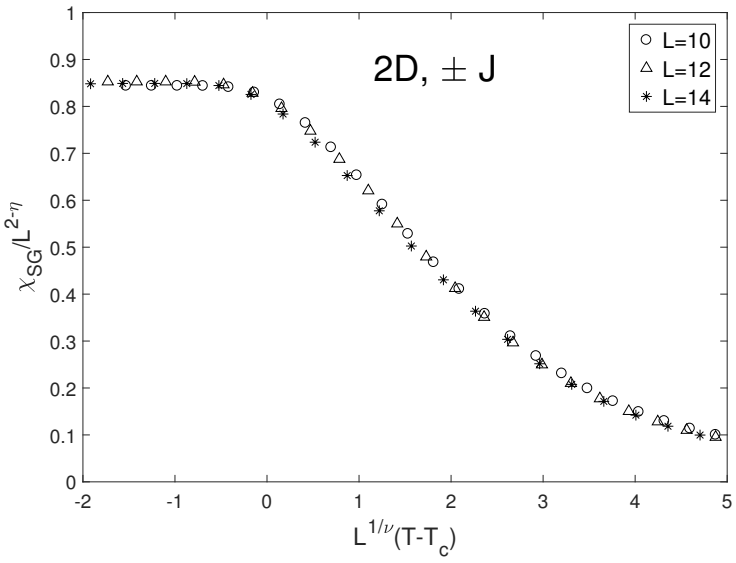

Figure 6.22: Scaling plot of χ_{SG} of the 2D $\pm J$ Ising spin glass according to Eq. (6.28) with $\nu = 1.5$, $\eta = 0.20$ and $T_c = 0.43J$.

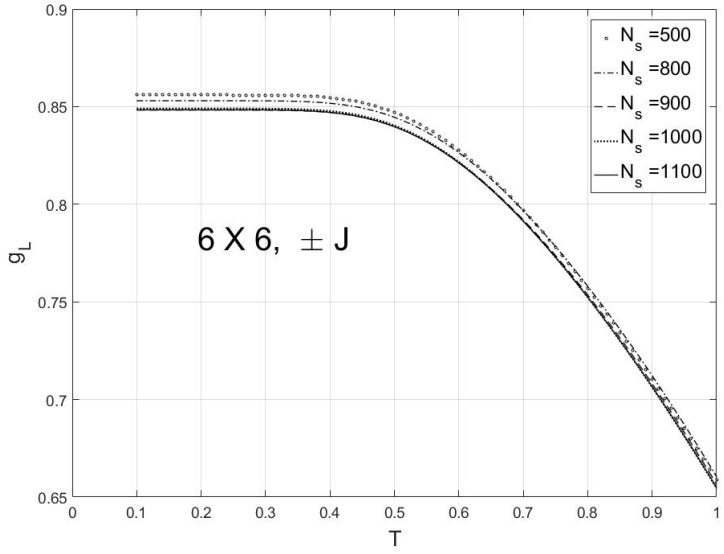

Figure 6.23: Binder parameters with different number of samples for a 6×6 Ising spin glass with the bimodal interactions.

how the Binder parameter changes as the number of samples increases for 6×6 $\pm J$ Ising spin glass. Although g_L changes more slowly as more samples are taken, as can be seen in FIG. 6.24 which magnifies at lower temperatures, it is still possible that g_L keeps changing extremely slowly even for a very large number of samples.

Regarding the T_c of the 2D Ising spin glass, I think the above results imply three possible scenarios. One is that the evidences for $T_c \neq 0$ disappear extremely slowly as more samples are taken, thus $T_c = 0$. Another scenario is that the results supporting $T_c \neq 0$ are true up to a certain system size L^* and for $L > L^*$ the results chage to support $T_c = 0$. The third scenario is that simply $T_c \neq 0$, which is unlikely at this point but still possible. To determine which scenario is true, the extensive simulations for larger systems with more samples of random couplings should be performed using more powerful computer resources.

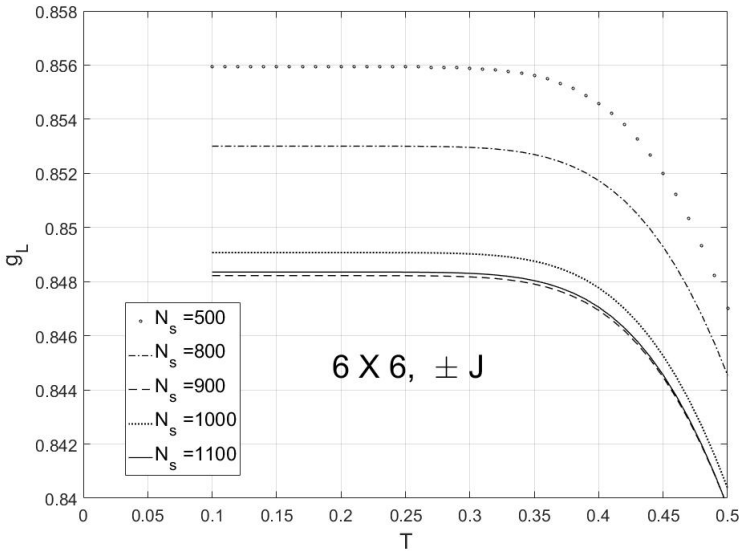

Figure 6.24: Magnified plot of FIG. 6.23 at lower temperatures

Chapter 7

Conclusions and Future Work

In this thesis, the transition matrix Monte Carlo method is employed to evaluate the densities of states for various systems. Since the accuracy of the DOS generated by the transition matrix Monte Carlo method depends on how the transition matrix is constructed, the TMMC needs to combine with appropriate broad sampling techniques. I explored the numerical methods of several different combinations and presented the test results of them. In chapter 2, I discussed the theoretical basis of the TMMC and explained how to construct the TM by all of the accepted and rejected transitions. The higher accuracy of the TMMC than other methods mainly results from the utilization of all the proposed transitions.

In chapter 3, I explained the regulated temperature method which populates the transition matrix by the Metropolis algorithm with continuously varying temperature according to a certain schedule. This method is simple and straightforward since the random walker can be controlled by adjusting temperature. However, finding the optimized *self-adapting* temperature schedule is not an easy task. In the context of the 2D Ising model, I introduced new techniques that can produce the optimized temperature schedule based on the autocorrelation time and the magnetization distribution. Next I proceeded to present the multicanonical transition matrix Monte Carlo method in which the transition matrix is constructed through the multicanonical iteration procedure. Although TMMC is highly accurate, it also suffers from the scalability problem; the CPU times grows according to $\tau_{CPU}^{TMMC} \sim V^{2.19}$, $\tau_{CPU}^{TMMC} \sim V^{2.36}$ for 2D and 3D Ising model respectively. The simulation speed of the TMMC could be significantly improved by the renormalization idea which utilizes the simulation results for a small system to obtain an accurate initial estimate of the DOS for a large system through the convolution procedures. I explained how to implement the RMCTM for the 2D and 3D systems. As the system size increases, the CPU time of the RMCTM grows according to $\tau_{CPU}^{RTMMC} \sim V^{1.75}$, $\tau_{CPU}^{RTMMC} \sim V^{1.64}$ for 2D

and 3D Ising model respectively. The decrease of the exponent in the formula of a power law implies tremendous increase of the simulation speed especially for large systems.

In chapter 6, I explained how to obtain JDOS $g(E, q)$ by the *bivariate* MCTM in which the transition tensor W_{IJKL} is constructed through the bivariate multicanonical iteration procedure. Since the transition tensor is stored in a four dimensional array, it is very cumbersome to handle and it takes long time to find the eigenmatrix which corresponds to the JDOS. I introduced a simple technique that can transform the transition tensor W_{IJKL} to a transition matrix $\tilde{W}_{\tilde{I}\tilde{J}}$ which can be manipulated by the methods developed in the monovariate TMMC. As a pilot test, I applied BMCTM to the Potts model as well as the Ising model and found its results correctly described the existence as well as the nature of phase transitions. Subsequently I applied it to the Edward-Anderson spin glass model to obtain the JDOS from which the Landau free energy and the probability distribution of the spin overlap were calculated. For the 3D $\pm J$ Ising spin glass, from the analysis of the Binder parameters, I obtained the critical temperature $T_c/J \approx 1.15$ which is almost identical to the consensus. For the 2D $\pm J$ Ising spin glass, contrary to the majority of the previous studies ($T_c = 0$), I found evidences for the nonzero temperature phase transition; the estimated critical temperature is $T_c/J \approx 0.45$. However, a definite conclusion could not be made due the limitted number of samples. Although I can not definitely exclude a few different possibilities regarding the T_c for the 2D Ising spin glass, I believe my results of the JDOSs for the 2D spin glass are reliable because I obtained correct results in the applications to the 3D $\pm J$ Ising spin glass, the Potts model as well as the Ising model. At least my results indicate the further study is required to fully understand the critical behavior of the 2D Ising spin glass.

I introduced several TMMC methods including a few newly developed techniques that can be used to evaluate the DOS or the JDOS of a system with high accuracy. I presented very accurate results obtained by those methods when applied to various models such as Ising model, Potts model ans Ising spin glasses. For the RTTM method, the optimized temperature schedule could be generated by monitoring the magnetization distribution in a self-adapting manner. I expect the accuracy and speed of the RTTM can be further improved by incorporating the *cluster spin flip* in the single spin flip dynamics since intermittent introduction of the cluster spin flip can reduce the correlations between samples. Promising results have been already obtained even though further refinement is required [75]. Regarding the finding of novel evidences of a nonzero temperature phase transition in the 2D Ising spin glass, since I could perform the BMCTM simulations only up to $L = 14$ with limited number of samples (different realizations of the random bonds), to confirm the results, I need to increase further the system size as well as the number of samples using more extensive and powerful computer resources.

References

[1] H. G. Ballesteros, A. Cruz, L. A. Fernández, V. Martín-Mayor, J. Pech, J. J. Ruiz-Lorenzo, A. Tarancón, P. Téllez, C. L. Ullod, and C. Ungil. *Phys. Rev. B*, 62:14237, 2000.

[2] P. D. Beale. *Phys. Rev. Lett.*, 76:78, 1996.

[3] B. A. Berg. *J. Stat. Phys.*, 82:323, 1996.

[4] B. A. Berg, U. Hansmann, and T. Neuhaus. *Phys. Rev. B*, 47:497, 1993.

[5] B. A. Berg and T. Neuhaus. *Phys. Lett. B*, 267:249, 1991.

[6] B. A. Berg and T. Neuhaus. *Phys. Rev. Lett.*, 68:9, 1992.

[7] S. Bhar and S. K. Roy. *Comput. Phys. Commun.*, 180:699, 2009.

[8] R. N. Bhatt and A. P. Young. *Phys. Rev. Lett.*, 54:924, 1985.

[9] R. N. Bhatt and A. P. Young. *Phys. Rev. B*, 37:5606, 1988.

[10] K. Binder and D. W. Heermann. *Monte Carlo Simulation in Statistical Physics: An Introduction*. Springer, 2010.

[11] K. Binder and A. P. Young. *Rev. Mod. Phys.*, 58:801, 1986.

[12] V. Cannella and J. A. Mydosh. *Phys. Rev. B*, 6:4220, 1972.

[13] P. M. C. de Oliveira. *Eur. Phys. J. B*, 6:111, 1998.

[14] P. M. C. de Oliveira, T. J. P. Penna, and H. J. Herrmann. *Braz. J. Phys.*, 26:677, 1996.

[15] S. F. Edwards and P. W. Anderson. *J. of Phys. F: Metal Phys.*, 5:965, 1975.

[16] B. Anderson et al. *J. Phys.*, 49:1485, 1988.

[17] R. Faller, Q. Yan, and J. J. de Pablo. *J. Chem. Phys.*, 116:5419, 2002.

[18] L. A. Fernandez, E. Marinari, V. Martin-Mayor, G. Parisi, and J. J. Ruiz-Lorenzo. *Phys. Rev. B*, 94:024402, 2016.

[19] A. M. Ferrenberg and R. H. Swendsen. *Phys. Rev. Lett.*, 63:1195, 1989.

[20] D. S. Fisher and D. A. Huse. *Phys. Rev. Lett.*, 56:1601, 1986.

[21] M. Fitzgerald, R. R. Picard, and R. N. Silver. *J. Stat. Phys.*, 98:321, 2000.

[22] C. J. Geyer. in Computing Science and Statistics: Proceedings of the 23rd Symposium on the Interface, edited by E. M. Keramidas (Interface Foundation, Fairfax Station, VA, 1991), p. 156.

[23] R. G. Ghulghazaryan, S. Hayryan, and C. Hu. *J. Comput. Chem.*, 28:715, 2007.

[24] U. H. E Hansmann and Y. Okamoto. *J. Comp. Chem.*, 14:1333, 1993.

[25] A. K. Hartmann and A. P. Young. *Phys. Rev. B*, 64:180404(R), 2001.

[26] N. Hatanoi and J. E. Gubernatis. *Phys. Rev. B*, 66:054437, 2002.

[27] F. Heilmann and K. H. Hoffmann. *Europhys. Lett.*, 70:155, 2005.

[28] K. Hukushima and K. Nemoto. *J. Phys. Soc. Jpn*, 65:1604, 1996.

[29] M. Suman Kalyan, R. Bharath, V. S. S. Sastry, and K. P. N. Murthy. *J. Stat. Phys.*, 163:197, 2016.

[30] N. Kawashima and A. P. Young. *Phys. Rev. B*, 53:R484, 1996.

[31] H. Khoshbakht and M. Weigel. *Phys. Rev. B*, 97:064410, 2018.

[32] S. Kirkpatrick, C. D. Geltt, and M. P. Vecchi. *Science*, 220:671, 1983.

[33] J. Lee. *Phys. Rev. Lett.*, 71:211, 1993.

[34] Y. H. Lee and D. Yevick. *Phys. Rev. E*, 94:043323, 2016.

[35] Shing-Te Li. *Transition Matrix Monte Carlo Method*. PhD thesis, Carnegie Mellon University, 1999.

[36] E. Marinari and G. Parisi. *Europhys. Lett.*, 19:451, 1992.

[37] E. Marinari, G. Parisi, and J. J. Ruiz-Lorenzo. *Phys. Rev. B*, 58:14852, 1998.

[38] F. Matsubara, A. Sato, O. Kseki, and T. Shirakura. *Phys. Rev. Lett.*, 78:3237, 1997.

[39] W. L. McMillan. *J. Phys. C*, 17:3179, 1984.

[40] N. Metropolis, A. W. Rosenbluth, A. H. Teller, and E. Teller. *J. Chem. Phys.*, 21:1087, 1953.

[41] M.Mézard, G. Parisi, and M. A. Virasoro. *Spin Glass Theory and Beyond*. World Scientific, Singapore, 1987.

[42] I. Morgenstern and K. Binder. *Phys. Rev. B*, 22:288, 1980.

[43] M. E. J. Newman and G. T. Barkema. *Monte Carlo Methods in Statistical Physics*. Oxford University Press, 1999.

[44] H. Nishimori. *Statistical Physics of Spin Glass and Information Processing: An Introduction*. Oxford University Press, Oxford, 2001.

[45] M. Palassini and S. Caracciolo. *Phys. Rev. Lett.*, 82:5128, 1999.

[46] G. Parisi. *Phys. Rev. Lett.*, 43:1754, 1979.

[47] R. B. Pearson. *Phys. Rev. B*, 26:6285, 1982.

[48] D. Perera, Y. W. Li, M. Eisenbach, T. Vogel, and D. P. Landau. in The Minerals, Metal and Materials Society(TMS) 2015 144th Annual Meeting and Exhibition.

[49] Sheldon M. Ross. *Introduction to Probability Models*. Academic Press, 2010.

[50] M. S. Shell, P. G. Debenedetti, and A. Z. Panagiotopoulos. *J. Chem. Phys.*, 119:9406, 2003.

[51] D. Sherrington and S. Kirkpatrick. *Phys. Rev. Lett.*, 35:1792, 1975.

[52] M. Shiomi, F. Matsubara, and T. Shirakura. *J. Phys. Soc. Jpn.*, 69:2798, 2000.

[53] T. Shirakura and F. Matsubara. *Phys. Rev. Lett.*, 79:2887, 1997.

[54] R. R. P. Singh and S. Chakravarty. *Phys. Rev. Lett.*, 57:245, 1986.

[55] G. R. Smith and A. D. Bruce. *J. Phys. A*, 28:6623, 1995.

[56] D. L. Stein and C. M. Newman. *Spin Glasses and Complexity*. Princeton University Press, 2013.

[57] Y. Sugita and Y. Okamoto. *Chem. Phys. Lett.*, 329:261, 2000.

[58] R. H. Swendsen and J-S. Wang. *Phys. Rev. Lett.*, 57:21, 1986.

[59] R. H. Swendsen and J.-S. Wang. *Phys. Rev. Lett.*, 58:86, 1987.

[60] C. K. Thomas, D. A. Huse, and A. A. Middleton. *Phys. Rev. Lett.*, 107:047203, 2011.

[61] T. Vogel, Y. W. Li, T. Wust, and D. P. Landau. *Phys. Rev. Lett.*, 110:210603, 2013.

[62] T. Vogel, Y. W. Li, T. Wust, and D. P. Landau. *Phys. Rev. E*, 90:023302, 2014.

[63] F. Wang and D. P. Landau. *Phys. Rev. Lett.*, 86:2050, 2001.

[64] F. Wang and D. P. Landau. *Phys. Rev. E*, 64:056101, 2001.

[65] F. Wang and D. P. Landau. *Phys. Rev. E*, 64:056101, 2001.

[66] J. S. Wang. *Eur. Phys. J. B*, 8:287, 1999.

[67] J. S. Wang and R. H. Swendsen. *J. Stat. Phys.*, 106:245, 2002.

[68] J. S. Wang, T. K. Tay, and R. H. Swendsen. *Phys. Rev. Lett.*, 82:476, 1999.

[69] U. Wolff. *Phys. Rev. Lett.*, 62:361, 1989.

[70] D. Yevick. *Int. J. Mod. Phys. C*, 27:1650033, 2016.

[71] D. Yevick. *Int. J. Mod. Phys.*, 27:1650041, 2016.

[72] D. Yevick. *Eur. Phys. J. B*, 91:221, 2017.

[73] D. Yevick and Y. H. Lee. *Int. J. Mod. Phys. C*, 28:1750012, 2017.

[74] D. Yevick and Y. H. Lee. *Eur. Phys. J. B*, 90:81, 2017.

[75] D. Yevick and Y. H. Lee. *arXiv:1902.08870 [cond-mat.stat-mech]*, 2019.

[76] D. Yevick and M. Reimer. *Photon. Technol. Lett.*, 19:1529, 2007.

[77] D. Yevick, M. Reimer, and B. Tromborg. *J. Opt. Soc. Am.*, 26:184, 2009.